VOL. VI No 2 AUGUST 2009

JMR

JOURNAL OF MARITIME RESEARCH

Spanish Society of Maritime Research

VOL. VI No2
AUGUST 2009

JMR JOURNAL OF MARITIME RESEARCH

JMR
JOURNAL OF MARITIME RESEARCH

UNIVERSITY OF CANTABRIA

Escuela Técnica Superior de Náutica
c/ Gamazo nº1, 39004 SANTANDER
Telfno (942) 201362; Fax (942) 201303
e-mail: info.jmr@unican.es
http://www.jmr.unican.es

Layout: JMR

Printed bay: Gráficas Fisa, S.L.

ISSN: 1697-4840

D. Legal: SA-368-2004

CONTENTS

Automar Scientific Committee

Gabriel Oliver *(UIB)*

Manel Frigola *(UPC)*

Rafael García *(UdG)*

Yolanda González *(UIB)*

Pablo González de Santos *(IAI-CSIC)*

Antoni Mánuel *(SARTI/UPC)*

Jaume Piera *(UTM-CSIC)*

Pere Ridao *(UdG)*

Roque Saltarén *(UPM)*

Carlos Silvestre *(IST)*

Francisco Velasco *(UC)*

Automar network

Some of the participants of the *Jornadas Automar 2008*

Automar is a research network in automatic control and robotics for the marine industry and marine sciences. Automar brings together scholars from universities and research centres, encouraging knowledge exchange, training and cooperation among the different members of the scientific and industrial community. To that end, the members of the network organize scientific and technical meetings, courses, tutorials and conferences on a regular basis.

Since its initial steps in 2002, Automar has organized more than ten events, promoting scientific education or cooperation and disseminating know-how among its partners, industrial companies and marine technology end-users. Throughout that time, the size of the network has progressively expanded to include more than fifteen research groups.

In September 2008, around forty researchers and students attended the *Jornadas Automar*, a three-day event held at the Universitat de les Illes Balears campus, in Palma (Spain). The first day Prof. Carlos F. Silvestre, from the *Instituto Superior Técnico* of Lisbon, conducted a tutorial about the design of tracking controllers for unmanned vehicles. During the second and third days, both researchers and PhD students presented twenty-one research and development projects.

In this issue, the reader will find some of the research works presented during the above-mentioned Automar meeting. The original manuscripts of the selected papers were extended and adapted to meet the JMR publication guidelines. They were additionally reviewed by an ad-hoc technical committee. As a matter of fact, the present selection does not intend to cover all the top-

ics in marine robotics and automation. Still, it can be considered representative of Automar partners' activity.

Four papers focus on AUV design and applications, probably one of the more dynamic and challenging areas at the moment. Sousa et al. present the design and preliminary results of a low-cost AUV for acoustic inspection. Researchers at the Technical University of Catalonia in Vilanova describe an autonomous hybrid (surface/underwater) vehicle as a solution for intensive vertical profile logging in oceanographic systems. Gliders are also extensively used in many oceanographic tasks and thus the paper from researchers at IMEDEA-CSIC proposes a path-planning strategy that uses large-scale current fields information to optimize power consumption and guarantee the completion of long-term missions with that type of vehicles. Ortiz and Antich present a new solution, based on particle filters, for visual vehicle guidance in underwater cable inspection. The article authored by Moreno et al. focuses on the path following control of an unmanned surface vehicle, which is a highly relevant and topical issue in autonomous navigation. Last but not least, researchers from Universities of A Coruña and Cádiz present a new methodology to ensure sensor fault detection and isolation applied to the thruster equipment of a dynamic positioning control system.

To end with, I would like to thank all the individuals and institutions that made this Special Issue of JMR possible. I remain indebted to all the members of the research groups involved in the Automar network for actively participating in this fruitful experience and to the University of Balearic Islands for hosting the *Jornadas*. Thanks are also due to the authors for their contributions and to the reviewers for their interest and efficient fulfilment of all the requirements in the submission process. Finally, my gratitude goes to people from the *Journal of Maritime Research*, who have provided us with constant guidance and support.

A special mention should be made to the Spanish Ministry of Education and Science for funding Automar network activities with the project DPI2006-28345-E.

Gabriel Oliver Codina
DPI2006-28435-E Project Leader

JMR

Journal of Maritime Research, Vol. VI. No. II, pp. 5-22, 2009

ISSN: 1697-4840

PATH PLANNING FOR AUTONOMOUS UNDERWATER VEHICLES IN REALISTIC OCEANIC CURRENT FIELDS: APPLICATION TO GLIDERS IN THE WESTERN MEDITERRANEAN SEA

B. Garau[1*], M. Bonet[1], A. Alvarez[2], S. Ruiz[1] and A. Pascual[1]

Received 22 September 2008; received in revised form 29 September 2008; accepted 15 April 2009

ABSTRACT

Autonomous Underwater Vehicles (AUVs) usually operate in ocean environments characterized by complex spatial variability which can jeopardize their missions. To avoid this, planning safety routes with minimum energy cost is of primary importance. This work revisits the benefits, in terms of travelling time, of path planning in marine environments showing spatial variability. By means of a path planner presented in a previous paper, this work focuses on the application to a real environment of such techniques. Extensive computations have been carried out to calculate optimal paths on realistic ocean environments, based on autonomous underwater glider properties as the mobile platform.

Unlike previous works, the more realistic and applied case of an autonomous underwater glider surveying the Western Mediterranean Sea is considered. Results indicate that substantial energy savings of planned paths compared to straight line trajectories are obtained when the current intensity and the vehicle speed are comparable. Conversely, the straight line path betwe en starting and ending points can be considered an optimum path when the current speed does not exceed half of the vehicle velocity. In both situations, benefits of path planning seem dependent also on the spatial structure of the current field.

Keywords: path planning, autonomous underwater vehicles, ocean variability.

[1] Instituto Mediterraneo de Estudios Avanzados, Mallorca, Spain. [2] NATO Undersea Research Centre, La Spezia, Italy. *Corresponding author (tomeu.garau@uib.es) IMEDEA (UIB-CSIC). C/Miquel Marques, 2107190, Esporles, Islas Baleares, Spain.

INTRODUCTION

Autonomous underwater vehicles (AUVs) must frequently operate in ocean environments characterized by complex spatial variability (Schmidt and Bovio, 2000). This spatial complexity is induced by the turbulent nature of the ocean, described by the continuous change of a wide range of spatial and time scales. Energetic flows induced by tides and topographic perturbations, instabilities and currents induced by local wind effects, are only few examples of ocean variability. This variability can strongly perturb the development of AUVs operations (Galea, 1999). In particular, AUVs usually encounter strong current fields in the marine environment that can jeopardize their missions. Determining and predicting ocean currents is then a fundamental requirement to optimize certain aspects of the AUV's performance, specifically when vehicles have to operate energy-exhaustive missions in ocean areas characterized by comparatively strong currents. In such cases, it is of primary importance to plan safety routes with minimum energy cost.

Nowadays, several systems can provide an estimation of the existing current field in a certain region. Numerical ocean models can provide nowcasts and forecasts of ocean variability (Holland and McWilliams, 1987). A typical numerical ocean model consists of finite difference equations representing the momentum, heat and salt balance in a determined area. These equations are integrated forward in time to predict the time evolution of the horizontal and vertical structure of the fluid flow as well as the temperature and salinity within the domain, given the wind stresses and buoyancy forcing at the sea surface. Satellites can also provide current fields derived from their observations of the sea level. The procedure consists of merging into one map the sea level anomalies measured by altimetric satellites along their tracks. Current fields can be derived applying the geostrophic assumption on the resulting merged map. Information of the environmental current field, obtained either from the ocean models or from satellites observations, can be incorporated into existing path finding algorithms to plan safety routes with minimum energy cost (Alvarez and Caiti, 2001).

Traditionally in AUVs, path planning has been related to safety conditions. The path should be devoid of known obstacles or hazardous areas. Different computational methods were employed to plan safety paths for AUVs. Warren (Warren, 1990) used potential field algorithms to solve the path planning problem. The algorithm used artificial potential fields applied to the obstacles and goal positions, employing the resulting field to influence the path of the AUV. Graph searching techniques were employed by Carroll et al. (Carroll et al, 1992) for AUV path planning. In this case, a chart or graph is produced showing free space where no collision will occur and forbidden spaces where a collision will occur. Based on this graph, a path is selected by piecing together the free spaces or by tracing around the forbidden spaces. Techniques such as case-based reasoning (Vasudevan and Ganesan, 1996) and genetic algorithms (Sugihara and Yuh, 1997) have also been applied to the motion planning for underwater robotic vehicles.

Alvarez and Caiti (Alvarez and Caiti, 2002) employed dynamic programming to carry out a systematic simulation study of the energy savings obtained through optimal AUV path planning, taking into account the spatial structure of the current velocity field. The study had the objective of putting in relation the spatial scales of the current field variability with the expected energy saving due to the optimized path planning. Results indicated a substantial energy saving, as compared to straight line paths, when ocean eddy structures were greater than one-third of the total crossing distance. Finally, the problem of AUV mission planning optimizing the energy cost in ocean environments with real current fields was considered by Alvarez et al. (Alvarez, Caiti and Onken, 2004). The developed planning algorithm integrated the current predictions obtained from the Harvard Ocean Prediction System (HOPS) (Robinson et al, 1996) to an evolutionary navigator, providing the path with minimum energy requirements. In these studies incorporating the current field, the AUV speed with respect to the bottom was assumed to be constant. Thus, the considered AUV was able to adapt its speed depending on the current field where it was immersed, being the total speed constant through the planned path.

Recently, Garau et al (Garau, Alvarez and Oliver, 2005) considered a more common situation on actual AUVs, where the thrust power is usually kept constant during the mission. Thus, in the usual situation the optimization of energy consumption agrees with finding the minimum-time path. This defines an optimization problem in oceans with spatial variability, different from the previously studied. Minimum-time paths were computed in simulated ocean basins with different eddy sizes and current speeds. Results showed the path planner performance depends on different parameters like current strength or eddy size.

In this article we apply the proposed techniques in the abovementioned paper, in the more realistic and applied case of current fields derived from different models as well as satellite altimetry. The real path followed by an actual platform is also compared to the planned path.

The paper is organized as follows: Section II details the designing of the route planner while Section III describes the different ocean environments employed in the simulations. A real platform is presented in section IV. Results from two different deployments are shown in Section V and discussed in Section VI.

THE PATH PLANNER

The presented path planner considers the case of AUV motion on the horizontal plane. This simplification is justified by the interest in the effect of horizontal ocean structures on AUVs because vertical motions in ocean structures are generally negligible. Moreover, the scales of variability that can be forecasted by models or observed from satellites are large enough to suppose that the main movement of the vehicle will be on a horizontal plane.

The dimensions of the AUV are considered much smaller than the dimensions of the ocean basin and ocean structures. Thus static route planning, which does not account for the AUVs dynamics, is appropriate. Consider the two-dimensional underwater environment discretized in space over a grid. Any point in the grid defines a node whose coordinates units will be measured in degrees (latitude and longitude), a coherent decision taking into account the size of the region to be considered. This grid, conversely to the previous version of the path planner, can be regular or irregular, and it can even be a triangular mesh like the ones produced by finite element methods. A path between a starting node and a destination node is defined through a sequence of nodes which are interconnected, and it is made by straight-line segments connecting any two adjacent nodes. In practice, it is assumed that the AUV navigation is defined through via-points that are the nodes of the grid. A current velocity vector is defined at any point in space.

Within this setting, the path planning problem can be enunciated as follows: given a start node *s*, a destination node *d* and a current velocity field, find a path such that the time required for a vehicle travelling along the path at a constant thrust power is minimum, subject to the constraints that the path does not intersect any solid obstacle.

The travelling time required by a given path is evaluated computing and adding up the time required covering each segment constituting the path. Consider a segment connecting two nodes $n_{i-1}n_i$ of any arbitrary path; let d_i indicate its length, and let $\vec{e}_i$ be a unitary vector oriented along the segment in the direction of desired motion of the vehicle. At any point (x,y) along the segment the vehicle must have a nominal velocity $\vec{v}_i(x,y)$ given by:

$$\vec{v}_i(x,y) = \vec{v}_r(x,y) + \vec{v}_c(x,y), \forall (x,y) \in n_{i-1}n_i \tag{1}$$

where $\vec{v}_r$ is the speed of the vehicle relative to the current, $\left|\vec{v}_r\right|$ is constant and proportional to the cubic root of the constant thrust. The time to cross the segment is given by,

$$t_i = \frac{\left|d_i \vec{e}_i\right|}{\left|\vec{v}_i\right|} \tag{2}$$

and the total travelling time of the path is finally given by the summation $\sum_1^m t_i$.

Computational difficulties on evaluating expression (2) appear when current speeds are different in the surrounding nodes. In these cases, a unique velocity cannot be defined for the entire segment. A recursive approach has been implemented

to overcome the problem. The segment is split into sub-segments until the difference between the interpolated current speeds at the end points of each subsegment, do not exceed a given threshold. Then, equation (2) is applied to each sub-segment with a current speed obtained from averaging the current velocities at the subsegment end points. The total time required to cover the segment is the summation of the travelling times of each sub-segments.

An A* algorithm has been implemented as a search engine to find the optimum path in a given ocean environment. The traditional Euclidean distance between the field point and the destination goal, divided by the maximum possible nominal speed (maximum current speed plus the vehicle speed) was employed like heuristic function. This election ensures that the heuristic cost will be always lower than the actual cost to reach the goal from a given node and thus, the optimum solution is guaranteed. Moreover, previous works have showed that this simple heuristic function guides the search, reducing the computation time.

An improvement applied on the initial path planner is made on the conversion from the initial grid to graph, which is the input to the path planner. While the previous version considered the typical 8-connectivity to generate the edges between nodes of the grid, in this study it has been increased to 16-connectivity. This is a subset of the 24-connectivity, dismissing the edges that represent a path reproducible exactly with edges from the 8-connectivity. This improvement provides more flexibility to the path planner to adapt the path to the current direction. It also increases the number of edges in the searching graph, increasing the computational effort. Nevertheless, the heuristic function guides the search and helps in not increasing the computation time due to the larger number of edges.

In order to test the path planner performance in the work presented by Garau et al (Garau, Alvarez and Oliver, 2005), the current fields used for their simulations were obtained from a streamfunction field $\Psi(x,y)$ randomly generated from a specific isotropic power spectrum peaked at determined scales with random phases. This procedure allows the generation of current fields with controlled features. Therefore, it is feasible to study the path planner performance based on the predominating scales over the field, their maximum current intensity or any other parameter of interest. The current fields were defined on a regular grid with a fixed distance between grid points, expressed in meters, for easiness of computation.

REALISTIC OCEAN ENVIRONMENTS

While the abovementioned work evaluated path planner performance, this work presents the application of the same path planner on realistic situations. The previous assumptions of a regular grid points equidistant and the randomly generated stream function fields are not used. Instead of a regular grid, a graph is used, allowing either for regular or irregular grids, as well as meshes produced by finite elements

methods. These changes are introduced to improve the adaptability of the path planner to different sources of oceanographic information.

Oceanographic environmental information can be extracted either from in-situ or remote observations, or numerical forecast models. The oceanographic observations are characterized by their spatial distribution as point time-series, trajectories, profiles or 2D grids. Examples of that are moorings, gliders, CTD ship cruises or satellite observations, respectively. The numerical models usually provide 2D or 3D information about marine environment properties. For the case of the path planner, the gridded data is the required information, and so, several trials will be done with satellite observations as well as forecast model outputs.

Several model outputs and satellite observations can be used for the realistic path planning. Examples of these sources are, among others, MFS (Mediterranean Forecast System), IFOSY (IMEDEA Forecast System), ESEOO (Establecimiento Español de un Sistema de Oceanografía Operacional) or AVISO.

MFS is the output of the numerical forecast model that has been setup and is running operationally at INGV (Istituto Nazionale di Geofisica e Vulcanologia). It uses GFDL-MOM (Geophysical Fluid Dynamics Laboratory-Modular Ocean Model, Pakanowsky et al., 1990) which is a three-dimensional primitive equation ocean general circulation model designed by Bryan, (1969) and Cox (1984). MFS provides forecasts outputs on a regular grid with a resolution of 1/16° that covers the whole Mediterranean Sea.

AVISO provides near real time images of absolute dynamic topography and geostrophic currents obtained from a process of optimal interpolation combining all the available altimeters (Jason-1, Envisat, Geosat Follow-On). The absolute dynamic topography is obtained through the sum of the sea level anomaly measured by the altimeter plus a mean dynamic topography (Rio et. al., 2007). Currents are computed applying the geostrophic approximation. The spatial resolution of this product is 1/8°.

Besides the different spatial resolution and limits, the heterogeneity of data sources is an issue to be tackled. The Centro Operacional de Datos Oceanográficos (CODO) located in Mallorca as part of the Tecnologías Marinas, Oceanografía Operacional y Sostenibilidad (TMOOS) department of the Institut Mediterrani d'Estudis Avançats (IMEDEA) is working on the standardization of the data from different sources in the Western Mediterranean Area for its distribution. The path planner has been tested with information resulting of this work. This standardization allows using different data sources over the same area without changing the path planner software.

An international data format standard for the oceanographic data has been adopted. NetCDF (network Common Data Format) is a set of software libraries and machine-independent data formats that support the creation, access, and sharing of array-oriented scientific data. The oceanographic data is associated to a geospatial location that can be stored in the NetCDF files. However, the format does not

determine the relationship between the data and its spatial distribution in terms of latitude and longitude or depth. The conventions for climate and forecast (CF) metadata are designed to promote the processing and sharing of files created with the NetCDF API.

CF are increasingly gaining acceptance and have been adopted by a number of European projects and groups as a primary standard. The conventions define metadata that provide a definitive description of what the data in each variable represents, and the spatial and temporal properties of the data. This enables data users from different sources to decide which quantities are comparable, and facilitates building applications with powerful extraction, regridding, and display capabilities. Using data with these conventions makes it easier to the path planner for reading the input current fields. The path planner uses the NetCDF/CF format due to its advantage and because CF conventions generalize and extend other conventions on NetCDF such the COARDS conventions, thus, being backward compatible.

Besides the data format, the access mechanism to it has to be taken into account, since it tends to be distributed over internet and the datasets are relatively large. For the distribution of oceanographic data the most extended protocol is the OpenDAP (Open-source Project for a Network Data Access Protocol). OpenDAP is a framework that simplifies all aspects of scientific data networking. OpenDAP provides software which makes local data accessible to remote locations regardless of local storage format. The OpenDAP protocol allows the access to a concrete variable of the file without downloading the whole file. In the case of the path planner, the current fields are extracted from a remote file, and the software works with them as if the data was stored locally.

IMEDEA has a data catalog using THREDDS (TDS, Thematic Real-time Environmental Distributed Data Services) [http://dataserver.imedea.uib-csic.es:8080/thredds]. TDS is a web server that provides metadata and data access for scientific datasets, using OPeNDAP, OGC WMS and WCS, HTTP, and other data access protocols.

IMEDEA has been using a special type of AUV as an in-situ observing platform for several purposes. The platform is integrated in the CODO data management system as well as other platforms such as moorings, uses NetCDF/CF as data format delivery and its information is organized on the same Thredds catalogue as the models and the satellite information. This AUV, which is presented in the next section, and some of its missions have been used in this work to test the path planner performance.

OCEANOGRAPHIC AUV PLATFORM

An underwater glider is a type of autonomous underwater vehicle (AUV) that uses small changes in its buoyancy in conjunction with wings to convert vertical

motion to horizontal, and thereby propel itself forward with very low power consumption. Gliders follow an up-and-down, sawtooth-like profile through the water, providing data on temporal and spatial scales unavailable to previous AUVs.

In the presented experiment the deployed platform was a Slocum shallow electric glider manufactured by Webb Research Corporation. The Slocum glider, named after Joshua Slocum, the first person to solo circumnavigate the world, is a torpedo shaped, winged vehicle that is 1.5 meters long, weighs 52 kilograms and has a hull diameter of 21.3 cm (Creed et al, 2002). The wings, made of composite material are mounted just aft of the centre of buoyancy.

There are three main hull sections plus wet fore and aft sections. The front wet section or nose dome houses a 200 kHz transducer for altimeter use. This section also has a hole on the centerline for large bore movement of water as is created by the displacement piston pump. The first main hull section contains the displacement piston pump, pitch vernier mechanism, altimeter electronics, ballast weights and a large alkaline battery pack that supplies power and serves as the mass moved by the pitch control during ascent and descent. The middle hull section encloses the science payload, additional energy and ballast weights. The third main hull section houses the back chassis that holds the navigation and communication electronics, the catalyst, the air pump system for the air bladder, battery power, vehicle controller, hardware interface board and attitude sensor.

A pressure transducer is ported through the aft end cap. The aft battery pack can be manually rotated for static roll offsets. The air bladder, steering assembly, burn wire, jettison weight and power umbilical are housed in the wet tail section. This section also has provisions for external trim weights and wet sensors. Protruding through the aft end cap and through the tail cone is the antenna fin support. This boom is a pressure proof conduit for the antenna leads and low noise amplifier for the GPS. Below the boom is a protected conduit for the steering motor linkage. Attached to the boom is the antenna fin.

Prior to a mission, the glider is ballasted to make it neutrally buoyant in the waters it has to operate in. To dive, the displacement piston pump moves water into the nose making the vehicle's nose heavy. To ascend, water is pushed out of the nose by the piston pump making the glider buoyant. The volume of water is approximately 233 cm^3, and causes two effects on the glider: changes its buoyancy and moves the centre of gravity along the longitudinal axis of the vehicle. The buoyancy change induces on the glider a force that accelerates the vehicle in the vertical axis. This acceleration increases the glider vertical speed. The drag force, proportional to the square of the speed, also increases until an equilibrium point is reached. When both forces are equal, the glider vertical speed is kept constant through the dive or climb. It is designed to operate between the surface and 200 m of depth. During the ascent or descent, the glider moves the pitch batteries to fine adjust the centre of gravity and therefore the diving angle.

Typical values for its vertical speed are around 0.2 m/s. The vehicle is designed also to acquire a pitch angle close to 26°. Therefore, adding a small angle of attack (approx. 1°) of the glider, the horizontal speed it can reach is $\frac{0,2}{\tan(27)} \approx 0.4 m/s$.

This nominal speed, without taking currents into account, will be the one used by the path planner as the thrust produced by the vehicle.

The air bladder in the aft section provides buoyancy and stability while the glider is surfaced. The inflated air bladder also lifts the tail fin out of the water to facilitate communication of the glider with its Command Center. To steer the glider the back portion of the tail fin is moved as a controlled plane that acts as a rudder. Communication with the glider is done using line of sight radio frequency (RF) modem (FreeWave) for local high speed communications, ARGOS for a recovery beacon and Iridium for bi-directional satellite communications.

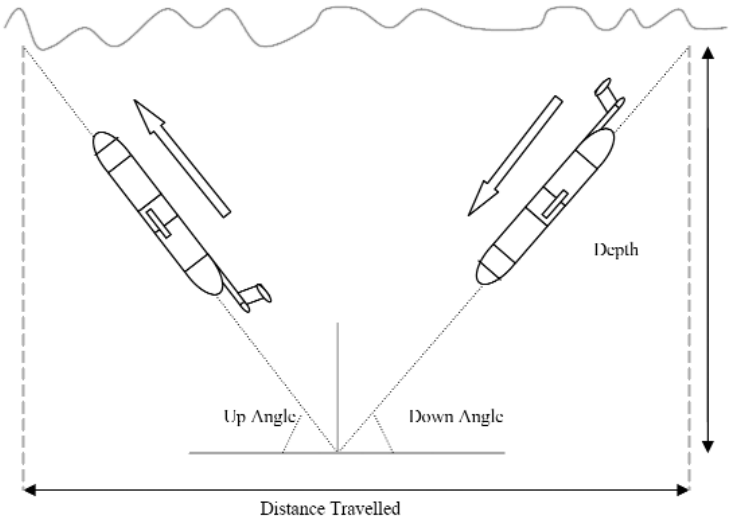

Figure 1. Schema of a glider inflection.

Deployment region and duration, dependent upon what scientific measurements are being taken and what type of communication is being used averages 30 days with a range of 1500 km. The deployment is defined as a set of waypoints that the glider has to navigate.

Glider navigation is done using GPS, internal dead reckoning and the altimeter. While underwater, the glider dead reckons its position relative to the water. When surfaced, the glider receives a precise location from its gps. Assuming that the dead reckoning and GPS are perfect, any errors between the gps fix and the final dead

reckoned position must be due to the currents fields. The glider can use the measured water current in its next underwater segment to navigate better.

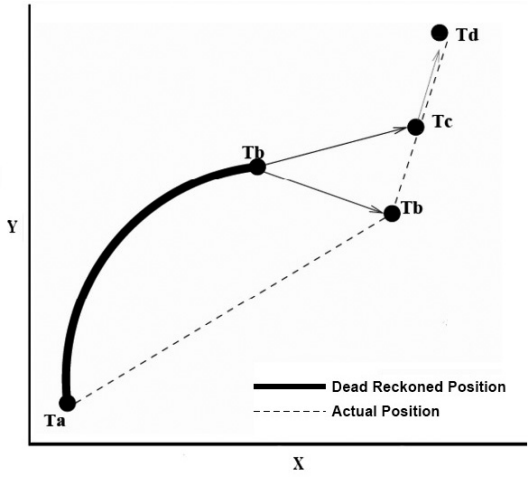

Figure 2. Schema of glider current estimation.

As shown in figure 2, at time Ta, the glider dives and surfaces at time Tb. The dotted line connecting Ta and Tb represents the actual path the glider performed underwater. The solid line linking Ta and Tb represent the dead reckoned trajectory of the glider. Tc represents the first GPS fix position. During this time, the glider drifts on surface due to the wind effect. To estimate this drift, the glider waits until Td to fix a new GPS position. Assuming a constant surface drift, the glider is able to estimate the position where it surfaced. Then, it can compute the distance between the dead reckoned position and the actual one in order to estimate the integrated drift while underwater.

RESULTS

Previous works established that path planning provides substantial improvements when currents strengths are close to the AUV nominal speed. In this work, two different glider deployments have been considered to exemplify in a real scenario such conditions. First, a glider mission in the North of the Balearic Islands is shown to provide the case of weak currents. Also, a more interesting case in the Alboran Sea is shown, where the current intensities are even higher than the vehicle nominal speed.

Missions and Scientific Goals

During the JASMIN cruise, performed in August 2008, between the 12th and the 27th, a coastal glider followed the JASon satellite 70 track from MINorca to the Iberian Peninsula coast. This track is of particular interest because it runs perpendicular to the main oceanographic features in the Balearic Sea (Ruiz et al, 2008; Bouffard et al, 2009). The JASMIN cruise was conducted during the calibration phase of the satellite Jason-2 in the frame of the OST Proposal "Improvement, validation and merging of altimeter products for coastal and regional applications".

One month before, in the framework of the EU funded SESAME project, the same glider was deployed in July 2008, starting on the 2nd and ending on the 21st.

There were several specific objectives of this mission. One of them was to test the feasibility of the gliders technology usage in an area with intense current and high mesoscale variability. There was interest in exploring the feasibility of new assimilation techniques of data from different platforms (gliders, satellites, buoys, etc…) on high resolution models (2km) and also providing boundary conditions for SESAME numerical models. And finally, one of the major interests was to characterize the ocean variability and interaction between the Atlantic and Mediterranean water in the eastern Alboran Sea.

Figure 3 shows a general map of the region. Figure 4 presents two maps, one for each mission, showing the glider trajectories along with its own currents estimation during navigation. Endpoints are marked also in figure 4 as WP1 and WP2. The first segment of each mission covers the navigation between WP1 and WP2, while the second segement goes from WP2 to WP1

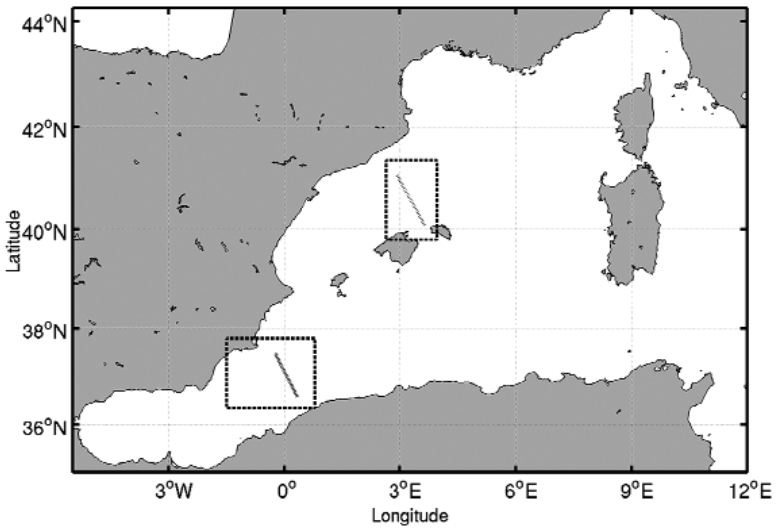

Figure 3. Map of WMED with the study areas marked with dashed lines and tracks marked with dotted lines.

Environmental Conditions

During the two abovementioned missions, the Thredds catalogue provided access to environmental information. Several model outputs as well as altimetry maps where available to evaluate the current field the glider was to be operating in. Figures 5 and 6 show the current fields that were considered most relevant: MFS model output and altimetry maps. The maximum agreement between the current fields and the currents estimated by the glider is achieved with altimetry.

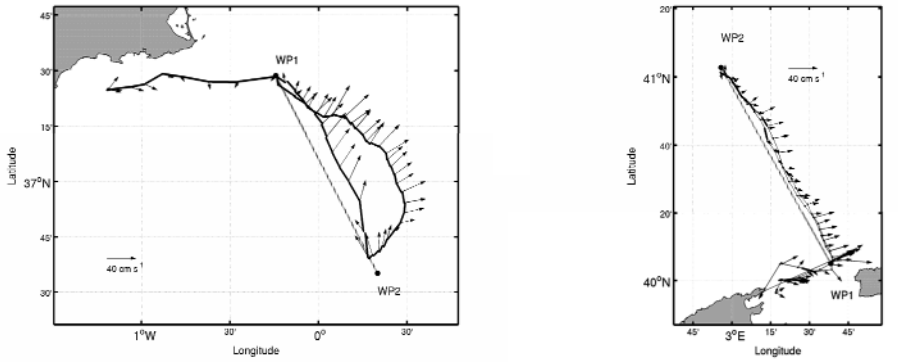

Figure 4. Glider trajectories and its estimated currents.

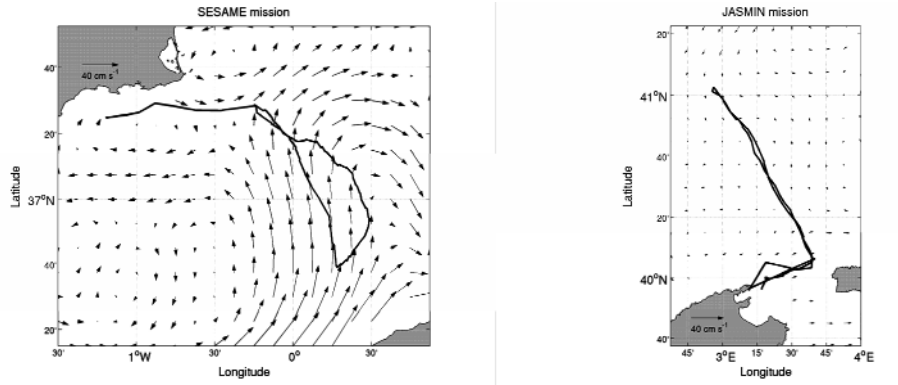

Figure 5. SESAME and JASMIN missions and altimetry derived current field.

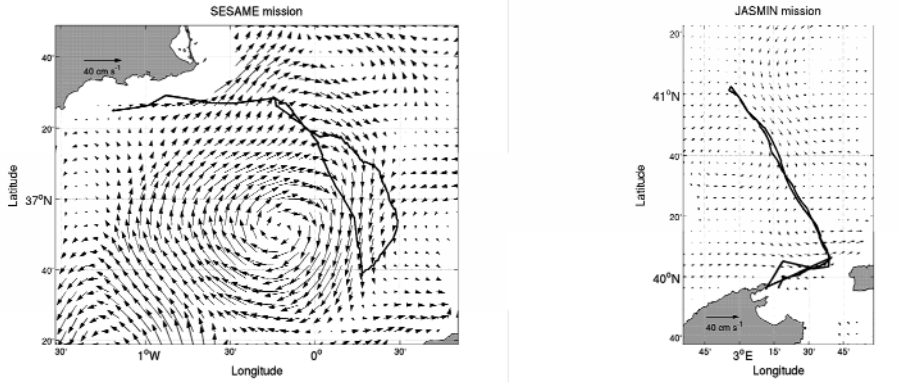

Figure 6. SESAME and JASMIN missions and MFS current field.

Figures 5 and 6 also show the trajectory that the glider followed when commanded to navigate along the satellite tracks. In the case of JASMIN mission, at the right hand side of both figures, currents were weak, and the glider was able to follow the expected straight line path when moving towards the northwest and southeast. However, during the SESAME mission, on the left hand side of both figures, a instability with strong currents was found on the glider path. This feature made the glider unable to follow the commanded route, and it was advected by the flow when performing the first segment. The second segment, where the glider moved northwest, was accomplished correctly by the glider since it was helped by the currents.

For JASMIN mission, the glider needed 5.53 days to travel the first segment (from south to north) and 4.45 days to make the second segment on its way back. During SESAME mission, the glider spent 7.73 days performing the first segment of the mission, and just 3.09 days for the second part. Moreover, the glider was unable to reach the southest point, so the first segment was never completed as in the original mission design. The travelling time difference for the same segment performed in different directions provides an indication of the currents effects on the glider.

Planned Paths

Using the current fields derived from altimetry and the MFS model output, minimum travelling time routes have been computed. Figures 7 and 8 show the results of the path planner.

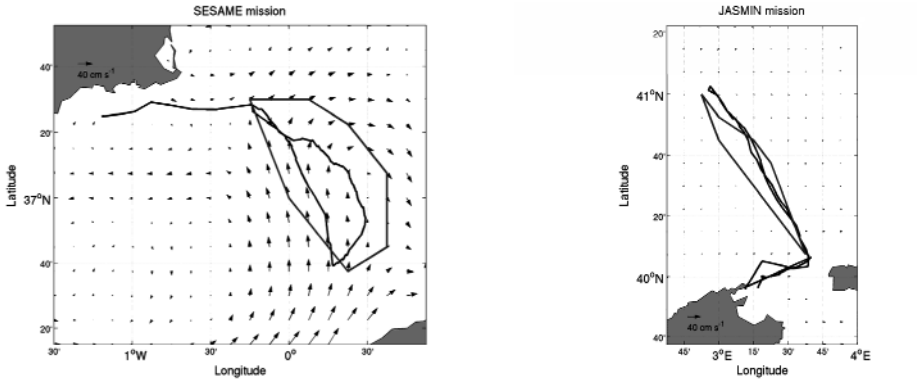

Figure 7. SESAME and JASMIN planned paths on altimetry derived current field.

Using ADT for JASMIN mission, the path planner provided a near-straight path. Thus, the improvement with respect to the straight line was almost zero. However, the estimated time to perform each segment was around 3.6 days. This fact is due to the difference between the ADT derived currents and the real currents felt by

the glider. Altimetry was providing currents in the correct direction but magnitude was lower.

When MFS model output was used for JASMIN mission, the path planner provided a slightly different pattern, but also close to the straight line. In this case, the path planner showed a higher improvement (close to 10%) than with ADT. The time estimation in this case was around 4.5 and 3.3 days for each segment, respectively. The explanation of the difference between results from each source is the fact that MFS was providing currents with higher intensity, but the circulation pattern was different. Therefore, the current intensities and their spatial distribution played an important role in both the shape of the path and the time estimation provided by the path planner.

Using ADT for SESAME mission, the path planner provided a very different path for both segments. While the first segment should be performed describing a curve, the second segment was to be performed in almost straight line path. The improvement with respect to the straight line was very high in the first segment (around 57%). For the second segment, as it was already straight, no improvement was made by the path planner.

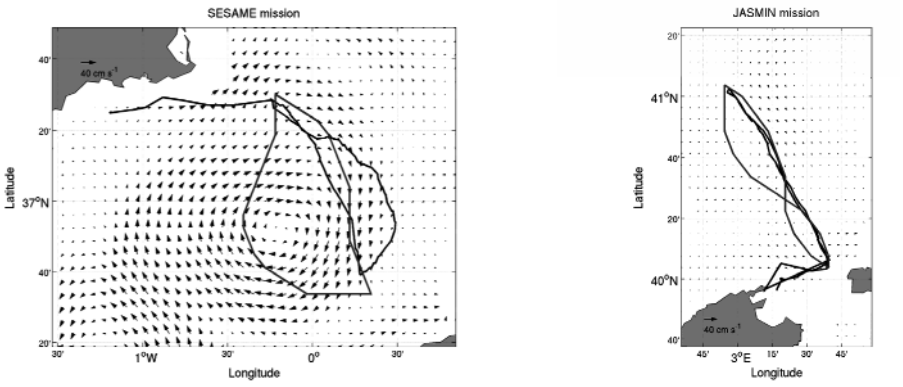

Figure 8. SESAME and JASMIN planned paths on MFS current field.

When MFS model output was used for SESAME mission, the path planner provided a very different pattern. In this case, results were dismissed because of the big misfit between glider estimated currents and current field. The model output was reproducing the eddy on the west of its position. Thus, the path planner results were computed over a wrong current field.

Given these two examples of deployments, it is reasonable to say that the path planner could not improve the glider performance in JASMIN mission, but could have improved travelling time significantly during SESAME mission, where the

currents were much stronger. This fact agrees with previous works conclusions about the path planner applicability.

DISCUSSION

In this work, extensive computations have been carried out to calculate by means of the A* based path planner, optimal paths (in terms of energy cost) in realistic ocean environments. Different sources of information have been used to capture the uncertainty of the current field used as input. The study is focussed on practical cases where the AUV develops a constant thrust independently of the current field where it is immersed. This substantially differs with previous works where the AUV was considered to adapt its speed to keep constant the total velocity with respect to the ground [9]. Now, minimum energy paths are also paths with minimum travel time being the problem more restrictive.

Concerning the benefits of path planning, results indicate that these are scarce when the vehicle velocity is clearly superior to the background current field. Substantial benefits of path planning are only obtained when the vehicle and current speeds are comparable. The velocity of present AUVs developing missions in the ocean is usually superior to current speeds normally found at the ocean. Nevertheless, path planning is required in those ocean areas characterized by strong currents. There, current intensities can reach values equal or even superior to the AUV velocity. In these cases, coupling a numerical ocean model or any other current field observation with a path planning algorithm constitutes an optimum solution to ensure the success and safety of the AUV mission.

The proposed techniques provide robustness and efficiency to AUVs. Robustness can be seen in the feasibility analysis of the path planner results. The reachability of a location is proven if the path planner is able to find a route to that destination. Thanks to the completeness of the searching algorithm, an impossible mission could be dismissed before deploying an AUV in a hazardous area. Efficiency plays an important role even when the straight path is feasible. Using the path planner, the scientists can replan the AUV trajectory to visit the same locations in a shorter time. This time saving allows for longer (in distance) or energy exhaustive (more sensors) missions.

REFERENCES

Alvarez, A. and Caiti, A. (2001): A genetic algorithm for autonomous underwater vehicle route planning in ocean environments with complex space-time variability. *Proceedings of the IFAC Control Applications of Marine Systems* (CAMS 2001).

Alvarez, A. and Caiti, A. (2002): Interactions of autonomous underwater vehicles with variable scale ocean structures. Proceedings of the IFAC World Conference Systems.

Alvarez, A.; Caiti, A. and Onken, R. (2004): Evolutionary path planning for autonomous underwater vehicles in a variable ocean, IEEE *Journal of Oceanic Engineering* 29, no. 2, 12. pp. 418-429.

Bouffard, J.; Roblou, L.; Birol, F.; Pascual, A.; Fenoglio-Marc, L.; Cancet, M.; Morrow, R. and Ménard, Y. (2009): Assessment of improved coastal altimetry strategies over the NMW Sea. Costal altimetry. S. Vignudelli, A. Kostianoy, P. Cipollini and J. Benveniste Eds. Springer-Verlag. Submitted

Bryan, K. (1969): A numerical method for the study of the circulation of the world ocean. *Journal of Computational Physics*, 4, 347-376.

Carroll, K. P.; McClaran, S. R.; Nelson, E. L.; Barnett, D. M.; Friesen, D. K. and Williams, G. N. (1992): AUV path planning: An A* approach. Proceedings of the *Symposium on AUV Technology* (AUV92), pp. 3-8.

Cox, M.D. (1984). A primitive equation, 3-dimensional model of the ocean. GFDL *Ocean Group Tech. Rep.* N^. 1, 143 pp.

Creed, E.L.; Mudgal, C.; Glenn, S.M.; Schofield, O.M.; Jones, C.P. and Webb, D.C. (2002): Using a fleet of slocum battery gliders in a regional scale coastal ocean observatory, *Oceans '02 MTS/IEEE*, Volume 1, 29-31 Oct. 2002 Page(s):320 – 324

Galea, A. M. (1999): Various methods for obtaining the optimal path for a glider vehicle in shallow water and high currents. *Proceedings of the 11th International Symposium on Unmanned Untethered Submersible Technology.* pp. 150-161.

Garau, B.; Alvarez, A. and Oliver, G. (2005): Path Planning of Autonomous Underwater Vehicles in Current Fields with Complex Spatial Variability: an A* Approach, *Proceedings of the 2005 IEEE International Conference on Robotics and Automation*, pp. 195-199.

Holland, W. R. and McWilliams, J. C. (1987): *Computer modelling in physical oceanography from the global circulation to turbulence*. Physics Today pp. 51-57.

Pacanowski, R. C.; K. Dixon, and A. Rosati (1990): Readme file for GFDL-MOM 1.0, *Geophys*. Fluid Dyn. Lab., Princeton, N. J.

Rio, M-H.; Poulain, P-M.; Pascual, A.; Mauri, E. and Larnicol, G. (2007): A mean dynamic topography of the Mediterranean Sea computed from altimetric data and in-situ measurements. *Journal of Marine Systems*, 65, pp. 484-508

Robinson, A. R.; Arango, H. G.; Warn-Varnas, A.; Leslie, W. G.; Miller, A. J.; Haley, P. L. and Lozano, C. J. (1996): *Real-time regional forecasting*. Modern approaches to data assimilation in ocean modeling, Amsterdam, NL: Elsevier, pp. 377-410.

Ruiz, S.; Pascual, A.; Garau, B.; Faugere, Y.; Alvarez, A. and Tintoré, J. (2008): Mesoscale dynamics of the Balearic front integrating glider and satellite data. J*ournal of Marine Systems.* In press.

Schmidt, H. and Bovio, E. (2000): Underwater vehicle networks for acoustic and oceanographic measurements in the littoral ocean. *Proceedings of the 5th IFAC Conference Manoeuvring and Control of Marine Craft* (MCMC2000) pp. 323-326.

Sugihara, K. and Yuh, J. (1997): GA-based motion planning for underwater robotic vehicle. *Proceedings of the 10th International Symposium on Unmanned Untethered Submersible Technology,* pp. 406-415.

Vasudevan, C. and Ganesan, K. (1996): *Case-based path planning for autonomous underwater vehicles*. Autonomous Robots. pp. 79-89.

Warren, C. W. (1990). A technique for autonomous underwater vehicle route planning. IEEE *Journal of Oceanic. Engineering.* vol. 15, pp. 199-204.

Journal of Maritime Research, Vol. VI. No. II, pp. 23-36, 2009

ISSN: 1697-4840

AN AUTONOMOUS VEHICLE DEVELOPMENT FOR SUBMARINE OBSERVATION

S. Gomariz[1], J. Prat[2], P. Gaya[3] and J. Sole[4]

Received 22 September 2008; received in revised form 29 September 2008; accepted 25 de April 2009

ABSTRACT

This work proposes the development of a low-cost ocean observation vehicle. This vehicle, a hybrid between Autonomous Underwater Vehicles (AUV) and Autonomous Surface Vehicles (ASV) moves on the surface of the sea and makes vertical immersions to obtain profiles of a water column according to a pre-established plan. Its design means production costs are low and efficiency is increased. Also, the vehicle is able to make high resolution space and time measurements simultaneously. GPS navigation allows the platform to move along the surface of the water while a radio-modem provides direct communication links and telemetry. The vehicle measures 1885 mm by 320 mm wide. It weighs 76 kg. It navigates at a speed of 1.5 m/s at 80% at full propulsion power and reaches a maximum depth of 20 m. It is a vehicle of electrical propulsion with an autonomy of 3-5 hours. This work outlines the mechanical and electronic design of the vehicle, as well as considerations for navigational and immersion experiments.

Key words. Autonomous Underwater Vehicle, vertical profiler, computer embedded.

INTRODUCTION

Despite major advances in ocean research by oceanographic ships and anchorages, tests on the marine environment are still insufficient. The limitations of convention-

[1] Titular professor.Universitat Politècnica de Catalunya (spartacus.gomariz@upc.edu), Avda. Victor Balaguer s/n 08800 Vilanova i la Geltrú. Spain. [2] Titular professor. Universitat Politècnica de Catalunya (jordi.prat@upc.edu), Avda. Victor Balaguer s/n 08800 Vilanova i la Geltrú. Spain. [3] Titular professor. Universitat Politècnica de Catalunya (pgaya@eel.upc.edu), Avda. Victor Balaguer s/n. 08800 Vilanova i la Geltrú. Spain. [4] Titular professor. Universitat Politècnica de Catalunya (jsole@em.upc.edu), Av. Victor Balaguer s/n. 08800 Vilanova i la Geltrú. Spain.

al oceanic observation platforms cannot carry out tests in the sea and provide the required space and time measurements. For this reason and with the aid of recent technological advances, the development of new oceanographic observation platforms which are able to carry out high-resolution space and time interdisciplinary measurements simultaneously, have been tested. Observation platforms referred to as Gliders, Autonomous Underwater Vehicles (AUVs) and Autonomous Surface Vehicles (ASVs) have already been designed (Meyrowitz et al, 1996) (Blidberg, D.R, 2001). This project proposes the development of a low-cost oceanic observation vehicle which is a hybrid between the AUVs and ASVs. The vehicle moves along the surface of the sea and makes vertical immersions to obtain vertical profiles of a water column in agreement with a pre-established plan (Dabholkar et al, 2007) (Byron et al, 2007). These two characteristics of the observation platform lower the production costs and increase its efficiency. GPS navigation will allow the platform to move along the surface of the water while a radio-modem will provide direct communication links and telemetry.

MECHANICAL DESIGN OF THE VEHICLE

The design proposed here is a prototype which will have to be modified. The platform design is made up of a support structure on which the steering and propulsion mechanisms are attached. This structure is not watertight, thus allowing us to drill holes wherever required.

A watertight cylindrical module is located inside the support structure. It houses the immersion actuator and the electronics control, as well as the power supply provided by the batteries (Egeskov, 1994).

Support Structure

As figure 1 shows, the support structure is made up of a PVC cylinder, 1.2m in length by 32cm in outer diameter. The simple construction means it is easy to make modifications. The final result is a platform which can house the bulky elements of the vehicle such as the batteries and the immersion actuator in the minimum space possible. The main Seaeye(™) propulsion engine is located at one the end of the support structure (Seaye). This engine, without brushes, runs on a supply voltage of 24V DC and nominal current of 5A, which provides a maximum thrusting of 110N to 950rpm (Dewijs, 2000).

Individual Seabotix(™) engines are located on the sides of the cylinder. These engines have a maximum thrust of 25N at a maximum power of 80W and are powered with 24V DC (Seabotix). When these engines are used, the course of the vehicle can be altered. This solution was favoured instead of a rudder system with a hydraulic cylinder because its construction is simple. (Desset et al, 2005). The engines, located on the sides of the device are attached to the support structure by

means of a stainless steel telescope tube that allows the spindle, located on both of the vehicle's engines, to be altered during testing.

The main engine is attached to the support structure by means of a stainless steel tube and mechanized nylon blocks provide adequate rigidity.

Finally, depth and direction auto-stabilizers are located on the stern once again to ensure stability.

The bow is finished with a carbon fibre hemisphere.

Watertight Module

As figure 1 shows, the watertight module contains the set of immersion equipment, the electronic signal reception modules and engine control, and the power supply batteries.

All these parts are joined to the watertight PVC cylinder by means of a metallic structure. See below.

The watertight module is covered in black nylon. An o-ring and 12 M6 screws guarantee watertightness.

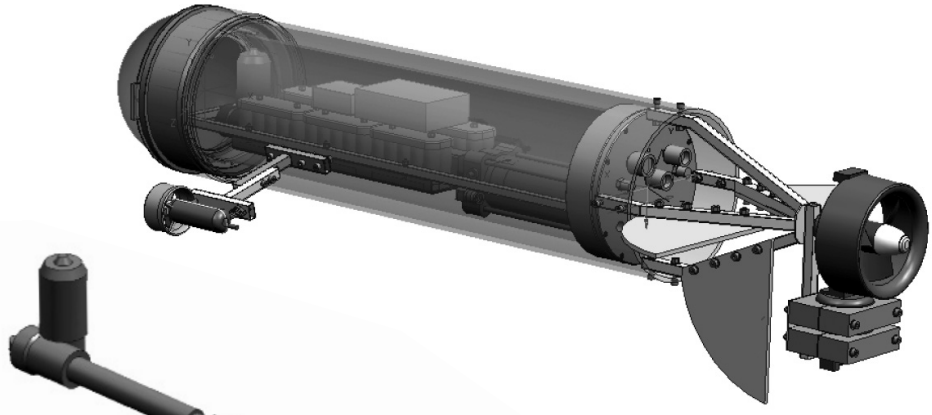

Figure 1. Frame.

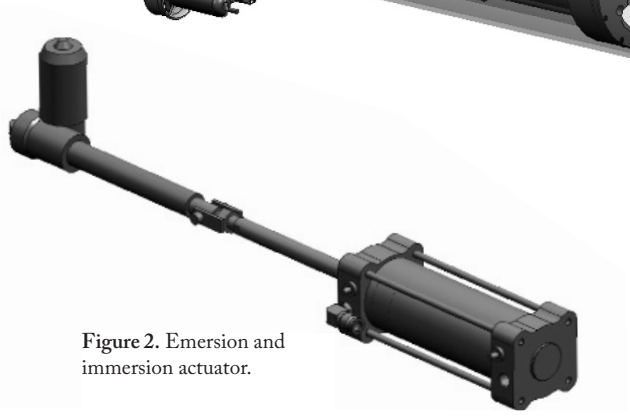

Figure 2. Emersion and immersion actuator.

The design of the emersion and immersion equipment is composed of a commercial pneumatic stainless steel cylinder with a displacement of 1500 cm^3 and a linear electrical actuator which can cover a maximum distance of 200mm and a thrust force of 3KN. See figure 2.

Complete structure of the vehicle.

Figure 3 and figure 4 show the external structure and watertight module of the constructed vehicle, respectively.

It is worth highlighting, that the position of the center of gravity ensures stability in immersion/emersion operations.

The payload works out at 5kg, approximately, on a gross weight of the 76kg platform.

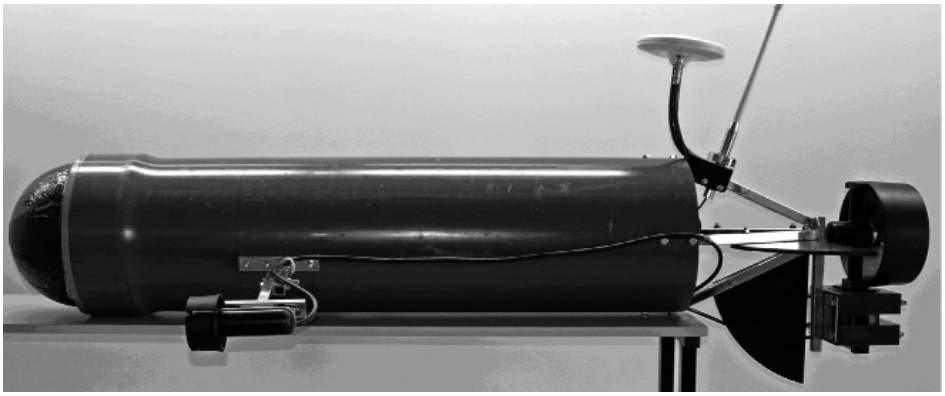

Figure 3. Constructed vehicle.

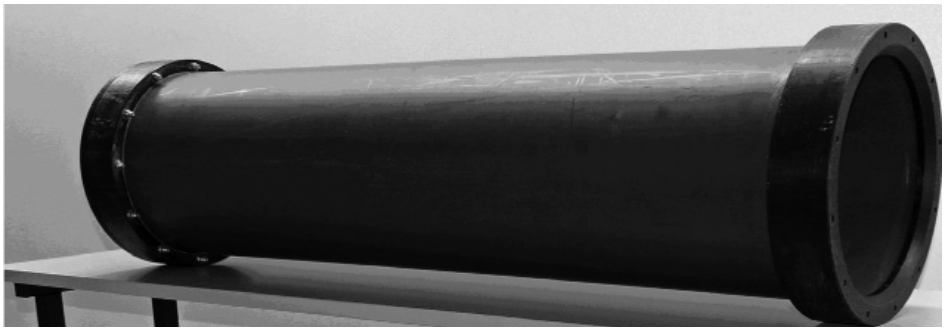

Figure 4. Constructed watertight module

ELECTRONIC DESIGN. CONTROL PHASE

The autonomous navigation control system is made up of an embedded computer and the elements necessary for communication, navigation and propulsion and data acquisition. Safety elements are also included (Desa et al, 2007). In figure 5 the diagram for the autonomous control of the vehicle is described.

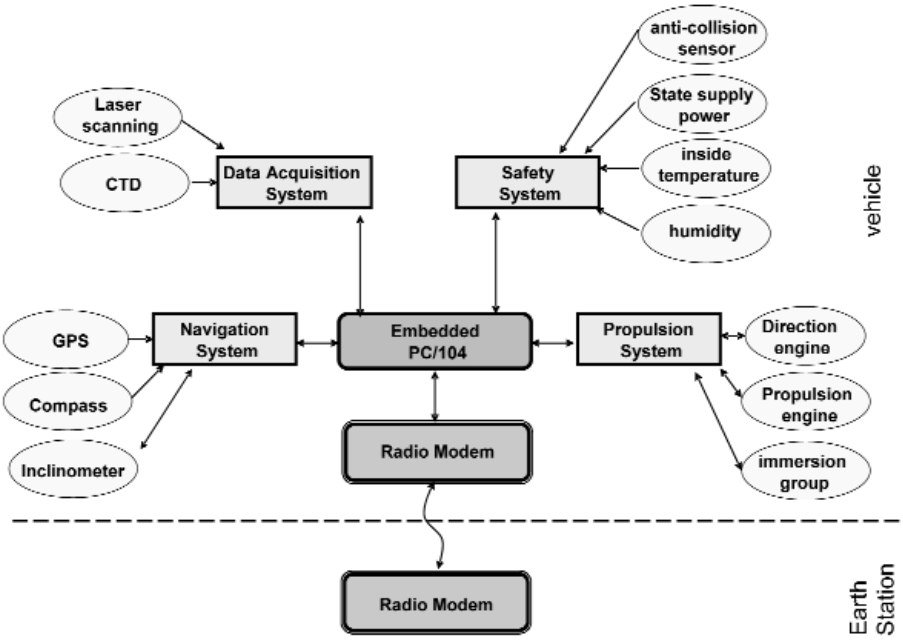

Figure 5. Diagram of the autonomous control system

Communication between the vehicle and the station located on shore is bidirectional and a Farell Instruments(™) industrial modem T-MODC48 has been used. See figure 6. Its features include a data rate of 4800 bps, protocol-transparent and a configurable carrier power of 100mW/5W that allows a maximum range of 10km and +/- 1 ppm stability level from -30ºC to 60ºC. (Farell).

A PC/104 embedded computer (PM-6100 AEWIN) makes up the central control of the vehicle, see figure 7. It has an embedded AMD® Geode™ LX800 CPU up to 500MHz. This is of limited size, weight and power consumption (max 12W). It also has a low heat loss (Aewin). It is managed by a Windows XP operating system stored in a compact flash memory which provides good protection from vibration.

Figura 6. Radio módem T-MODC48.

The propulsion control system is a SSC32 Lynxmotion driver. See figure 8. This transforms the RS232 signal from the PC/104 in a modulated PWM signal that acts on the engine power driv-

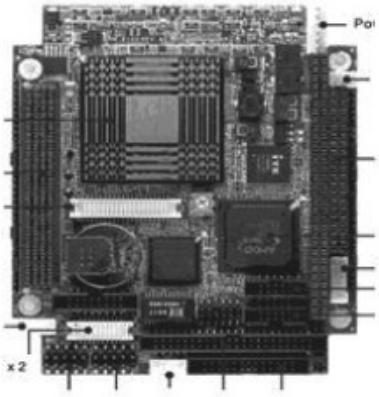

Figure 7. PC/104+ PM-6100

ers. This servo-controller has 32 channels with 1uS-0.09º resolution and 1uS/Second speed. This can work at a velocity of 2400, 9600, 38.4k, 115.2k bauds. (Lynxmotion)

Several power drivers have been developed to adapt the modulated PWM signal received from the SSC32 so that the vehicle's engines can execute the control orders.

Power steering driver. The steering orders received are transferred to individual adjustable-speed drives that control the engines responsible for moving to the left and right. These adjustable-speed drives incorporate the power electronics necessary to adapt to the engines changing requirements.

Power driver of immersion/emersion. The immersion/emersion orders are applied to a control circuit that acts on the engine-cylinder equipment.

This control circuit incorporates a microcontroller PIC 16F88 that interprets the signal received and consequently executes the stop/immersion/emersion orders on the electrical engine of the immersion/emersion equipment.

The pneumatic cylinder incorporates individual magnetic limit switches which can block the electric engine's actuators and also act as a security system limiting the total displacement of the cylinder.

Power driver for propulsion. The propulsion orders are processed on a microcontroller PIC16F873, which provides the control signal via RS485 to the propulsion engine. This engine includes the control and power electronics necessary to decode the orders received via RS485.

Figure 8. Controlled SSC32.

The navigation system is a digital compass and a three-axis inclinometer, PNI TCM-2.6, see figure 9a. The TCM 2.6 is a 3-axis tilt-compensated compass-heading (also known as azimuth, yaw, or bearing angle) module with electronic gimballing to provide accurate heading, pitch, and roll measurements over a ±80˚ tilt range. This high-precision (heading accuracy 0.8˚), high-resolution (Compass heading 0.1˚) navigation system runs on low power (< 20 mA typical draw) (PNI).

The navigation system also has a global positioning system GPS, Magellan DG14™, which provides the precise location of the vehicle during a mission, see figure 9b.

The DG14™ is a sub-meter GPS+Beacon+SBAS receiver. It incorporates signals from Satellite Based Augmentation Systems (SBAS), such as WAAS, EGNOS & MSAS, or an embedded beacon receiver, to provide sub-meters differential positioning. DG14 can emit SBAS ranging, ephemeris and differential corrections through the serial port. Although DG14 offers three standard RS232 ports, it is also capable of single port operation.

It can provide up to 20-Hz precise three-dimensional positions and raw data for real-time guidance and navigation (Magellan).

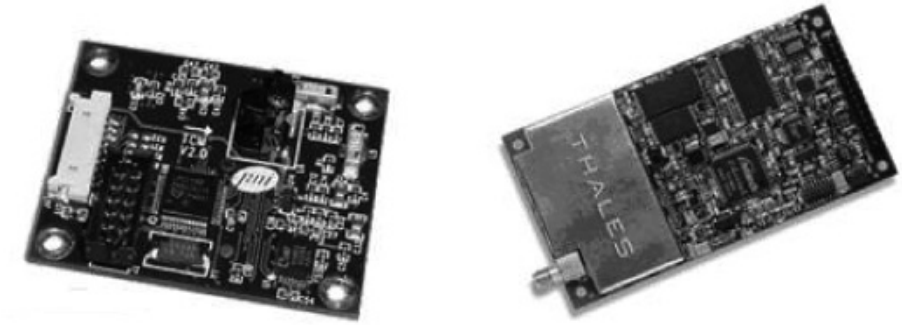

Figure 9. Navigation System. (a) PNI TCM-2.6 (b) DGPS, DG14

All this equipment is assembled inside two PVC boxes, as seen in Figure 10. One box houses the PC/104 with the navigation system and the other is equipped with the propulsion system. For both boxes a power bus which uses 24V, 12V and 5V has been installed. These voltages are generated from 6 Ni-Cd batteries, 24V nominal voltage and 21AH capacity, through a power stage implemented using

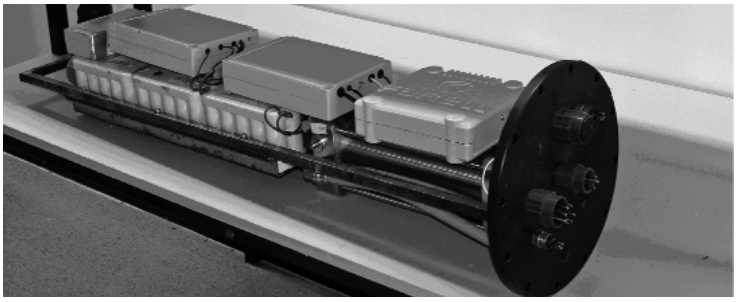

Figure 10. Inside layout of the watertight module

switched dc-dc converters, located in a separate box.

Safety elements for the vehicle and a data acquisition system will be developed in the second stage of the project. Figure 10 shows the layout of all the elements in the watertight module.

SOFTWARE DESIGN. TRACKING STATION

The vehicle needs user interaction in terms of control parameters, operational verification and data acquisition and downloading. A program has been designed which reads/writes the data received/sent by radio-modem, checks for transmission errors and represents the information graphically. Figure 11 shows the graphical user interface (GUI). The GUI has a two-page front-end. The main page incorporates direction, roll and pitch angles indicators and also an artificial horizon to view the data transmitted by the compass / inclinometer. This page also includes a series of Scrollbars and buttons to control the vehicle's engine. The second page presents the user with each of the parameters that the GPS receiver provides using TextBox and a variety of geo-maps to locate the position of the vehicle.

EXPERIMENTAL TESTS

When the vehicle was initially placed in the water, balance had to be adjusted. It was obtained by incorporating a 3.6kg ballast in the prow and a 1.5kg push in the stern. This was sufficient to allow the navigation and immersion tests to begin. In the navigation test the speed was approximately 1.5m/s with the control of the propulsion engine at 80% at full power. By using the lateral engines at full power and decreasing the propulsion of the first engine the trajectory, variation is obtained very easily. The immersion tests were carried out with complete normality acting on the engine-cylinder equipment.

CONCLUSIONS

The result so far is a robust platform which is relatively small and light, factors which facilitate its manageability and operability. To sum up we can say that a low-cost oceanic observation platform has been developed which is able to navigate on the surface of the sea and make vertical immersions to obtain water column profiles.

ACKNOWLEDGMENT

This work has been funded by the Spanish Ministry of Education and Science and the European Union (FEDER), project nº: CTM2006-12072/MAR.

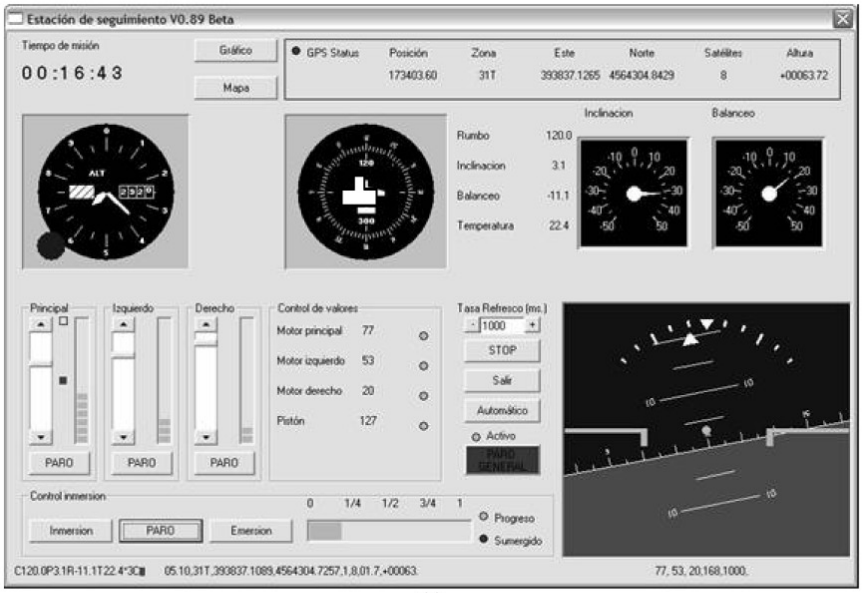

(a)

(b)

Figure 11. Tracking Station (a) GUI Main Page (b) Geo-Map.

REFERENCES

Aewin http://www.aewin.com.tw/main/product_info.aspx?fid=2&sid=3&sname=Embedded+Board&pname=PM-6100&tname=PC%2F104+CPU+Module&fname=&pid=27

Byron, J. and Tyce, R. (2007) Designing a Vertical / Horizontal AUV for Deep Ocean Sampling. *Proceedings of MTS/IEEE Conference and Exhibition Oceans* 2007. Sept. 29 2007-Oct. 4. Vancouver, Canada pp. 1 - 10

Blidberg, D. R. (2001) The development of Autonomous Underwater Vehicles (AUV); A brief summary. *Autonomous Undersea Systems Institute publications (AUSI), ICRA, May, Seoul, Korea,*.

Dabholkar, N., Desa, E., Afzulpurkar, S., Madhan, R., Mascarenhas, A.A.M.Q., Navelkar, G., Maurya, P.K., Prabhudesai, S., Nagvekar, S., Martins, H., Sawkar, G., Fernandes, P. and Manoj, K.K. (2007) Development of an autonomous vertical profiler for oceanographic studies, *Proceedings of the International Symposium on Ocean Electronics (SYMPOL-2007),* 11-14 December, Cochin, India, pp. 250-256.

Desa, E., Maurya, P.K.,Pereira, A., Pascoal, A.M., Prabhudesai, R.G., Mascarenhas, A., Madhan, R., Matondkar, S.G.P., Navelkar, G., Prabhudesai, S. and Afzulpurkar, S. (2007) Small Autonomous Surface Vehicle for Ocean Color Remote Sensing. *IEEE Journal of Oceanic Engineering,* April, pp. 353 – 364 Vol. 32, Issue 2.

Desset, S., Damus, R., Hover, F., Morash, J. and Polidoro, V. (2005) Closer to deep underwater science with ODYSSEY IV class hovering autonomous underwater vehicle (HAUV). *Proceedings of MTS/IEEE Conference and Exhibition Oceans 2005 – Europe*, 20-23 June, Brest, France, pp. 758-762 Vol.2

DeWijs, B. (2000) AUV/ROV propulsion thrusters. *Proceedings of MTS/IEEE Conference and Exhibition OCEANS 2000.* 11-14 September, Providence, Rhode Island, U.S.A, pp 173 - 176 vol.1

Egeskov, P., Bjerrum, A., Pascoal, A. Silvestre, C., Aage, C. and Wagner Smith, L. (1994) Design, construction and hidrodinamic testing of the AUV MARIUS. *Proceedings of the AUV 94*, Cambridge, Massachusetts, USA.

Farell, http://www.farell-i.com/farell/eng/productos.php

Lynxmotion, http://www.lynxmotion.com/Product.aspx?productID=395&CategoryID=52

Magellan, http://pro.magellangps.com/en/products/product.asp?PRODID=174

Meyrowitz, A.L.; Blidberg, D.R. and Michelson, R.C. (1996) Autonomous vehicles

Proceedings of the IEEE. Volume 84, Issue 8, pp 1147 – 1164

PNI, http://www.pnicorp.com/products/all/tcm-2-6

Seabotix, http://seabotix.com

Seaeye, http://seaeye.com/thrusters.html

DESARROLLO DE UN VEHÍCULO AUTÓNOMO PARA OBSERVACIÓN SUBMARINA

RESUMEN

En este proyecto se desarrolla un vehículo de observación oceánica de bajo coste, híbrido entre los *Autonomous Underwater Vehicles (AUV) y los Autonomous Surface Vehicles (ASV),* esto es, que se traslada por la superficie del mar y realiza inmersiones verticales para la obtención de perfiles de la columna de agua de acuerdo con un plan previamente establecido. Estas dos características de la plataforma de observación propuesta, abaratan los costes de producción e incrementarían su eficiencia. El desplazamiento superficial de la plataforma permite la navegación mediante GPS y la comunicación directa y telemetría mediante radiomódem. Las dimensiones del vehículo son 1.885 mm de longitud y 320 de diámetro exterior, y posee un peso de 76 kg. En las pruebas de navegación alcanzó una velocidad de 1.5 m/s a un 80% de potencia de propulsión y una profundidad máxima de 20 m. El vehículo posee una propulsión eléctrica con una autonomía de 3-5 horas.

DISEÑO MECÁNICO DEL VEHÍCULO

Teniendo en cuenta que el diseño actual corresponde a un primer prototipo sobre el que, necesariamente, deberán realizarse sucesivas modificaciones, se propone un diseño mecánico constituido por una estructura de soporte sobre la que se acoplarán los motores de dirección y propulsión. Esta estructura no es estanca, lo cual va a permitir realizar cualquier tipo de mecanizado. En el interior de la estructura de soporte se acopla un módulo cilíndrico estanco que contiene el actuador de inmersión y la electrónica de control, así como las baterías de alimentación.

Tal como muestra la figura 1, la estructura de soporte se compone de un cilindro de PVC de 1.2 m de longitud y 32 cm de diámetro exterior. En uno de los extremos de la estructura de soporte se acopla un motor principal de propulsión de la empresa Seaeye. Este es un motor sin escobillas con tensión de alimentación de 24V DC y corriente nominal de 5A. Proporciona un empuje máximo de 110N a 950 rpm. En los laterales del cilindro se acoplan sendos motores de la empresa Seabotix con un empuje máximo de 25N a una potencia máxima de 80 W alimentados también a 24V DC. Dichos motores permiten modificar la dirección de navegación.

Tal como muestra la figura 1, el módulo estanco contiene el grupo de inmersión y emersión, que se ha diseñado a partir de un cilindro neumático comercial de acero inoxidable con desplazamiento de 1.500 cm^3 y un actuador eléctrico lineal con una carrera de 200 mm y un empuje de 3KN de fuerza, alimentado a 24V. Ver figura 2.

En las figuras 3 y 4 se puede observar el vehículo construido.

DISEÑO ELECTRÓNICO. FASE DE CONTROL

Se ha diseñado y desarrollado un sistema de control, basado en un ordenador embebido PC/104+ PM-6100 de AEWIN, que permite una navegación autónoma del vehículo. En la figura 5 se describe el diagrama de bloques del control autónomo.

La comunicación entre el vehículo y la estación terrestre es bidireccional y se ha realizado a través de un radio módem industrial T-MOD400 de la empresa Farell Instruments. La figura 6 muestra una imagen del equipo que posee una velocidad de transmisión de datos 4.800 bps, una potencia configurable de 5 W que permite un largo alcance (10 Km) y una estabilidad ±1 ppm desde -30ºC a +60ºC.

El control central del vehículo se ha encargado a un ordenador embebido PC/104+ PM-6100 de AEWIN, cuyas dimensiones y consumo son reducidos. Además, posee una baja disipación de calor que favorece su ubicación en el interior del módulo estanco. Está gestionado por un sistema operativo Windows XP almacenado en una memoria compact Flash, que proporciona mayor fiabilidad frente a vibraciones que un disco duro. La figura 7 proporciona una imagen del equipo.

El sistema de de control de la propulsión lo constituye un controlador SSCC32 de Lynxmotion que transforma la señal RS232 procedente del PC/104 en una señal modulada PWM que actúa sobre la etapa de potencia de los motores. Este controlador posee 32 canales con salida desde 0,50 ms hasta 2,50 ms y con una resolución de 1uS. Puede trabajar a velocidades 2.400, 9.600, 38.400 y 115.200 baudios. En la figura 11 se puede observar el controlador de servos. Para la etapa de potencia se han desarrollado diversos circuitos que permiten a los motores ejecutar las órdenes recibidas.

El sistema de navegación lo constituye un compás digital con un inclinómetro de tres ejes, PNI TCM-2.6, que proporciona el rumbo y los ángulos de cabeceo, guiñada y avance (ver figura 9). El rango de inclinación es de ±80º con una precisión de 0.8º y una resolución 0.1º. También se ha incluido un sistema de posicionamiento global GPS, DG14 de Magellan (ver figura 9), que proporciona una ubicación precisa del vehículo durante la misión.

Todos estos equipos se han montado en el interior de dos cajas de PVC, tal como se dispone en la figura 10. Por ambas cajas circula un bus de alimentación con 24V, 12V y 5 V. Estas tensiones se generan desde las baterías de Ni-Cd, de tensión nominal 24V y 21AH de capacidad, mediante una etapa de potencia implementada mediante conversores conmutados dc-dc, ubicados en una caja independiente.

DISEÑO SOFTWARE. ESTACIÓN DE SEGUIMIENTO

Para disponer de una buena operatividad con el vehículo se ha creado un software que permite leer/enviar datos por el radio-modem, gestionar los eventuales errores de transmisión y presentar gráficamente estos datos. Se incorpora la posibilidad de realizar un control manual del vehículo desde la estación de seguimiento.

RESULTADOS EXPERIMENTALES

La primera vez que se introdujo el vehículo en el agua se procedió a ajustar su perfecto equilibrado. Se consiguió incorporando un lastre en proa de 3.6 kg y un empuje en popa de 1.5 kg. Esta situación permitió el inicio de las pruebas de navegación, de direccionamiento y de inmersión.

En la prueba de navegación se obtuvo una velocidad aproximada de 1,5 m/s con el control del motor de propulsión al 80%. La variación de rumbo se consigue con gran facilidad utilizando los motores laterales a plena potencia y decrementando la potencia del motor de propulsión. La operación de inmersión/emersión se realizó con toda normalidad actuando sobre el grupo motor-cilindro.

CONCLUSIONES

Como resultado, actualmente, se dispone de un vehículo de unas dimensiones y peso no excesivo que permiten una buena maniobrabilidad y operatividad. Como valoración final se puede decir que se ha desarrollado un vehículo para la observación oceánica de bajo coste que permite navegar por la superficie del mar y realizar inmersiones verticales con el objetivo de obtener datos de una columna de agua.

JMR

Journal of Maritime Research, Vol. VI. No. II, pp. 37-52, 2009

ISSN: 1697-4840

LOW-COST AUTONOMOUS UNDERWATER VEHICLE FOR UNDERWATER ACOUSTIC INSPECTIONS

O. Calvo[1*], A. Sousa[2*], J. Bibiloni[3*], H. Curti[4*], G. Acosta[5] and A. Rozenfeld[6]

Received 23 September 2008; received in revised form 30 September 2008; accepted 5 May 2009

Abstract

The design considerations of a low-cost Autonomous Underwater Vehicle (AUV) are presented in this article. Periodic surveys are needed in the preventive maintenance of submarine structures of offshore industries. The advantages of performing them with AUVs instead of Remote Operated Vehicles (ROV) or Towed Unmanned Devices are the lower costs involved and a better data quality in the inspection missions. Through EU funded projects (AUVI and Autotracker), and Spanish funded project IOGECS, the construction of a low-cost prototype for depths of 100m AUV was initiated. Previous results and design considerations and proposed solutions, as well as a description of the hardware employed, the sensors in the payload, and the mission replanning, are described in this work.

Keywords: Autonomous Underwater Vehicles (AUV). Trajectory planning. Knowledge-based systems. Underwater pipeline inspection.

INTRODUCTION

One of the most outstanding applications of autonomous underwater vehicles (AUV) is the inspection of submerged structures for maintenance purposes. These

[1] Professor. University of the Balearic Islands (oscar.calvo@Uib.es), Physics Department, Palma de Mallorca, Spain. [2] PhD Student, University of the Balearic Islands (andre.sousa@uib.es), Physics Department, Palma de Mallorca, Spain. [3] Graduate student, University of the Balearic Islands (jaume.corro@gmail.com), Palma de Mallorca Spain. [4] PhD Student. University of the Balearic Islands (hcurti@fio.unicen.edu.ar), Palma de Mallorca, Spain. [*] GTE Group, Physics Dept., Universitat de les Illes Balears-UIB, Spain. [5] Professor. Universidad Nacional del Centro (gerardo.acosta@ieee.org), CONICET and INTELYMEC Group, Electromechanical Dept., Engineering Faculty, Universidad Nac. del Centro Prov. de Buenos Aires-UNCPBA, Argentina. [6] Researcher. Universiti o the Balearic Islands IFISC (alex@ifisc.uib.es), Palma de Mallorca, IMEDEA-UIB, Spain.

inspections, performed to avoid infrastructure damage and to preserve the ecosystem, are usually done with remotely operated vehicles. This approach has two basic drawbacks when compared to untethered vehicles: the low quality of acquired data due to the umbilical perturbation worsens with depth, and the operational costs of mother ship and its crew.

Figure 1a. Geosub AUV ready for trials.

During the last few years great advances had been made in inspections using AUVs. As an example, the Twin-burger 2 [Balasuriya et al, 1998], guided by camera images presented some interesting results. But, offshore oil exploration is moving into deep waters, since oil reservoirs near the cost are starting to dry. In deep and opaque waters, video becomes less practical for AUV inspections due to the lightening requirements; power needs and light scattering effects. In these cases it is preferable to use sonar or a fusion of many sensors as described in [Tena Ruiz et al, 2006].

The first commercial AUV capable of locating and following a pipeline with acoustic sensor was developed in the framework of an EU funded project: AUTOTRACKER (GRD1-2000-25150) [Acosta et al, 2005]; [Curti et al, 2005], in which the authors participated, along with oil and cable companies like British Petroleum (BP), Alcatel, Seas Power and Subsea7, and with a team of universities such as then UIB, Heriot Watt University (HWU) and the National University of Athenes, (NTUA). The project consisted on modifying a commercial AUV (Geosub by Subsea7) (figure 1a) with the purpose of developing autonomous searching, locating and tracking of submerged oil pipes, partially buried or exposed, using acoustic and magnetic sensors. The GTE at UIB developed an Expert System that was responsible for the real time path planning and re-planning based on the information of the sensor. We also built a HIL simulator that assisted in the development of the rules and to try all possible situations. The vehicle utilized was the Geosub AUV (Figure 1), designed to operate in water depths to 3000 m and with mission times of between 30 and 60 hours, depending upon payload configuration. The vehicle measures 6.82 m long and 900mm in diameter, and weights 2400 kg. This vehicle is an ideal stable platform, operating with a comprehensive range of survey sensors close to the seabed. Experimental trials were performed at the North Sea in Scotland (Orkney

Islands) in which the UIB participated. A trajectory of a search and locate of the real pipe is shown in figure 1b. Companies are now exploiting the technology developed. Driven by these successes, we applied to the EU and the Spanish government for further funding and they were both awarded as a Marie Courie Fellowship (6PM IIF2006 Ref. 3027) and by the former Spanish Ministry of Science and Education under the Transport National Program (TRA2006-13318), in collaboration with the Ocean System Lab at HWU. We decided then to build a cheaper prototype, the AUVI vehicle, which would navigate mainly in shallow waters but allowing us to test computational intelligence algorithms for planning and replanning of vehicle's trajectories and tasks.

AUVI PROTOTYPE DESIGNED FOR PIPELINE SEARCH AND INSPECTION

Working hypotheses

The central working hypothesis was to design a low cost and easy to deploy AUV, that could be used as a testbed for different control algorithms and pipeline detection routines. It should be software compatible with the previous platform used in the Autotracker project, where most of the pipe tracker was developed, and it should run under the OceanShell environment developed jointly with the researchers from Heriot Watt University [Acosta et al, 2005] [Evans, 2003]. The same software that runs on the vehicle can run on a real time simulator previously developed by UIB [Curti et al, 2005] (Hardware in the Loop). Even though the Geosub AUV is an ideal platform for commercial autonomous inspections, being capable of diving at great depths with great accuracy and fairly good autonomy the operational costs of the trials were too expensive for a University budget. Then, the idea of having a shallow water AUV to test all the algorithms was very appealing, to minimize the costs of each sea trial. A light AUV capable of carrying the necessary sensors for specific missions, with a plug and play feature would be ideal to validate the algorithms product of our research. It should be backwards compatible with the software that runs on the full depth AUV.

Mechanical description

The AUV was built using two torpedoes with a diameter of 225 mm. Each of the cylinders has at one end a half sphere with 225 mm of radius, it's the surface attack, and the opposite end is shaped like a cone with 225 m on your biggest diameter and 85 mm on your smallest one. The two bodies matching the structure of the vehicle are linked with metal tubes keeping at a distance of 430 mm between the centers of the cylinder.

The current design of the vehicle was based as a strategy to increase the passive stability and to optimize the torque on the thrusters, resulting in better navigation control given the interaction of the vehicle with the environment

Prototype AUVI GTE-UIB	
Length	78.74 cm
Width	81 cm
Max depth	52 meters
Weight without batteries	16.5 kg
Weigth with batteries	39.5 kg
Recharging time	4 to 6 horas
Batteries	Sealed lead GEL
Capacity	6 x 12v 33 AH
Autonomy	75 to 150 minutes
Speed	1 a 2 m/s
Motor thrust	2x13.64 kg (horiz)
Motor Type	4 12V DC motors
Comunicaciones	Radiomodem 115 Kbps/WiFi
Positioning	GP, dead reckoning, compass and Accelerometer
Manual Control	Joystick via UHF
CPU sensores	dsPic
CPU control Naveg.	Linux PC104
Distance to bottom	AUTOHELP ST30 (NMEA)
Extra payload Payload sonar Depth sensor	15 kg Tritech SeaKing Duck PTX 1400

Tabla I. Main Specs of the AUVI.

Hardware Architecture

Two main processor boards compose the AUV hardware: a low level and a high level electronics. The low level electronics is based on an Ingenia microcontroller board: the iCm4011 board, that uses a dsPIC 30F4011 as main processor. This board provides I^2C and RS232 interfaces to communicate with sensors and high level CPU. The high level board is an intel X86 single board computer running LINUX made by Compulab, a 5Watts small footprint PC. This is where most of the planning and controlling software resides.

The microcontroller board gets the position either from the GPS when surfaced, or from an accelerometer, integrating both x and y readings. The GPS sends its data using RS232 streams following NMEA format. The accelerometer is based on the Analog Devices ADXL 202, dual axis accelerometer. This inexpensive device measures accelerations with a full-scale range of ±g. The outputs are analog voltages or digital signals whose duty cycles (ratio of pulse width to period) are proportional to the acceleration. The duty cycle outputs can be directly measured by the microprocessor. The MBE sonar (Tritech Seaking) converts it readings into RS232 streams following proprietary data format. The Obstacle avoiding sonar, an Autohelm ST30 depth finder send measures acoustic echoes to the seabed and send it to the microprocessor using Seatalk protocol, (NMEA) by RS422 electrical signals that can be easily turn into an RS232 signal. The microcontroller communicates with the Linux host by USB. The digital compass, a CMPS03 robotics board, based on the Philips KMZ51 magnetic field sensor, provides the AUV orientation with respect to earth magnetic field. This device provides a PWM signal with the positive width of the pulse representing the angle. It interfaces directly with the dsPIC. The vertical propellers are attached to DC motors controlled by an MD22 - 50V 5A Dual H-

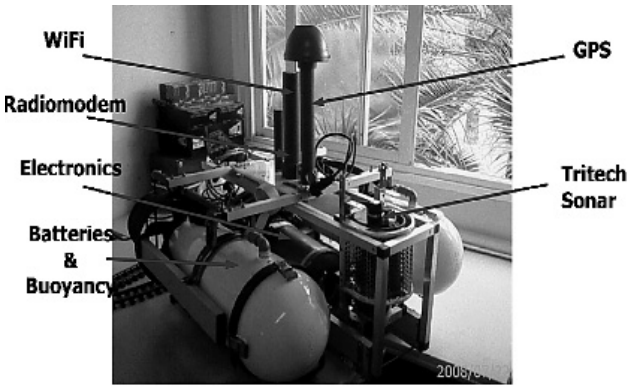

Figure 2. Experimental prototype.

Bridge made by Robot Electronics. The MD22 controller accepts I2C among the possible control signals. The two horizontal thrusters are driven by MD03 motor controllers, that were modified to accept direct control of the PWM signals from the dsPIC. All signals are opto-coupled for noise immunity. Isolation amplifiers are also used to measure motor speed and battery charge. An alarm circuit prevents water leaks. The electronics resides in a steel high pressure hull. Batteries are stored inside the torpedoes. A picture of the prototype is shown in figure 2 and a block diagram of the electronics can be observed in figure 3.

Software development and runtime environments

The central idea of this development was to employ the same environment for software development than for runtime. Also, special emphasis was placed in keeping backward/forward compatibility between the commercial AUV with the shallow water prototype. A modular philosophy was used in the design and development of the small AUV, re-using many modules previously developed and tested in other applications. This software architecture, running on a Debian Linux CPU, is based on communications messages between modules implemented using the UDP layer. The system is divided in modules specialized in a particular task. The software is based on messages going from sensors to actuators. The pipe is detected with acoustic, optical or magnetic sensors. Positioning data obtained by GPS, INS or DVL are fused in the sensor fusion module to provide accurate position of the pipe and vehicle. This information is used by the Dynamic Mission Planner that decides the trajectory to follow. That trajectory is verified against the exclusion zones and probable obstacles detected by the Obstacle Avoidance Sonar (OAS) and modified accordingly before is sent to the path planner. The path planner also receives information from a Static Mission planner, that could take control at any time modifying the final trajectory (i.e. safety reasons, beginning of mission, abort, etc). Finally the actual command is sent to the Autopilot that controls thrusters, rudders and buoyancy.

The simulation environment could communicate with the vehicle through the serial port, using an adaptor between the NMEA protocol and the proprietary communication protocol among modules. In this way, once the software is operative, the

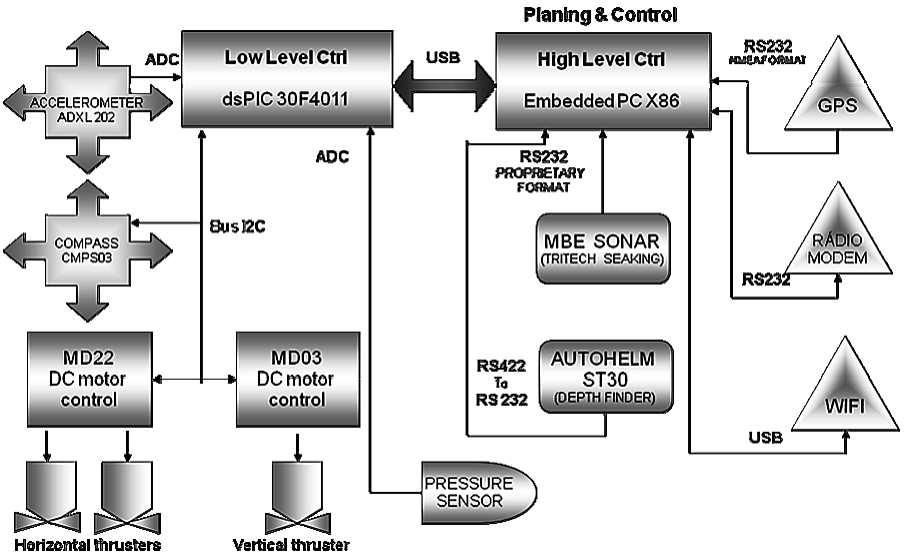

Figure 3. AUVI Electronics.

simulator is easily and straightforward replaced by the real hardware prototype. The adapted architecture for this prototype is shown in Figure 4.

The dynamic Mission Planner (DMP) [Acosta et al, 2005] and the Obstacle Avoidance Software (OAS) are in cascade. Thus, if the OAS does not detect any object through the forward-looking sonar, its output will be simply the desired trajectory from the DMP. On the contrary, if an obstacle is detected, the OAS changes the necessary waypoints in the trajectory provided by the DMP.

The tracking system employs a TriTech Seaking imaging sonar. For obstacle avoidance we replaced the multi-beam sonar by a low cost ST-30 sonar. In the first dry trials a Garmin GPS and an integrated compass were used to acquire the 2D position (x,y) and the yaw y, respectively.

As regards as the observer module in Figure 4, it simply listens to the position messages broadcasts and shows the vehicle's trajectory on the screen. The human machine interface is also employed to set the mission settings and start the simulation. A Graphical User Interface was built and it is shown in figure 5. UDP messages between threads are shown in the interface. This is a useful feature for debugging or to assist the operator when the AUV navigates on surface and radio link is available. The general architecture of an AUV used for pipe detection works with the dataflow going from sensors to actuators. The pipe is detected with acoustic, optical or and magnetic sensors. Positioning data obtained by GPS, INS or DVL are fused in the sensor fusion module to provide accurate position of the pipe and vehicle. This information is used by the Dynamic Mission Planner that decides the trajectory to

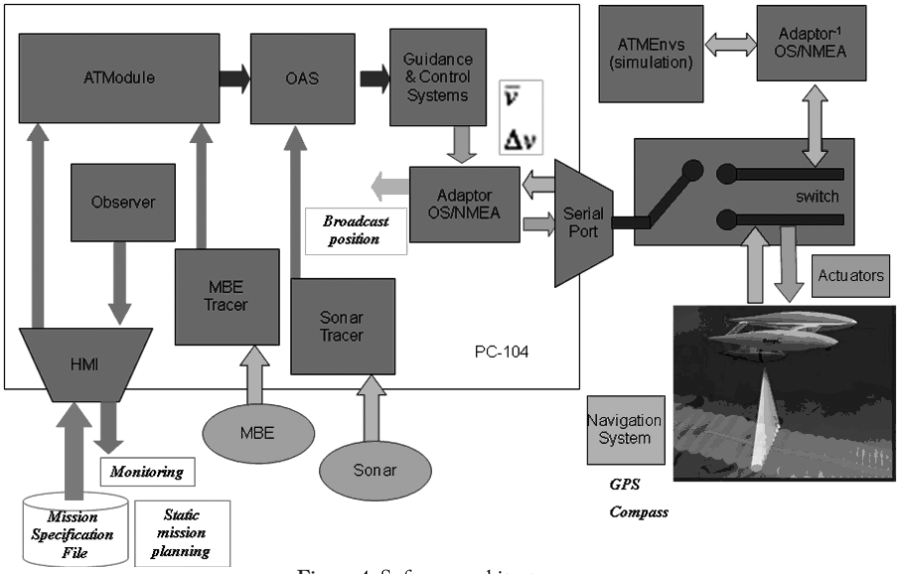

Figure 4. Software architecture.

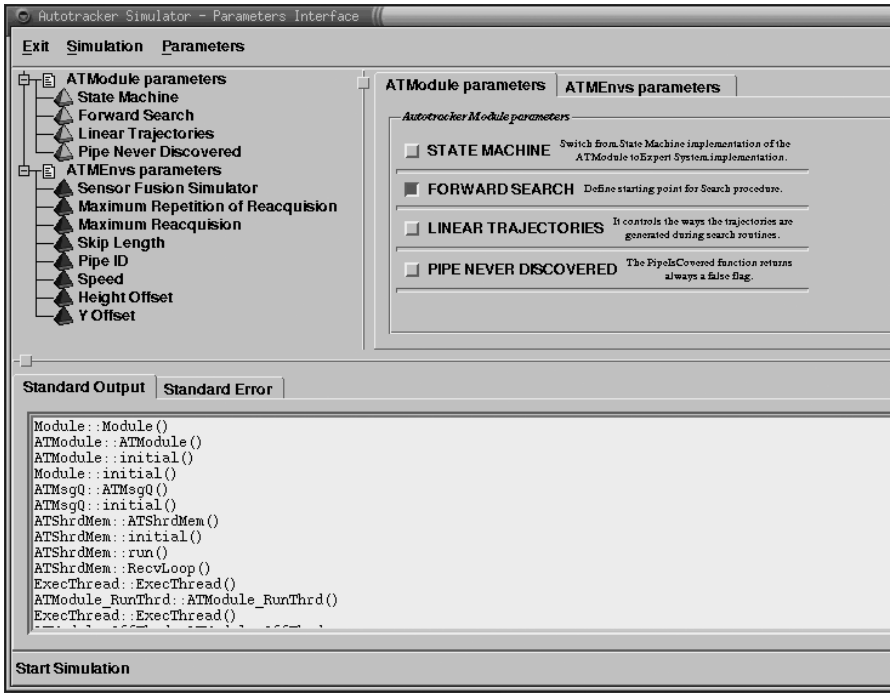

Figure 5. Graphical User Interface for mission planning.

follow. That trajectory is verified against the exclusion zones and probable obstacles detected by the Obstacle Avoidance Sonar (OAS) and modified accordingly before is sent to the path planner.

The path planner also receives information from a Static Mission planner that could take control at any time modifying the final trajectory (i.e. safety reasons, beginning of mission, abort, etc). Finally the actual command is sent to the Autopilot that controls thrusters, rudders and buoyancy.

Dynamic path Planning and re-planning

The dynamic path planner (DMP) must provide the desired vehicle trajectory formed by a series of waypoints. New waypoints are decided based on pipe estimates coming from the Sensors and different situations. The DMP software contains built-in reasoning to mimic human surveyors decisions. Its switches from different states: find/track/skip/reacquire the target or abort the mission. The software controls the AUV to descend, acquire the pipe/cable, follow it at a given offset, speed, .etc, reacquire. Two different mission planners were built: a state based and an Expert system based. The State machine approach is basic and simple what makes it very robust. On the other hand the Expert System based is more flexible, expandable and incorporates the ROV operator's knowledge in the form of rules.

State Machine path planning

The state machine implementation can be seen in figure 6. The vehicle is dropped in the water and navigates towards known coordinates where search operation will begin. The AUV starts the search navigating in zig-zag within a corridor known from legacy data. If the pipe is found it will track it with its sensor. If the pipe is lost it will search it again in the same area or in a different area after skipping a zone. This process can be repeated a programmable number of iterations, defined in the mission planning.

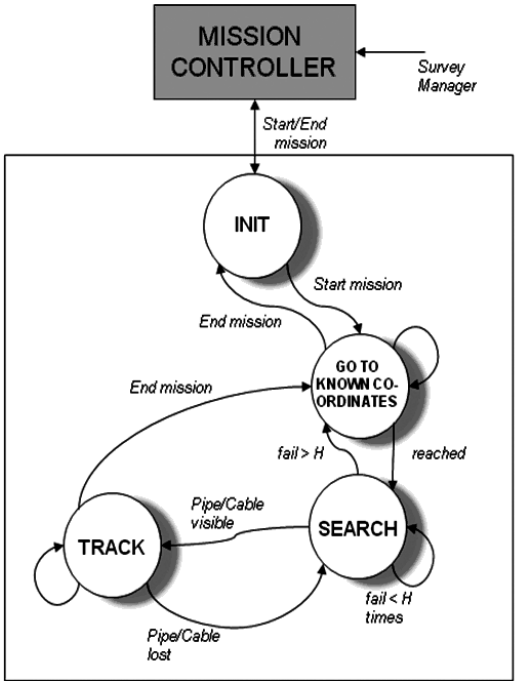

Figure 6. State Machine approach.

Expert System based dynamic mission planner (DMP)

When performing an inspection, many situations might come up (like the sudden appearance of a fishing net, a complex pattern of more than one pipeline over the seabed, or a detour due to obstacle detection, and many others) in which the DMP should exhibit an "intelligent" behavior. To cope with these real situations in the marine world, we resorted to the experience and skills of ROV operators. A little part of their knowledge was elicited and codified in the form of a real time expert system. This expert system, named EN4AUV (Expert Navigator for Autonomous Underwater Vehicles) [Acosta et al, 2006], was constructed using CLIPS, a C based shell. Its main feature is to assess a current situation to act accordingly, in a clearly data driven/reactive behavior. Thus, EN4AUV is a reactive expert system, taking the proper action for every different situation, and considering the pipeline/cable status, the type of survey, the different mission settings, and others. These situations were coded as possible scenarios, in about fifty rules, like the one presented in Figure 4. As the knowledge about different situations increases, the knowledge base (KB) describing new scenarios can be completed and updated, yielding an incremental KB growth. Each scenario triggers different searching or tracking strategies, which are then subtasks with their own features. Scenarios are based mainly on two ideas: the survey types and the tracking states. The type of survey is defined a priori in the SMP, to establish the number of pipelines/cables to be tracked, the navigation depth, and other mission features. The other basic component of the scenario determination is the tracking state that changes when the SFM updates its sensors. From this, the EN4AUV may decide the status of the pipeline/cable (if buried, exposed, intermittent or freespan) and how is the AUV as regards as the pipeline/cable (if avoiding an obstacle, with the object under study considered as found or lost, or returning to a previous known position). Once scenarios are established, a typical situation assessment task, EN4AUV must output a desired trajectory or must decide a pipe/cable reacquisition. To yield a desired trajectory, the actions are organized in a set of few simple subtasks: findstart, search, back to start, skip, and track. Then the final trajectory of the AUV is built by one of these subtasks, or by a concatenation of them.

The Knowledge-Base

Such expert system, named EN4AUV (Expert Navigator for Autonomous Underwater Vehicles), was built using CLIPS, a C based shell [Giarratano, 2002]. The classical steps followed were: (a) problem identification, (b) conceptualization, (c) formalization, (d) implementation, and (e) evaluation. As it is well known, these phases are progressive and there is a dynamic feedback among them during system development.

The problem to be solved by the Expert System is to generate the vehicle's trajectory, based on the position coordinates (x, y, z) provided by a sensor's module, and

a confidence in the measurement of such co-ordinates, called certainty error. The EN4AUV then proposes a desired trajectory, formed by four points to be reached and surpassed by the submarine (waypoints). This desired trajectory is in global co-ordinates indicating latitude, longitude and altitude. Then EN4AUV is clearly a reactive expert system, behaving according to the situation, taking into account, for instance, the pipeline status, the type of survey, the different mission settings, and others. The concept of scenario was used to classify different situations. Examples of scenarios developed for the sea trials were the following:

Scenarios

A scenario is defined as a set of input variables that describe a situation. The AUV shall react in different ways from one scenario to another. Through data abstraction, the collection of scenarios may then be considered as the world model to solve situations. For the trials described in this article, fourteen scenarios were programmed. As a consequence of the scenario a set of few parameterized subtasks are fired: findstart, search, backtostart, skip, and track. A concatenation of these subtasks constructs the final AUV trajectory.

1st Scenario: The AUV is tracking an exposed pipeline, navigating on top, at a fixed offset smaller or equal than 5 meters. Both the MBE and the MAG can detect it.

2nd Scenario: The AUV is tracking a buried pipeline on top, at a fixed offset, smaller or equal than 5 meters. The MBE may not be able to detect it, but the MAG can track it anyway.

3rd Scenario: The AUV is tracking an intermittently exposed and buried pipeline at a fixed offset. This is a sequence of alternative appearance of scenarios number one and two. MBE, MAG and LD are used.

4th Scenario: The AUV is tracking a free-span pipeline at a fixed offset. The pipe is tracked mainly based on MBE readings, which may be detecting the pipe itself or the trench.

5th Scenario: The AUV is tracking a pipeline in the presence of one or more pipes (like infield pipelines) or other magnetic objects in the area. Measures from MBE as well as MAG are needed.

6th Scenario: The AUV is tracking a pipeline but avoiding an obstacle. In such scenario the certainty error may increase beyond its thresholds, but the EN4AUV knows where the pipe is and ignores the pipe_lost flag. The path planner module (PPM) outputs a flag indicating this condition and the EN4AUV may query the legacy data to confirm the existence of an exclusion zone. Although sensor readings are not reliable, they are not turned off to be ready when the AUV is again over the pipeline.

7th Scenario: The AUV is searching a buried pipeline. No readings from MBE, just MAG will yield detection when the AUV is right over the pipe. With two detection (crossing) points the pipeline direction vector is computed and the AUV starts tracking from the last known point with this direction.

8th Scenario: The AUV is searching the pipeline, which is considered as lost. EN4AUV shall have an estimate of the trajectory from SFM considering the whole inputs: MBE, MAG, SSS and LD.

9th Scenario: The AUV is searching a pipeline in the presence of one or more pipes (like infield pipelines) or other magnetic objects in the area. Every information source is operative to discriminate the target under study (MBE, MAG, SSS and LD).

10th Scenario: The AUV is skipping from one point to another. MBE, SSS and MAG are off to save energy. This special situation appears when changing from one pipe to another to track, or from one zone of interest to another over the same pipeline.

11th Scenario: The AUV is going back to the last known position to start tracking, after founding the pipeline as a consequence of a successful search. MBE, SSS and MAG are off.

12th Scenario: The maximum number of reacquisition after unsuccessful searches was reached. The mission is ended with a failure message.

13th Scenario: The AUV is tracking an exposed pipeline, navigating on top, at a fixed z_offset greater than 5 meters. The detection is done mainly with the MBE.

14th Scenario: The AUV is tracking a buried pipeline on top, at a fixed z_offset greater than 5 meters. The blind tracking is done mainly based on legacy data, and cannot last more than half a minute. After this, if there are no more sensor readings, a new search must be started.

```
(defclass WORKING_SCENARIO (is-a SYM_VAR)
   (role concrete)
   (pattern-match reactive)
   (multislot Movie (type SYMBOL) (create-accessor read-write))
   (slot Navigation_type (type SYMBOL) (create-accessor read-write))
   (slot Incident_point (create-accessor read-write))
   (slot Error_Budget (type FLOAT) (create-accessor read-write))
   (slot Avoiding (type INTEGER) (create-accessor read-write))
   (slot Tracking_status (type INTEGER) (create-accessor read-write))
   (slot Follow_status (type SYMBOL) (create-accessor read-write))
   (slot Quantity_of_sensed_object (type SYMBOL)(create-accessor
read-write))
   (slot Risky_situation (type SYMBOL) (create-accessor read-write))
   (slot Within_corridor (type INTEGER) (create-accessor read-write))
   (slot Count_Reacq (type INTEGER) (create-accessor read-write))
   (slot Count_Rep_Reacq (type INTEGER) (create-accessor read-
write))
   (slot Error_distance (type INTEGER) (create-accessor read-write))
   (slot Navigation_Height (type FLOAT) (create-accessor read-write))
   (slot Search_results (type INTEGER) (create-accessor read-write)))
```

Figure 7. A framework representing a Working Scenario

```
(defrule R05.1
      (R4SD)
      ?a <- (R4SD)
      ?ws <- (object (is-a WORKING_SCENARIO)
(Count_Reacq ?cr)(Search_results ?sr) (Movie $?MOVIE)
(Follow_status ?FS))
      ?sv <- (object (is-a SURVEY) (Max_Reacquire ?mx))
      (test (<= ?cr ?mx))
      (test (eq ?FS LOST))
      (test (eq (send [OBJ_STUDY] get-
Present_Layout_Status) NOT_DETECTED_NOT_BURIED))
      test (= 0 ?sr))
=>
      (assert (Current_scenario SC8))
      (assert (PPLS notready))
      (retract ?ws)
      (insert$ $?MOVIE 1 SC8)
      (send ?ws put-Movie $?MOVIE)
      (retract ?a) ;to avoid the assertion of multiple scenarios in
the same KB query
      (printout t "CLIPSMACHINE: R05.1 Current Scenario is
SC8 -searching a pipe/trunkline" crlf)
      (printout t "CLIPSMACHINE: inserting movie" $?MOVIE
crlf))
```

Figure 8. A rule from the knowledge-base of the DMP for the 8th scenario determination, in the typical CLIPS syntax.

Rule base and objects

CLIPS allows the knowledge representation to be in the form of rules and frames (COOL or Clips Object Oriented Language). These formalisms are used in the knowledge base (KB) to represent the involved knowledge. Thus, there is a set of rules devoted to pipeline's layout determination (if it is or not detected, if buried or free span, etc.). Once this is assessed, rules determine the AUV "follow status" as regards as the pipeline. These "follow status" may be: avoiding an object, pipeline found, pipeline lost or pipeline intermittent. Then rules determine which scenario is present, and then select the corresponding action. These actions are modularly implemented as C++ routines. In Fig. 7, the class definition for the concept of "*working scenario*" is also shown and a rule for determining the AUV's follow status is presented in the CLIPS syntax in Fig. 8.

About 50 rules form the current KBPP. They are forward chained as usual in data driven, real time expert systems. The inference rule used is based on the Rete's algorithm. The objects used for formalization were: symbolic_variable, Waypoint, Type_of_Survey, Survey, Trajectory, Input_Trajectory (is-a-Trajectory), Output_Trajectory (is-a-Trajectory), Object_of_Study (is-a-symbolic_variable set to pipeline in this first approach), Working_Scenario (is-a-symbolic_variable).

EXPERIMENTAL RESULTS

The performance of the AUV navigation was tested with two different methods. The first one is a simple control method based on the line of Sight (LOS). With this simple scheme the AUV was able to follow a series of waypoints minimizing the angle computed as the difference between the actual heading and the angle of the line that joins the AUV with the target (next waypoint). A corrective signal proportional to the heading error is applied to the thrusters as a differential speed, adjusting the heading continuously to minimize this heading error. The scheme of the method is presented in figure 9. The control system in its present state is a simple proportional-integral (PI) control in the horizontal plane (2D) minimizing the angle β.

Recently, this DMP was integrated in the AUV described in this article. Preliminary guidance and control system approaches were tested in the new prototype. These trials were performed in shallow water, with the vehicle navigating just below water,

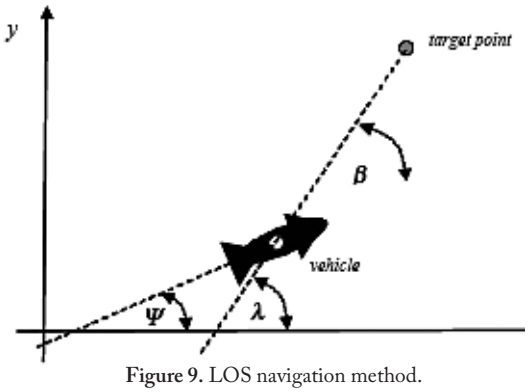

Figure 9. LOS navigation method.

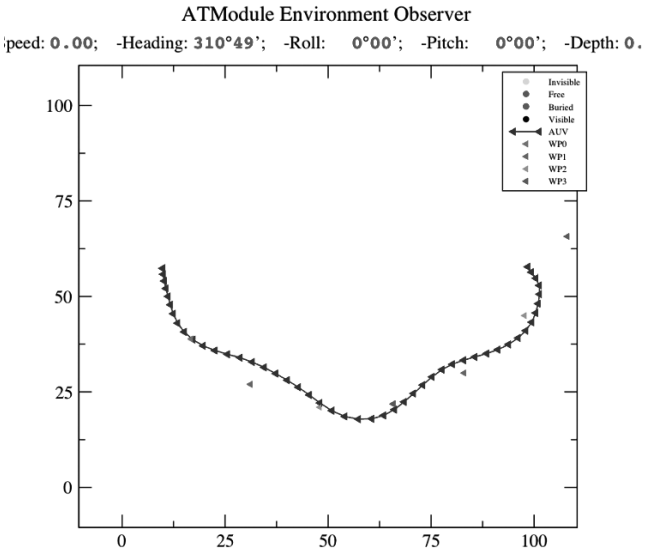

Figure 10. Sea trial of the AUV prototype in shallow Sea trial of the AUV prototype in shallow waters in Mallorca, Spain. Circular path.

obtaining position by GPS. In the first test a series of waypoints over a curved path was sent as a reference to follow using the line of sight algorithm (LOS). The desired path is a smooth trajectory that goes over the waypoints shown in figure 10, while the continuous blue line shows the real AUV positions. The area where the test was performed was quite limited and the controller was a simple non-optimized proportional producing some detours from the desired path. The AUV was programmed to go through a series of eight waypoints inscribed in a circle with a radius of around 45m. The vehicle followed the waypoints correctly though some oscillations were observed when passing over waypoints 2 and 4. It should be noted that an error tolerance was given to the control since the experimental area was small and turning radius was limited by software to avoid oscillations. Since the aims of the tests were to determine the maneuvering of the vehicle in water a proportional controller was used at this stage. Better results should be expected with a PI or PID controller. Trials were made in a shallow bay called Cala Estancia, near Palma de Mallorca, at the Balearic Islands. A second trial of the SEARCH condition was performed later. The search of a buried pipeline (emulated) was performed, as shown in figure 9. The sonar was simulated since the exact position of the pipe was known but it was assumed that the sonar would not see it. The vehicle starts at (58 m, 0 m) and moves to the initial position to start the search process at about (65 m, 25 m). This time the vehicle has more inertia than in the previous trial due to extra paylod electronics, this produces a couple of extra loops to reach to the start of search position. The pipeline is shown as a yellow continuous line in this figure. Since the pipeline is invisible the DMP decides to perform a search within a corridor. A series of waypoints describing a zig-zag movement are sent by the DMP as desired trajectories for the AUV's control system. These waypoints were joined by red straight lines in figure 11 for clarity. The AUV follows them reasonably well, though an improvement to the controller and a large area of tests should be done to give better results.

These experiments were performed on April 2008. A more sophisticated control system was designed combining a Lyapunov controller with the virtual particle path following strategy. Promising results were obtained through simulations and experimental test will follow soon. The control is composed by two blocks that allows to reach and track a pre-specified trajectory in real time, even in the presence of perturbations. The Control scheme is constituted by a Lyapunov based navigation block and a PI controller. The former creates robust references in order to guide the vehicle towards the desired trajectory.

CONCLUSIONS

This paper describes in detail hardware and software aspects of an inexpensive AUV developed for pipe/cable tracking for inspection.

The key aspects of the design consideration of the software and hardware elements in the AUVI prototype were presented in this article, as a low-cost adaptation of the AUTOTRACKER vehicle. In particular, the dynamic mission planner based on an expert system was described. This mission planner showed that this artificial intelligence approach is able to re-plan the vehicle trajectory while in the mission, taking into account the mission settings, the changing underwater environment and the situation of the target under inspection. The new low-cost experimental prototype presented here, will surely be an adequate test-bed for the new task and path planning algorithms. In particular we will focus in a near future in the enlargement of the knowledge-base within EN4AUV for untested use-cases. Design details of a dynamic path planning with state machine and AI based technique were also shown.

Once again, rule-based approaches show that incremental prototyping is an easy way to code user's experience. Besides, coding knowledge, easy to understand for an experienced ROV user is fairly simple. The design is reusable since it can be applied to different targets (pipelines, power cables, telephony cables). This inexpensive AUV was developed to test the algorithms that allow

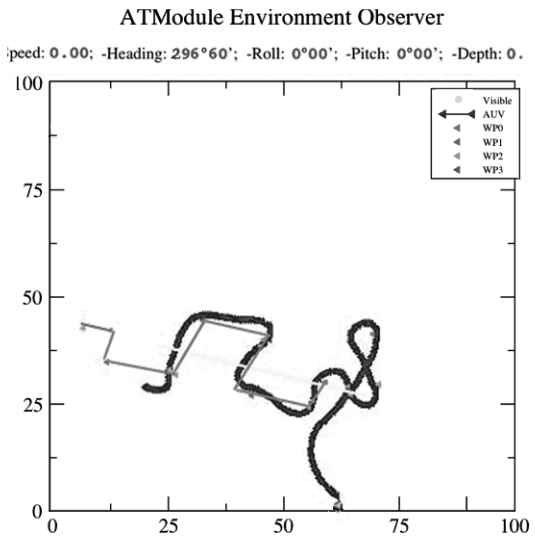

Figure 11. Sea trials of the AUV prototype in shallow waters in Mallorca, Spain. Searching a pipe.

the detection and tracking of the pipe with acoustic sensor. The paper presents a control method to govern the AUV performing lawmower searches of pipelines and cables. The simple method, is based on the LOS algorithm and was tested in a prototype AUV, passing through a series of waypoints. A more sophisticated control, based on Lyapunov to achieve better performance with guaranteed convergence was tested in simulations. Work is in progress to mount the MBE and Sidescan sonar and test the image recognition algorithms. The new designed vehicle will perform full 3D navigation so the control algorithms well have to be redesigned accordingly.

ACKNOWLEDGMENTS

The authors acknowledge financial support by the MEC (Spain) and FEDER (EU) through projects TRA2006-13318 and PCI2005-A7-0356, the University of the Balearic Islands, the University of La Plata, CONICET and ANPCyT.

REFERENCES

Acosta, G. G. , Curti, H. , Calvo, O. (2005): Autonomous Underwater Pipeline Inspection in AUTOTRACKER PROJECT: the Navigation Module, *Proceedings of IEEE/Oceans'05 Europe Conference,* June 21-23, Brest, France, pp. 389-394, Vol. 1.

Acosta, G. G., Curti, H., and Calvo, O. (2006): A Knowledge-based approach for an AUV Path Planner Development, *WSEAS Trans. on Systems,* Issue 6, Volume 5, pp. 1417 – 1424

Balasuriya and T. Ura (1998): Autonomous Target Tracking by Underwater Robots Based on Vision, *IEEE Proc. Int'l Symposium on Underwater Technology*, 15-17 April, Tokyo, Japan, pp. 191-197.

Curti, H. J., Acosta, G. G., Calvo, O. A. (2005): Autonomous Underwater Pipeline Inspection in AUTOTRACKER PROJECT: the Simulation Module", *Proceedings of IEEE/Oceans'05 Europe Conference,* June 21-23, Brest, France, pp. 384 - 388, Vol. 1.

Evans, J., Petillot, Y., Redmond, P., Wilson, M. and Lane, D. (2003): AUTOTRACKER: AUV Embedded Control Architecture for Autonomous Pipeline and Cable Tracking", *Proceedings of IEEE-OCEANS*, Sept., Volume 5, 22-26, pp. 2651-2658.

Fernández León, J. A.; Acosta, G. G.; Mayosky, M. A., and Calvo Ibáñez, O. (2008): A Biologically Inspired Control based on Behavioural Coordination in Evolutionary Robotics", Book chapter 7 in *Advancing Artificial Intelligence through Biological Process Applications,* Idea Group Inc.

Fossen, T. (2002): Marine Control Systems, *Marine Cybernetics AS,* Trondheim, Norway.

Giarratano, J. (2002): *CLIPS User's Guide*, NASA LB Johnson Space Center – Software Technology Branch.

Tena Ruiz, Y. Petillot, D.M. Lane (2003): Improved AUV navigation using side-scan sonar, *Proceedings of IEEE OCEANS,* Volume: 3 , 22-26 Sept. pp. 1261 – 1268.

Valenciaga, F., Puleston, P. F., Calvo, O., Acosta, G. (2007): Trajectory Tracking of the 'Cormoran' AUV Based on a PI-MIMO Approach, *IEEE/Oceans'07 Europe Conference*, Aberdeen, UK, June 18-22.

Journal of Maritime Research, Vol. VI. No. II, pp. 53-70, 2009

ISSN: 1697-4840

ON SENSOR FDI BY FUNCTIONAL AND PHYSICAL REDUNDANCY APPLIED TO DP SYSTEMS

R. Ferreiro[1], R. Haro[2] and J.L. Calvo[3]

Received 24 September 2008; received in revised form 2 October 2008; accepted 20 May 2009

Abstract

The research work is focused on sensors fault detection and isolation (FDI), exploiting the synergy of functional and physical redundancy. Functional and physical redundancy is applied under a novel methodological approach to isolate individual sensor faults. The contribution uses a heuristic algorithm which combines a rule based strategy associated to a process parameter identification procedure to be applied on instrumentation FDI tasks. Implementation procedure is carried out on a dynamic positioning system (DP) equipped with supervision facilities, which efficiently manage databases, rule based systems and appropriate identification algorithms on a simulation basis.

Keywords: Dynamic Positioning Systems, Fault detection, Fault isolation, Expert systems, Functional redundancy, Physical redundancy, and Rule based system.

INTRODUCTION

Most of the supervisors design methods are based on the plant models. Additionally, the implementation of intelligent control technology based on soft computing methodologies such as expert systems and artificial intelligent techniques can notably enhance the supervision and advanced control capabilities of many industrial processes such as process engineering industries and many other complex chemical engineering processes (Lippmann, R. P., 1987). A necessary requirement to succes-

[1] Professor. University of A Coruna (ferreiro@udc.es), ETS. Náutica y Máquinas, Paseo de Ronda, A Coruna, Spain. [2] Professor. University of Cadiz (manuel.haro@uca.es), Facultad de Ciencias Nauticas, Cadiz, Spain. [3] University of A Coruna.

sfully be applied, such state of the art techniques needs to operate with highest-quality data, which means a considerable effort on applying sensors faults isolation and/or faults tolerant strategies. The typical faults encountered in industrial applications are commonly classified into some of the following typical groups: Process parameter changes, Disturbance parameter changes, Actuator malfunctions, and Sensor malfunctions.

The sequence of subtasks to be carried out to ensure correct process operation is at the heart of process supervision, usually referred to as process monitoring tasks, including, fault detection, fault identification, fault diagnosis, and fault removing by process intervention, process recovery or process reconfiguration. Process monitoring is based on data acquisition and data processing procedures. An introduction on this topic can be found at (Ferreiro García R., 2007).

Among data driven methods, Partial Least Squares (PLS) are data decomposition methods for maximizing covariance between predictor block and predicted block for each component (Wise B. M. and Gallagher N. B., 1996) (MacGregor J. F., 1994) (Piovoso M. J. and Kosanovich K. A., 1992) (Piovoso M. J. and Kosanovich K. A., 1994).

Regarding analytical methods, they use residuals as features which are commonly referred to as analytical redundancy methods. The residuals are the result of consistency checks between plant observations and their math-model. The residuals will be sufficiently large values in the presence of faults and small or negligible in the presence of disturbances, noise and/or modeling errors (Frank P. M., 1993), (Gertler. J. J. 1998) (Hodouin D. and Makni, 1996). Three main methods are commonly used to generate residuals: Parameter estimation, Observers and Parity relations.

In the case of parameter estimation, the residuals are the difference between the nominal model parameters and the estimated model parameters. Deviations in the model parameters are an indicator used as the basis for detecting and isolating faults (Isserman R., 1998) (Mehra R. K. and Peschon J., 1971).

In the observer-based methods, system output is reconstructed from measurements or a subset of measurements with the aid of observers. The differences between actual measured output and estimated output are the residuals (Frank P. M., 1990) (Clark R.N. et all., 1975).

The parity relations strategy checks the consistency of the mathematical equation of the system with real time measurements. The parity relations are subjected to a linear dynamic transformation as the transformed residuals are used in detection and isolation tasks (Gertler, J. J., 1995) (Mironovski L. A., 1979) (Mironovski L. A., 1980). The aforementioned analytical approach that has been commented on requires error-free mathematical models in order to be effective.

Knowledge-based methods, extensively applied in process monitoring tasks, include: Causal analysis, Expert systems and Pattern recognition (Doyle R. J. et all., 1993).

These techniques are based on qualitative models, which can be obtained via one of the following ways:

— Causal modeling of the systems (Lee G. et all., 1999) (Mo K. J. et all., 1998) (Mo K. J. et all. 1997).

— Expert knowledge (Kramer M. A and Palowitch J.B.L., 1987) (Li X, and Yao X, 2005) (Kramer M. A. and Finch F. E., 1988) (Bakshi B.R. and Stephanopoulos G., 1994).

— A detailed model describing the system (Nekovie, R. and Sun, Y., 1995), (Demuth, H. and Beale, M. 1998).

— Fault-symptom based cases. (Isserman R 1993) (Yong-Guang Ma, Liang-Yu Ma and Jin Ma, 2005).

Among the outlined supervision methods, none of them is qualified to carry out the overall safely supervision task on the vast amount of different processes and variety of instruments. As consequence of such drawbacks, the proposed research work is focused on a problem-solving strategy which combines into a heuristic search path driven on the basis of a flow chart, a rule base processor with an appropriate identification method. The proposed strategy supposes a novel, general and effective alternative on FDI sensors diagnosis. Thus, the work is centered on the task of detection and isolation sensor faults using a model based approach which deals with a model parameter identification technique associated to a rule based scheduler oriented to FDI tasks mainly applied in process supervision, including decision-making procedures according to well-known rule-based techniques. To carry out proposed tasks, the identification algorithm based on the collection of real-time data for transient state operation conditions is presented using the facilities of (DeltaV™. V.8.4. 2007).

The work is organized by describing the strategies to synthesize FDI rule bases on the basis of an analytical function approximation model based approach. Finally an illustrative example of sensors FDI is presented. Validation is based on the results achieved from an application on the pilot plant.

FAULT DETECTION AND ISOLATION STRATEGY

Being FDI a crucial part of an asset management task, as shown in (Chow M., 2000) (Kusiak A. and Shah S., 2006) (Li. T., 1989), the principles of predictive maintenance apply to all machines, processes and industrial applications, where expert systems play relevant and important role. However, the knowledge storage required for the implementation of an expert system is significant, particularly for systems that require decisions to be based upon the knowledge base. In fact, as stated in (Kusiak A. and Shah S., 2006), expert systems cannot respond creatively under unexpected scenarios or circumstances and no deterministic answer to determine when the input values go outside a predefined range is available but rather random.

Nevertheless, Rule Based Systems (RBS) may be used to solve difficult problems that typically require significant human expert intervention. By emulating the expertise and the decision-making ability of a human it is possible to reduce the effort and cost of making the knowledge of multiple experts available continuously, simultaneously, and permanently; thereby increasing reliability and performance.

In this work it is described how the inherent advantages of RBSs can be embedded into a scalable process control system. It also presents a prototype of a highly interactive and user friendly environment that simplifies and speeds the configuration of an expert system and makes it easy and intuitive for the typical plant engineer to incrementally apply his process knowledge.

Such a tool can be used to monitor and process and to address abnormal condition management by continuously evaluating real-time and historical data, watching for events and abnormal conditions, providing reliable diagnosis and advice, and taking corrective actions when necessary in order to support the plant operators to manage their monitoring operations. The core technology and functionality is implemented using DeltaV inference engine.

Analytic modeling is the modeling technique chosen to handle process changes detection tasks in this work. The main reason is that analytical modeling represents the process dynamics as function of available and accessible measured variables and parameters. Consequently it can be updated without via on-line parameter identification.

Sensor Faults Characteristics

A sensor fault can be defined as a deviation from its normal readings. Excluding complete failure, sensor faults are classified into four types (Abdelghani M. and Friswell M.I., 2007) (Qin S.J. and Li W.H., 1999): bias, drift, precision degradation, and multiplication fault. The reading of a fully functioning sensor at time t is $x^*(t)$. Sensor malfunction could cause the reading to deviate from the actual value. For bias fault, $x(t)$ is the sensor reading and can be expressed as

$$x(t) = x^*(t) + b \tag{1}$$

where b is constant and could be positive or negative. For the drift fault,

$$x(t) = x^*(t) + a \cdot (t - t_f) \tag{2}$$

where a is a constant, t_f is the time stamp when the drift begins. Over time the drift fault becomes larger.

For the precision degradation fault,

$$x(t) = x^*(t) + \varepsilon \tag{3}$$

where ε is a random variable following the normal distribution $N(0,\sigma^2)$. The value of ε usually has a larger variation than the white noise.

For the multiplication fault,

$$x(t) = c \cdot x^*(t) \tag{4}$$

where c is a constant. In a generic case, the sensors fault scenario could be due to a combination of the four types of faults. For this reason, the main goal is simply to isolate the faulty sensor in order to apply a decision making strategy and a problem solving procedure.

Proposed FDI Algorithm

In this work FDI tasks is associated with two aspects of redundancy combined among them as required:

— Functional redundancy
— Physical redundancy

Functional redundancy deals with two or more functions describing the same process, while physical redundancy is referred to several hardware devices applied to measuring the same variable. Since analytical models in general don't represent effectively the behavior of nonlinear processes, it is justified the use of back propagation neural networks (BPNN) based functional approximation techniques in nonlinear process modeling, not used in this work.

Functional Redundancy on the FDI Procedure

Let's consider a *free fault* (FF) process defined by means of an analytical function approximation procedure (Deckert J.C. et all., 1977). With regard to functional redundancy, to describe at least two functions of the same variable (manipulated variable) first principles are to be applied. Consequently, a manipulated variable can be described as an active function *MVa*, while a process inverse model provide a reactive function *MVr* as response to the excitation constituted by the manipulated variable.

The complete open loop process can be described by means of model based functions as shown in (5),

$$
\begin{aligned}
MVa &= f(X_1, X_2, ...X_N) \\
MVa' &= f(X_1', X_2', ...X_N') \\
MVr &= f(Z_1, Z_2, ...Z_M) \\
MVr' &= f(Z_1', Z_2', ...Z_M')
\end{aligned}
\tag{5}
$$

where *MVa'* and *MVr'* are respectively physically redundant functions of *MVa* and *MVr*.

where

$X_1, X_2, ...X_N$, are inputs from hardware devices to the function *MVa*,

$X_1', X_2', ...X_N'$ are the physical redundant inputs to *MVa'*,

$Z_1, Z_2, ..Z_M$ are inputs from hardware devices to the function *MVr*, and

$Z_1', Z_2', ..Z_M'$ are the physical redundant inputs from hardware devices to the function *MVr'*.

In figure 1 it is depicted the functional redundancy concept implemented on the basis of functional approximation architectures as defined by (5)

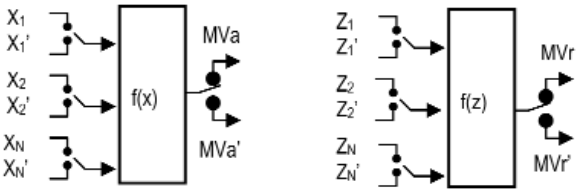

Fig. 1. Functional redundancy implemented under model based functions.

Furthermore, sub-index *N* is the number of instruments assigned to the active function, and sub-index *M* is the number of devices assigned to the reactive function. Described model based functions are experimentally obtained by means of an on-line parameter identification procedure.

Under normal and FF conditions the following functional relations are fulfilled:

First principles

$$MVa = MVr \tag{6}$$

Physical Redundancy

$$
\begin{aligned}
MVa &= MVa' \\
MVr &= MVr'
\end{aligned}
\tag{7}
$$

With such premises the basis for the proposed strategy is stated.

FDI Procedure

Considering equations (5) (6) and (7), a FDI scheduler is developed and represented by means of a close loop sequence of tasks, implemented by means of the flow-chart depicted with figure 2.

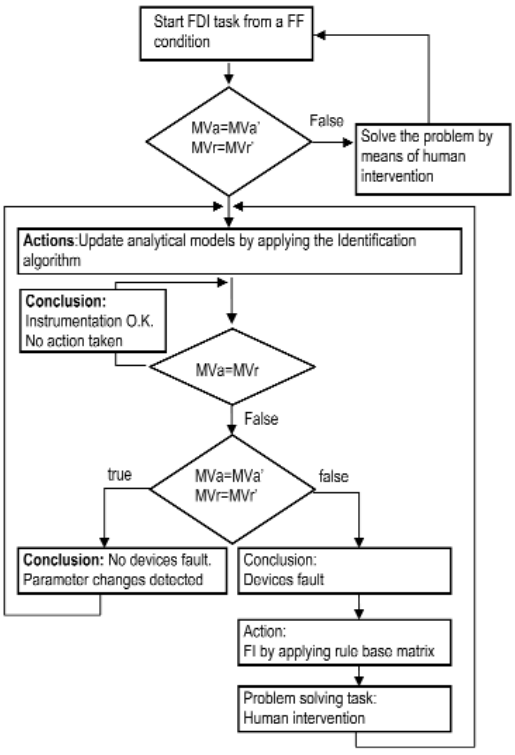

Fig. 2. Flow-chart of the FDI scheduler.

According this flow-chart, starting procedure requires a safety operating condition. Once system operation is verified as nominal free-fault or safe condition, then the diagnostic task begins. Human operator intervention is necessary since system reconfiguration doesn't solve the problem of repairing or substitution faulty sensors. Furthermore, if at least one of the sensor fails, in order to keep the required redundancy, this problem must be solved before to continue towards the next flow-chart step. In safety-critical systems, under severe situations a double redundancy may be applied. In such a case system reconfiguration consists in discard the faulty sensor thus avoiding human intervention, but assuming the disadvantage of hardware cost increment.

The Identification procedure

Although in many recent research works reasonably efforts on neural networks based fault detection techniques are being used, such in, in order to gets an analytical function describing the manipulated variable *MVa*, as function of its device outputs and model parameters, as well as an analytical function *MVr* describing the process inverse model as function of the process variables and parameters, an on-line identification method is then proposed and applied. The identification procedure of both models *MVa* and *MVr* is carried out simultaneously.

Experimental identification of process dynamics has been an active area of research in several areas of engineering. A Variety of techniques has been proposed. In this work it will be applied a conventional one widely used in process engineering. General nonlinear estimation uses linear estimation iteratively applied to linear

approximations of the model until coefficients converge. On the other hand the Extended Kalman Filter (EKF) is probably the most widely used estimation algorithm for nonlinear systems. However, more than three decades of experience in the estimation community has shown that is difficult to implement, difficult to tune, and only reliable for systems that are almost linear on the time scale of the updates. To overcome these drawbacks and limitations, the selected parameter estimation method is based on the time-domain fitting of step test data.

The most direct way of obtaining a linear dynamic model of a process is to find its parameters that fit the experimentally obtained step response data. It is based on applying a disturbance and record the output variable *x(t)* and its successive derivatives as a function of time. With achieved data it is possible to estimate a set of model parameters proceeding by means of the linear least squares algorithm. In order to be prepared to apply the estimation procedure let's review the method by starting from a linear model such that

$$y = X\grave{e} + e \tag{8}$$

where y is an N by 1 vector, X is N by K matrix, where K is the number of model variables, $\grave{e}$ is a K by 1 vector of unknown coefficients, and e is an N by 1 vector of errors.

The vector of parameter estimates is straightforward achieved from least squares algorithm according

$$\hat{\grave{e}} = \left(X^T X\right)^{-1} X^T y \tag{9}$$

where its covariance matrix is then

$$V\left[\hat{\grave{e}}\right] = s^2 \left(X^T X\right)^{-1} \tag{10}$$

with s^2 the estimated mean squared model error.

Rule Base Matrix

A rule base matrix is developed in order to deterministically decide the faulty group. The faulty device will be isolated by applying the properties inherent to physical redundancy. The rule base matrix is composed by an *m*.x.*n* order, where $m = n$, which means a square matrix. The corresponding entries of rows and columns are matched by means of an *If Then* rule of the form:

IF group (a) is equal to group (r) THEN Conclusion (True or False)

	MVa	MVr	MVa'	MVr'
MVa		0		
MVr	0		0	0
MVa'		0		
MVr'		0		

Table I. Full single redundancy rule matrix.

Every element of the rule base matrix is the conclusion of every processed rule that means a deterministic decision about the matched group of instruments by applying (6) and (7).

Table I shows the structure of a full single redundancy set of instruments associated by groups identifying the rule matrix entries. The shadowed cells are not applicable.

For instance, with regard to table I, if any device of the group of instruments *MVr* fails, then the result derived from the fact of matching this group against the remaining groups of the rule base matrix, is false (0). Otherwise, is true (1), according the decisions of the rules shown in rule matrix of table I. According to the given explanation, the decision of the rest of table cells is a logic one.

IMPLEMENTATION PROCEDURE ON DP PROPULSION SYSTEM

In order to show the supervision procedure under described methodology, a basic propulsion system equipped with a set of instruments for an autonomous vehicle dynamic positioning control system is to be described

This propulsion system is specifically selected in this work to test DP propulsion related instrumentation, being equipped with physical redundancy instrumentation for most of the relevant variables. The application is focused on the supervision of the instrumentation associated to the thrust forces caused by propulsion effectors. Such vehicle is equipped with a fully redundant positioning system designed to ensure that position monitoring can be carried out throughout all phases of ship operation and in the specified environmental condition.

The Propulsion Model

The analysed propulsion system correspond to a shunt DC motor driven by a full-bridge thyristor rectifier (SCR), which has separately supplied field winding and armature (rotor) winding. The armature current is transferred from the stationary terminals to the rotor by use of brushes connected to the rotating commutator.

In a shunt DC motor the induced armature voltage is proportional to the magnetic field and rotational speed. The magnetic field is a function of the field current,

and because of saturation effects, they are in practice not proportional. However, if neglecting the saturation, the armature voltage is:

$$V_a = k \cdot \Phi(I_f) \cdot n \approx k \cdot K_\Phi \cdot I_f \cdot n = K_V \cdot I_f \cdot n, \tag{11}$$

where K_V is the induced voltage constant, I_f is the magnetization (field) current, n is the rotational speed, K_Φ and K are proportional constants, and Φ is the motor flux.

The developed torque Q is proportional to armature current and magnetic field, according

$$Q = k \cdot I_a \Phi(I_f) \approx k \cdot I_a \cdot K_\Phi \cdot I_f = K_{TM} \cdot I_a \cdot I_f \tag{12}$$

where K_{TM} is the torque constant and I_a is the armature current. Since the DC motor must be supplied from a DC source with limited voltage, field, and armature currents, the characteristic boundary of operations will be also limited. Using expressions (11) and (12) conveniently, the motor torque can be expressed as function of the current and voltage of the armature. Furthermore the developed power is straightforward achieved according

$$\begin{aligned} Q &= \frac{1}{n} \cdot \frac{K_{TN}}{K_V} \cdot I_a \cdot V_a \\ Power &= Q \cdot n \cdot \frac{K_V}{K_{TN}} \end{aligned} \tag{13}$$

The torque control block diagram of an electric propulsion system is shown in figure 3.

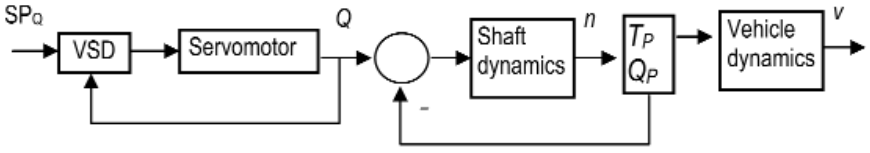

Fig. 3. Electric motor-propeller based propulsion scheme.

The torque Q is to be controlled by means of a variable torque/speed drive. The load is due to the propeller torque Q_P. The vehicle dynamics depends on propeller thrust T_P, hull resistances and external disturbances.

Propulsion system dynamics

It is assumed that the propeller shaft is driven by an electric motor, which generates a torque Q controlled by a variable speed drive (VSD) of the SCR type. The engine dynamics is split-up into two parts. The first part describes the relation between the developed torque (*PV*) and demanded torque (*SP*). The linear transfer function is modelled as a first order time constant according (R. Ferreiro, M. Casado, F.J. Velasco, 2005)

$$\frac{Q}{SP_Q} = \frac{K_Y}{T_c s + 1} \tag{14}$$

where K_Y is the gain constant and T_c is the time constant corresponding to the torque from motor and shaft inertia loads. The mentioned second part correspond to the shaft torque balance, being expressed as

$$Q = I_m \dot{n} + Q_f + Q_p \tag{15}$$

where I_m is the total moment of inertia of rotating parts, Q_p is the torque developed from the propeller and Q_f is the friction torque.

Propeller thrust dynamics

The propeller thrust and torque are modelled by the following relations

$$\begin{aligned} T_p &= K_T \rho D^4 |n| n \\ Q_p &= K_Q \rho D^5 |n| n \end{aligned} \tag{16}$$

where D is the propeller diameter and ρ is the mass density of water

Thrust coefficient

$$K_T = \frac{T_p}{0.5 \cdot \rho \cdot V_r^{\,2} \cdot A_0} \tag{17}$$

Torque coefficient

$$K_Q = \frac{Q_p}{0.5 \cdot \rho \cdot V_r^{\,2} \cdot A_0 \cdot D} \tag{18}$$

Where V_r is the relative speed of advance and A_0 is the propeller disc surface.

$$V_r^{\ 2} = V_A^{\ 2} + (0.7 \cdot R \cdot n)^2 \tag{19}$$

$$\beta = A\tan(V_A, 0.7 \cdot R \cdot n) \tag{20}$$

Where R is the propeller disc radius and V_A is the speed of advance (arriving water velocity to propeller)

Advance number

$$J = \frac{V_A}{n \cdot D} \tag{21}$$

By knowing experimentally the advance number of such particular hull-propeller vehicle, the speed of advance is calculated, and consequently, the relative speed of advance, the torque coefficient and the thrust coefficient which yields the propeller torque and propeller thrust necessary to establish the analytical redundancy.

Ship surge dynamics

The ship dynamics can be approached by the following non-linear differential equation

$$m\dot{v} = R(v) + (1 - t_T)T_p + T_{EXT} \tag{22}$$

where m is the total mass (ship mass plus added mass), $R(v)$ is the hydrodynamic resistance, $(1\text{-}t_T)$ is the thrust deduction factor, T_{EXT} is the total external forces and T_p is the thrust propulsion

After rearranging past equations, and neglecting the external forces, yields the final model for the shaft speed and vehicle speed as

$$Q = SP_Q \frac{K_Y}{T_c s + 1} \tag{23}$$

$$\dot{n} = \frac{1}{I_m}[Q - Q_f - Q_p] = \frac{1}{I_m}[Q - KF \cdot n - K_Q \cdot \rho \cdot D^5 \cdot n \cdot |n|] \tag{24}$$

$$\dot{v} = [-R(v) + (1 - t_T)T_p]/m = \frac{1}{m}[-R(v) + (1 - t_T) \cdot K_T \cdot \rho \cdot D^4 \cdot n|n|] \tag{25}$$

whose block diagram is achieved and shown in figure 4.

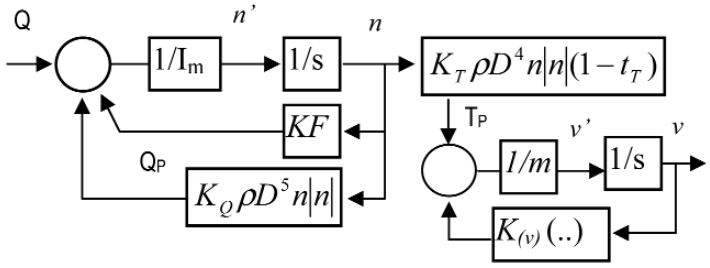

Fig. 4. Block diagram of propulsion system under state space phase variable model.

Implementation of the DP FDI Strategy

Given a DP propulsion plant corresponding to a marine vehicle described by means of analytical approximation procedures under *MVa*, *MVr*, and redundant groups of devices under *MVa' and MVr'*, by applying expression (5) on (13), (15) and (16) for the armature current, voltage and shaft speed it yields

$$\begin{aligned} MVa &= f(SP_Q, I_a, V_a) \\ MVa' &= f(SP_Q, I'_a, V'_a) \\ MVr &= f(Q_P, n) \\ MVr' &= f(Q_P, n') \end{aligned} \tag{26}$$

where (SP_Q, I_a,. V_a) are inputs to the function *MVa*, (I'_a, V'_a) are redundant inputs to *MVa'*, (n) is the input to the function *MVr*, and (n') is the redundant input to the function *MVr'*. With the model

Since the speed of advance V_A and consequently the advance factor J depend on the actual dynamic characteristics of the maneuver, estimation of thrust and torque coefficients according expressions (16-21) doesn't provide accurate results. Due to such ambiguity the actual measures of propeller thrust and motor current and/or power are available and measured. At zero vehicle speed, in keeping station conditions, a well experimental approach which relates the motor torque with propeller thrust is the used.

$$T_P = f_Q(Q) = f_n(n) \tag{27}$$

With the balance given by (27) expression (26) is being used on the FDI task. According (26), the corresponding rule base matrix is that of table V, in which a single full redundancy is being applied. Consequently, applying the FDI scheduler depicted by means of the flow-chart shown in figure 2, as part of the whole supervision system, yields the results (conclusions) of the on-line instrumentation supervisi-

on task. If there is full evidence of correct instrumentation operation, then the plant supervision task, which is beyond the scope of this research work, will be easier and deterministic. It must be also taken into account that if instrumentation operation is correct, then, standard plant FDI methods may be applied.

Simulation results

In order to verify a potential malfunction of the instrumentation (armature current, voltage and tachometer), the redundant current sensor is manually adjusted to be deviated from the actual value (shift) and consequently its behavior is the typical one of a faulty sensor affected by such fault. After starting up the FDI scheduler following the flow-chart shown in figure 2 with the rules described by (26), the FDI process begin.

	MVa	MVr	MVa'	MVr'
MVa		1	0	1
MVr	1		0	1
MVa'	0	0		0
MVr'	1	1	0	

Table II. Detection of the faulty group of instruments (Row and column of *MVa'=0*)

The rule base matrix which must be processed under the instrumentation structure is the one of table II according the flow-chart sequence. The results of processing the rule base are shown in table V, where the group of sensors denoted as *MVa'* is faulty.

As a fault has been detected, isolation of the faulty device is rather a straightforward action which consists in the comparison of every device of the faulty group with its redundant device. As consequence of the comparison between the readings on both groups of devices it yields $I_a \neq I_a^{'}$. Since a fault has been detected and acknowledged, it is expected to solve the problem by re-adjusting the faulty current sensor. After acknowledging the human intervention, then the signal flow is returned to the origin to continue the on-line supervision task.

CONCLUSIONS

A systematic methodology to implement the supervision task of process instrumentation applied on the thruster equipment of a DP control system has been proposed and developed. The approach combines model based approximation implemented on the basis of parameter identification, with rule based strategies, both

implemented with the facilities of an object oriented programming tool. This procedure solves an important task by deterministically deciding the health of the data acquisition system. The relevance of this fact is verified since the ambiguity on conventional system FDI tasks is avoided with the applied methodology. The problem associated with the most probable faults and decision making based on voting, as well as the most convenient number of redundant devices is solved by the procedure implemented by means of the developed supervision FDI scheduler.

ACKNOWLWEDGEMENTS

This work has been partially supported by the XUNTA DE GALICIA under grant DPI 1 IN825N cod_web: 772.

REFERENCES

Lippmann, R. P. (1987): An Introduction to Computing with Neural Networks; *IEEE Acoustic, Speech, and Signal Proc*. Mag. 4-22.

Ferreiro García R. (2007): "On fault isolation by neural-networks-based parameter estimation techniques", *Expert Systems*, Vol. 24, No 1, pp. 47-63.

Wise B. M. and Gallagher N. B. (1996): "The process chemometrics approache to process monitoring and fault detection". *Journal of Process Control*, Vol. 6:329-348

MacGregor J. F. (1994): Statistical Process Control of multivariate processes. *Proc. Of the IFAC Int. Symp. On Advanced Control of Chemical Processes*, pp 427-435, New York. Pergamon Press.

Piovoso M. J. and Kosanovich K. A. (1992): Monitoring process performance in real time. *Proc. Of the American Control Conference*, pp. 2359-2363, Piscataway, New Jersey. IEEE Press.

Piovoso M. J. and Kosanovich K. A. (1994): "Applications of multivariate statistical methods to process monitoring and controller design". *Int. Journal of Control*, Vol. 59:743-765

Frank P. M. (1993): "Robust model based fault detection in dynamic systems", *On line fault detection and supervision in the chemical process industries.* pp. 1-13. Pergamon Press. Oxford. IFAC Symposium series Number 1.

Gertler. J. J. (1998): "*Fault Detection and Diagnosis in Engineering Systems".* Marcel Decker, Inc. New York.

Hodouin D. and Makni (1996): S. "Real time reconciliation of mineral processing plant data using bilinear material balance equations coupled to empirical dynamic models". *Int. Journal of Mineral Processing* , Vol. 48, pp 245-264.

Isserman R. (1998): "Process Fault Detection based on modelling and estimation methods: A survey", *Automatica*, Vol. 20, pp 387-404.

Mehra R. K. and Peschon J. (1971): "An Innovation approach to fault detection and diagnosis in dynamic systems". *Automatica*, Vol.7, pp. 637-640

Frank P. M. (1990): "Fault diagnosis in dynamic systems using analytical and knowledge based redundancy.- A survey and some new results". *Automatica*, Vol. 26, pp 459-474.

Clark R.N. et all. (1975), "Detecting instrument malfunctions in control systems". *IEEE Trans. On Aerospace and Electrooninc Systems*, Vol. 11, pp 465-473.

Gertler, J. J. (1995): "Diagnosis of parametric fault – from identification to parity

Mironovski L. A. (1979): "Functional diagnosis of linear dynamic systems", *Automation and Remote Control*, Vol. Vol. 40: 1198-1205.

Mironovski L. A. (1980): "Functional diagnosis of linear dynamic systems- A survey". *Automation and Remote Control*, Vol. 41: 1122-1142

Doyle R. J. et all. (1993): "Causal modeling and data-driven simulation for monitoring of continuous systems", *Computers in Aerospace.*, Vol. 9, pp 395-405

Lee G. et all. (1999): "Multiple-fault diagnosis under uncertain conditions by the quantification of qualitative relations". *Ind. Eng. Che.Res.*, 38: pp988-998.

Mo K. J. et all. (1998): "Robust fault diagnosis based on clustered symptom trees". *Control Engineering Practice*, Vol.5: pp 199-208

Mo K. J. et all. (1997): "Development of operation-aided system for chemical processes". *Expert Systems with Applications*. Vol. 12: pp 455-464

Kramer M. A and Palowitch J.B.L. (1987): "A rule-based approach to fault diagnosis using the signed direct graph". *AIChE. Journal.* Vol. 37: pp.1067-1078

Li X, and Yao X, (2005), "Multi-scale statistical process monitoring in machining", *IEEE Transactions on Industrial Electronics*, vol. 52(3), pp 924-927, 2005

Kramer M. A. and Finch F. E. (1988): "Development and classification of expert systems for chemical process fault diagnosis". *Robotics and ComputerIntegrated Manufacturing*, Vol. 4: pp 437-446

Bakshi B.R. and Stephanopoulos G. (1994): "Representation of process trends, IV Induction of real time patterns from operating data for diagnosis and supervisory control". *Computers and Chemical Engineering.* Vol.18, pp 303-332.

Nekovie, R., and Sun, Y. (1995): Back propagation Network and its Configuration for Blood Vessel Detection in Angiograms, IEEE Trans. on Neural Networks, Vol 6, No 1.

Demuth, H. and Beale, M. (1998): "Neural Network Toolbox: User's Guide", The MathWorks, http://www.mathworks.com

Isserman R. (1993): "Fault diagnosis of machines via parameter estimation and knowledge processing.-Tutorial paper". *Automatica,* Vol. 29: pp. 815-835.

Yong-Guang Ma, Liang-Yu Ma, Jin Ma (2005): "RBF neural network based fault diagnosis for the thermodynamic system of a thermal power generating unit", *Proceedings of 2005 International Conference on Machine Learning and Cybernetics* Volume 8, Issue , 18-21 Aug. 2005, Page(s): 4738 - 4743 Vol. 8

DeltaV™. V.8.4. (2007): "Books on line", Copyright © 1994-2007, *Fisher-Rosemount Systems, Inc., Emerson process Management*. USA

Chow M. (2000): "Special session on motor fault detection and diagnosis" *IEEE Transactions on Industrial Electronics*, Vol 47, pp 982-983.

Kusiak A. and Shah S. (2006): "Data-Mining-based System for prediction of water chemistry faults", *IEEE Transactions on Industrial Electronics*, Vol. 53, pp 593-603, 2006

Li. T. (1989): "Expert Systems for Engineering Diagnosis: Styles, requirements for tools, and adaptability". Ed Tzafestas S. G. *Knowledge-based Systems Diagnosis, Supervision, and Control*, Plenum Press, New York, pp. 27-37.

Abdelghani, M. and Friswell, M.I. (2007): "Sensor validation for structural systems with multiplicative sensor faults", *Mechanical Systems and Signal Processing*, Vol. 21, N 1, pp 279-279.

Qin, S.J. and Li, W.H. (1999): "Detection, identification, and reconstruction of faulty sensors with maximized sensitivity", *AIChE., Journal*, Vol. 45, No. 9, pp. 1963-1976.

Deckert J.C. et all. (1977): "F-8 DFBW sensor failure identification using analytic redundancy". *IEEE Trans. On Automatic Control*, Vol. 22, pp 795-803.

R. Ferreiro, M. Casado, F.J. Velasco (2005): "Trends on modelling techniques applied on ship's propulsion systems monitoring", *Journal of Maritime Research*, Vol II. No1, pp. 87.104.

Journal of Maritime Research, Vol. VI. No. II, pp. 71-82, 2009

ISSN: 1697-4840

APPLICATION OF AN AERONAUTIC CONTROL FOR SHIP PATH FOLLOWING

D. Moreno[1], D. Chaos[1], J. Aranda[1], R. Muñoz[1], J. M. Díaz[1] and S. Dormido-Canto[1]

Received 25 September 2008; received in revised form 5 October 2008; accepted 30 May 2009

Abstract

Control design for marine autonomous vehicles is a subject of great interest in control systems. These vehicles are strongly non linear and show complex hydrodynamics effects that make the control design difficult. Besides, coordinated control deals with the control of several independent objects to reach a global goal. Therefore the CPF deals with the problem of controlling a group of unmanned vehicles along a given path, while they are keeping a desired formation. In a first approach to the problem of coordinated control of formations, the control of an underactuated autonomous vehicle, a ship, has been treated to reach and follow a given reference. For the control of the ship, it has been used a "Line of Sight" algorithm, initially developed for the control of an aircraft, applied to marine vehicles, allowing a smooth and accurate control and path following.

Keywords: nonlinear control, unmanned vehicles, path following, marine control.

INTRODUCTION

The problems of control of autonomous vehicles, that are dealt in a wide range (Aguiar 2003, 2007) (Fossen 2000), can be classified in three fundamental groups.

— Point stabilization: Its aim is to stabilize the vehicle in a fixed point in a particular orientation.
— Trajectory tracking: In this problem the vehicle must follow a trajectory parameterized with respect to the time.

[1] Universidad Nacional de Educación a Distancia, dmoreno@bec.uned.es, +34 913987147, +34 913987690, Juan del Rosal 16, 28040 Madrid, Spain.

— Path following: In this problem the vehicle must converge on a particular path and follow it with a desired speed. The main difference with respect to the trajectory tracking is that there are no time references in path following.

The difficulty to solve each of these problems is strongly dependent on the vehicle configuration and it is of very interest when the vehicle is underactuated.

It is important to emphasize that the drift velocity in the underactuated marine vehicles is often linearly independent respect to the forces that actuate over them, so that it is not possible to convert the model into another model without drifting.

Furthermore, the fully actuated systems are expensive and, in many situations, it is not convenient to equip the ship with more actuators due to weight problems, complexity, efficiency and other considerations. For this reason, the control of underactuated vehicles is a very active investigation topic.

The path following systems are widely studied in (Encarnação 2001) (Ghabcheloo, 2007) (Pettersen, 2006) for example.

In this control problem the vehicle's forward velocity does not have to be controlled with high precision, so that an adequate orientation control to drive the vehicle along the desired path is enough. Nevertheless, the forward speed can be controlled to fulfill some soft time references.

Usually, this kind of control reaches a convergence with the path smoother than the trajectory tracking control, and moreover, the control signals obtained do not have too much tendency to saturation.

In this line, this work deals with the path following of an unmanned surface vessel (USV) to be used in cooperative tasks with other ships in formation control (Ihle, 2007) (Barisic, Vukic, Miskovic, 2005).

CONTROL LAW

Path planning problems are related to the design of control laws that force a vehicle to reach and follow a reference. The degree of difficulty to solve this problem depends on the vehicle's configuration.

The control logic consists in a simple algorithm that calculates the necessary rudder rate to reach the desired path in a smooth way.

An anticipatory control element is used for the control which overcomes the inherit limitation of feedback control to follow curved paths. This anticipatory control element and guidance logic is described deeply in (Park, Deyst & How, 2006) for its use in unmanned air vehicles (UAVs), where its stability is demonstrated. Here lies one of the new approaches of this work: the use of this aeronautic control for marine vehicles.

The basic idea is to do path following by using an imaginary point moving along the desired path as a pseudo target, as in the common LOS control algorithm. It can be considered as an element of anticipation for the upcoming desired path.

In the forthcoming approach, we consider two reference frames, one inertial frame in which the variables referred to it will be expressed without sub index, and a body fixed frame, which will move with the vehicle fixed at its mass centre. This second frame has its x-axis aligned with the vehicle's forward velocity vector (figure 1).

A line of sight (LOS) of 1000m is used to compute the error between the desired and the real path followed by the vehicle. In figure 1 the variables used to calculate the error between the desired and the real path are shown, so the distance 'd' between them can be controlled.

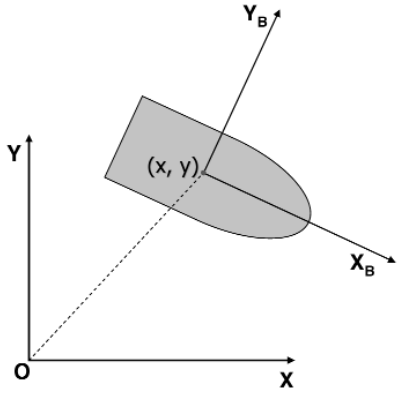

Figure 1: Reference frames.

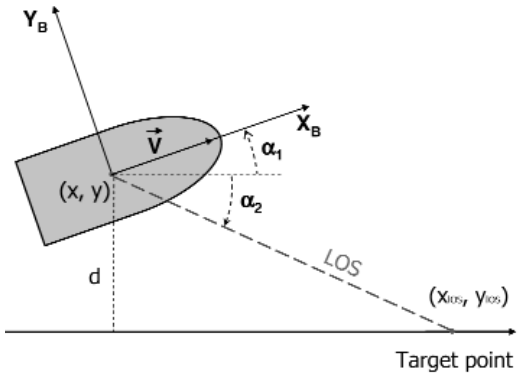

Figure 2: Control variables.

The algorithm consists firstly in finding the point in the desired trajectory that is at the distance of LOS. Then, the angles α_1 and α_2 are calculated, the first one as the inverse tangent of the ship's velocity coordinates, and the second one, as an inverse tangent as well, but in this case of the vector that joins the vessel to the point in the path at the distance of LOS.

$$\begin{aligned} \alpha_1 &= \arctan(v_y / v_x) \\ \alpha_2 &= -\arctan(y_{LOS} - y / x_{LOS} - x) \end{aligned} \tag{1}$$

The sum of these two angles is used to calculate the yaw rate, which will feed the control of the craft.

$$\begin{aligned} \alpha &= \alpha_1 + \alpha_2 \\ w &= -2 \cdot \frac{U}{L} \cdot \sin(\alpha) \end{aligned} \tag{2}$$

Where w is the yaw rate, U is the advance speed and L is the distance of LOS. The yaw rate is integrated to obtain the yaw angle as a control course input to obtain rudder angle for the ship.

From this equation we can observe two properties. The first one is that the direction of the acceleration depends on the sign of the angle between the line of sight segment and the vehicle velocity vector, so the vehicle will tend to align its velocity direction with the direction of the Line of Sight segment. The second one is that at each point a circular path can be defined by the position of the reference point, the vehicle position and that is tangential to the vehicle velocity vector. The acceleration command generated is equal to the centripetal acceleration required to follow this instantaneous circular segment.

Hence the guidance logic will produce a lateral acceleration that is appropriate to follow a circle of any radius R.

About the length Line Of Sight some considerations can be made:

— The direction of LOS makes a large angle with the desired path, when the vehicle is far away from the desired one.

— The direction of LOS makes a small angle when the vehicle is near to the desired path.

Therefore, if the vehicle is far from the desired path, then the control law rotates the craft so that its velocity direction approaches the desired path at a large angle. If the vehicle is close to the path, it is rotated so its velocity direction approaches the desired path tangentially (Park, Deyst & How, 2006).

SIMULATION EXAMPLES

Now we can see the control explained above in several simulations for different paths.

Straight lines

The first case that will be studied is when the ship must follow a path that converges to a straight line. Two cases will be considered: when the ship starts near or in the desired path, and when it does it in a distant position.

In this scenario, figure 3 shows when the ship starts the path following in the desired path, which converges to a straight line. The precision of the control law can be observed from this figure in the good performance made by it. It can be observed too how the ship converges to the desired path in an oscillating way at the beginning because it starts with an inadequate orientation of 45º instead of the 0º of the path.

Figure 4 shows when the ship starts in a distant position respect to the desired one. It can be seen how the ship reaches and follows the path as it is desired, achieving a simulated path of high accuracy.

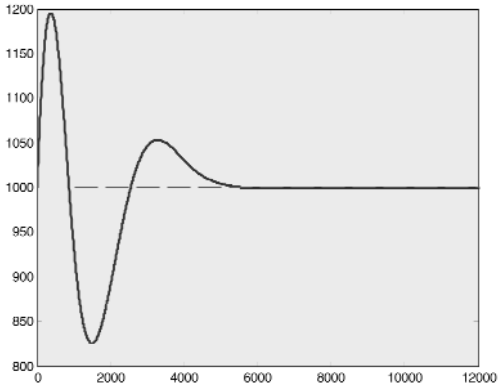

Figure 3: Desired (--) and followed path (-).

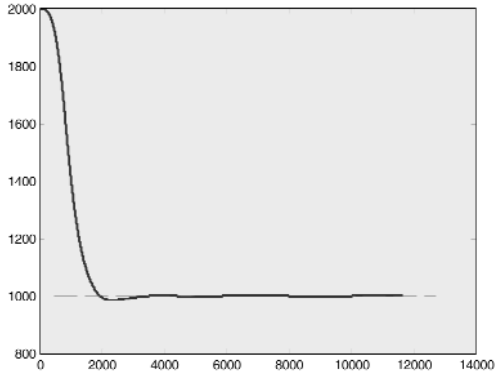

Figure 4: Desired (--) and followed path (-).

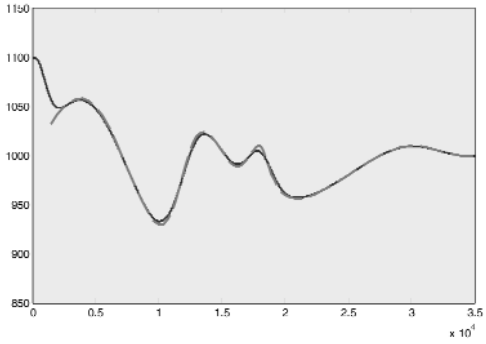

Figure 5: Desired (--) and followed path (-).

In this example, the ship searches the nearest point of the desired path and takes the adequate orientation to reach this point. Once this point has been reached, the 'line of sight' algorithm chooses the next point and so on along the path. As it can be seen from figure 4, the ship follows the desired path with a high precision once it has been reached, although in this case, despite of the ship starts far away from the desired position, it takes less time than before to reach accurately the desired path. It is because the ship can take a correct orientation while it is getting close to the desired path and it does not have to leave the path to converge to it adequately.

Perturbation from a straight line path

In this case, it is shown how the ship follows a path that is a perturbation from a straight line. The two possibilities commented above will be shown. First when the ship starts close to the desired path (figure 5).

The second case, when the ship starts far away from it, is shown in figure 6.

As it can be seen, the ship follows with great accuracy the desired path, but in this case it can be seen at the beginning how the path followed by the ship converges to the desired one a little bit rougher.

Circular path

As third scenario, it will be studied when a circle is defined as the desired

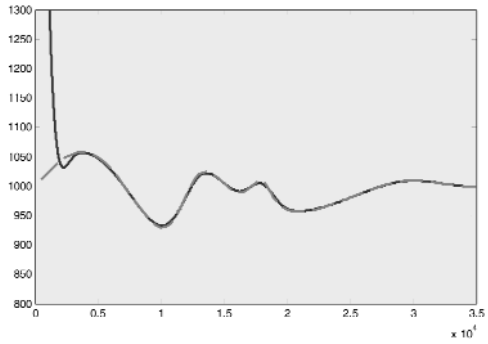

Figure 6: Desired (--) and followed path (-).

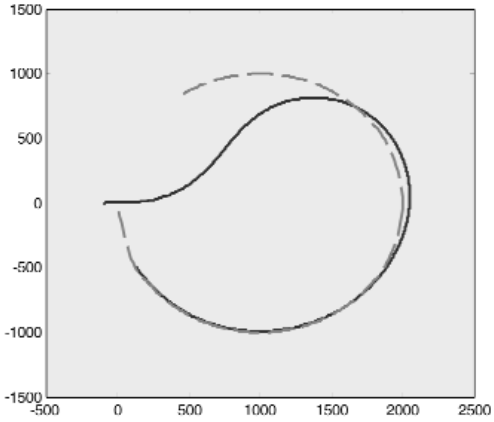

Figure 7: Desired (+) and followed path (-).

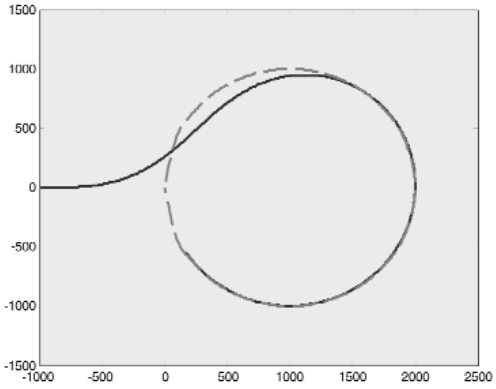

Figure 8: Desired (--) and followed path (-).

path. The two possibilities studied in the previous point will be considered too, when the ship starts near or in the desired path, and when it starts in a distant position.

First, when the ship starts in the desired path is shown in figure 7. It can be seen how, at the beginning, the vehicle does not follow the desired path because it has started with an inadequate orientation and must correct it. While the orientation is being corrected, the point to reach is changing to another nearer and easier to reach. Once the desired path has been reached, the vessel follows it with high accuracy as it can be seen at the end of the path.

Now, the case in which the ship starts in a distant point is shown in figure 8.

In this example it can be observed that the path is followed with higher accuracy at the beginning due to that the ship starts in a distant position and can reach the desired path in a smoother way.

It can be seen from the previous examples how the ship converges to the desired path as soon as it can, following the path with high accuracy once this path has been reached. It gives a simple control law with a very good fit in path following. In the next example it is shown how this control works very well not only in straight and circle paths, but also in a random path with sudden and smooth changes.

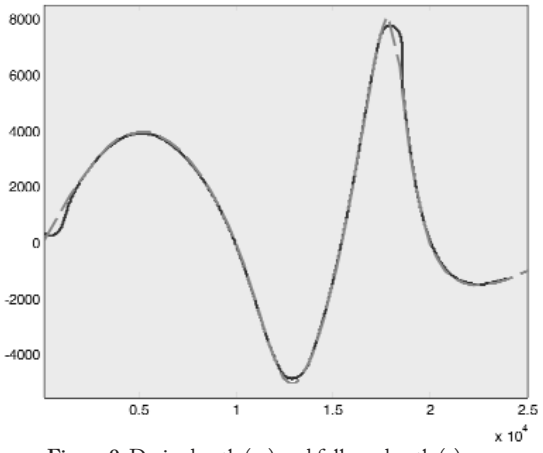

Figure 9: Desired path (--) and followed path (-).

Arbitrary path

In this case the advance speed is again maintained as a constant control input. In figure 9 it can be seen how the ship (blue line) follows the path (- red line) with high accuracy for a desired arbitrary way with sudden changes, and with a starting point out of this desired path.

In this case it can be seen how the control law fits very well the path to follow, achieving a very good control law for USV.

CONCLUSIONS

In this work a control law for aircrafts applied to Unmanned Surface Vessels (USV) has been presented. This control law shows a simple way to control USV for path following. In the different simulation examples a great fit in several situations has been demonstrated, showing that this kind of control can be used for formation control so the ship follows very well its desired path.

Besides this simple control law allows its experimental application that will be tested in future works, within the commented formation control.

ACKNOWLEDGMENTS

The authors wish to thank the Spanish Ministry of Education and Science for its support under PLACOMAR project, DPI2006-15661-C02.

REFERENCES

Aguiar, A. P., Cremean, L. and España, J. P.: Position tracking for a nonlinear underactuated overcraft: controller design and experimental results, *42nd IEEE Conference on Decision and Control,* 2003.

Barisic, M; Vukic, Z. and Miskovic, N. (2005): *Design of a Coordinated Control System for Marine Vehicles,* Department of Control and Comupeter Enginering, Zagreb, Croatia.

Fossen, T. I. (1994): *Control and Guidance of Ocean Vehicles,* Ed John Wiley and Sons.

Ghabcheloo, R. (2007): *Coordinated Path Following of Multiple Autonomous Vehicles*, Thesis (PhD), Instituto Superior Técnico, Technical University of Lisbon.

Ghabcheloo, R.; Pascoal, A.; Silvestre, C. and Kaminer, I. (2005): Coordinated path following control of multiple wheeled robots with directed communication links, in *Proc. 44rd IEE Conference on Decision & Control and 5th European Control Conference*, Sevilla, España.

Ihle, I. F. (2007): *Coordinated Control of Marine Craft*, Thesis (PhD). Thesis (PhD) Faculty of Information Technology, Mathematics and Electrical Engineering, Norwegian University of Science and Technology, Norway.

Park, S.; Deyst, J. and How, J. P. (2006): *A new nonlinear guidance logic for trajectory tracking,* AIAA Guidance, Navigation, and Control Conference and Exhibit, Providence, Rhode Island, Aug. 16-19, 2004.

Pettersen, K. Y.; Kyrkjebo, E. and Borhaug, E.: Trajectory tracking, path following and formation control of autonomous marine vehicles, *45th IEEE Conference on Decision & Control 2006 Workshop.*

SEGUIMIENTO DE UN CAMINO POR UN VEHÍCULO AUTÓNOMO

RESUMEN

El diseño de controladores para vehículos autónomos marinos es un tema de gran interés dentro de los sistemas de control. Esto es debido a que estos vehículos son fuertemente no lineales y exhiben complejos efectos hidrodinámicos que dificultan considerablemente el diseño de control.

Los problemas de control de movimiento de vehículos autónomos, que se tratan ampliamente en la literatura (Aguiar 2003, Fossen 2002), se pueden clasificar en tres grandes grupos fundamentales:

— Estabilización en un punto (point stabilization): Este problema es también conocido como posicionamiento dinámico, el objetivo es estabilizar el vehículo en un punto fijo y en una determinada orientación.
— Seguimiento de trayectoria (tracking): En este problema el vehículo debe seguir una trayectoria que se encuentra parametrizada en el tiempo.
— Seguimiento de camino (Path following): En este problema el vehículo debe converger hacia un camino preestablecido y después seguirlo con una velocidad de crucero. La diferencia fundamental con el seguimiento de trayectoria es que en el seguimiento de camino no hay referencias temporales.

Este trabajo se centra en este punto, en el seguimiento de un camino por parte de un vehículo autónomo, para aplicarlo en trabajos futuros a un conjunto de vehículos moviéndose en formación.

De este modo, en una primera aproximación al control coordinado de formaciones, se ha tratado el control de un vehículo autónomo subactuado, un barco, para alcanzar y seguir una determinada referencia, para aplicarlo posteriormente al control de varios barcos que actúen de forma coordinada siguiendo cada uno su propio camino previamente especificado.

Para el control del barco se ha usado un elemento de control anticipatorio el cual supera la limitación del control por realimentación para seguir caminos curvados. Este elemento anticipatorio y la lógica de orientación están basados en el control desarrollado por Park, Deyst & How (2006) para su uso en vehículos aéreos autónomos. En este aspecto reside uno de los nuevos enfoques de este trabajo, el uso de un control aerospacial en vehículos marinos.

La idea principal de este control es hacer el seguimiento de la trayectoria usando un punto imaginario que se mueve a lo largo del camino deseado como un pseudo

objetivo. Éste puede ser considerado como el elemento anticipatorio comentado para el camino deseado.

De esta manera, usando este control para el seguimiento de camino de los vehículos y una estrategia de coordinación y mantenimiento de formaciones es posible conseguir un movimiento coordinado de un grupo de vehículos.

MÉTODOS

Se usará el control aeronáutico explicado en Park S., Deyst J. and How J. P. (2006) para el seguimiento de camino por parte de un barco. La línea de horizonte (LOS) usada por el control para calcular el error entre el camino seguido por el barco y la trayectoria deseada será de 1000m. En la figura 10 se muestran las variables usadas para calcular el error entre los caminos deseado y real, y de este modo controlar la distancia 'd' entre ambos a través del control del timón.

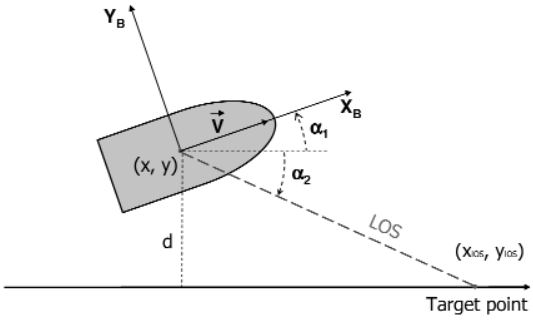

Figura 10: Variables para el cálculo del error de seguimiento de camino.

El algoritmo comienza buscando el punto en el camino deseado que se encuentra a la distancia de LOS. Tras esto, son calculados los ángulos α_1 y α_2, el primero como el arcotangente de las coordenadas de velocidad del barco, y el segundo de nuevo como un arcotangente, pero en este caso del vector que une el centro de masas del barco con el punto en el camino de referencia a la distancia de LOS.

$$\alpha_1 = \arctan(v_y / v_x)$$
$$\alpha_2 = -\arctan(y_{LOS} - y / x_{LOS} - x) \quad (1)$$

La suma de estos dos ángulos es usada para calcular la variación del timón, que alimentará el control del vehículo.

$$\alpha = \alpha_1 + \alpha_2$$
$$w = -2 \cdot \frac{U}{L} \cdot \sin(\alpha) \quad (2)$$

Donde 'w' es la variación de orientación del barco respecto al tiempo (velocidad angular), 'U' es la velocidad de avance y 'L' es la distancia de LOS. La velocidad angular de guiñada es integrada para obtener el ángulo de orientación como entrada del control de rumbo para obtener el ángulo de timón del barco.

En este caso la velocidad de avance se mantiene constante. En la figura 11 se muestra el resultado del seguimiento de camino de un barco usando el control explicado para un camino arbitrario deseado.

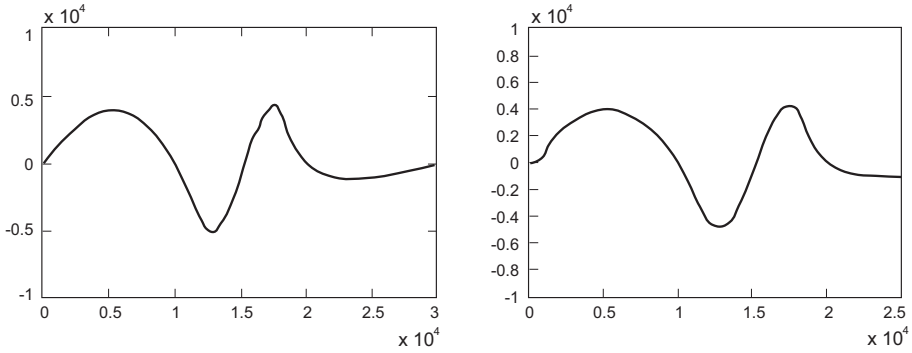

Figura 11: Camino deseado y camino seguido por el barco.

Se puede observar como el barco sigue de forma bastante fiel el camino deseado usando el control comentado.

CONCLUSIONES

Como conclusión al trabajo realizado, indicar que se ha utilizado un sistema de control aeronáutico adaptado a vehículos marinos, cuya lógica de funcionamiento se basa en dar una referencia de timón al vehículo en cuestión mediante un sencillo algoritmo que asegura la estabilidad del vehículo tanto en caminos rectos como circulares, proporcionando una convergencia exponencial al camino deseado.

Como se ha podido ver en los ejemplos mostrados, los vehículos, siempre que el camino definido esté dentro de lo permitido por su dinámica interna, siguen de forma fiel dicho camino deseado.

De la misma forma, este buen seguimiento de camino permite la creación de formaciones de vehículos moviéndose de forma coordinada, dejando este punto para futuros trabajos y desarrollos.

Journal of Maritime Research, Vol. VI. No. II, pp. 83-98, 2009

ISSN: 1697-4840

BAYESIAN VISUAL TRACKING FOR INSPECTION OF UNDERSEA POWER AND TELECOMMUNICATION CABLES

A. Ortiz[1] and J. Antich[2]

Received 26 September 2008; received in revised form 8 October 2008; accepted 10 June 2009

ABSTRACT

The surveillance and inspection of underwater installations such as power and telecommunication cables are currently carried out by trained operators who, from the surface, guide a Remotely Operated Vehicle (ROV) with cameras mounted over it. This manual visual control is, however, a very tedious job that tends to fail if the operator looses concentration. This paper describes a tracking system for underwater cables whose main objective is to allow an Autonomous Underwater Vehicle (AUV) to video-document the whole length of a cable. The approach is based on Particle Filters (PF) because of their natural ability to model multi-dimensional multi-modal probability density functions, what allows handling in a more appropriate way the ambiguities which naturally arise from undersea environments. Extensive experimental results over a test set of more than 10,000 off-line frames, for which a ground truth has been manually generated, have shown the usefulness of the solution proposed. All those images come from inspection runs captured by ROVs navigating over real power and telecommunication undersea cables. Besides, on-line results obtained from an unmanned vehicle guided by the cable tracker in a water tank are also available and are discussed in the paper.

Keywords: Autonomous Underwater Vehicles, Robot Vision, Cable Tracking, Bayesian Tracking, Particle Filter.

[1]Profesor Titular de Universidad, Universidad de las Islas Baleares (alberto.ortiz@uib.es), Escuela Politécnica Superior. Ctra.Valldemossa, Palma de Mallorca, Spain. [2]Profesor Colaborador, Universidad de las Islas Baleares (javi.antich@uib.es), Escuela Politécnica Superior. Ctra.Valldemossa, Palma de Mallorca, Spain.

INTRODUCTION

Due to the particularly aggressive conditions to which undersea cables are exposed, the feasibility of such installations can only be guaranteed by means of a suitable inspection programme. It must provide timely information on the current state of the installation or about potentially hazardous situations or damages caused by the mobility of the seabed, corrosion, or human activities such as marine traffic or fishing (Iovenitti et al., 1994; Whitcomb, 2000).

Inshore, divers can take care of part of the maintenance programme, but offshore —with increasing depth— *Unmanned Underwater Vehicles* (UUV) are preferably used. In such a case, the surveillance and inspection tasks are carried out using video cameras attached to *Remotely Operated Vehicles* (ROV) which must be steered by well-trained operators in a support ship. Such a manual visual control is a very tedious job and tends to fail if the operator looses concentration. Besides, undersea images possess some peculiar characteristics which increase the complexity of the operation: blurring, low contrast, non-uniform illumination and lack of stability due to the motion of the vehicle, to name but a few. Moreover, ROVs are connected to the support vessel by means of an umbilical cable which, on the one hand, requires a *Tether Management System* (TMS) and, on the other hand, due to its rigidity and floatability, limits the maneouverability of the vehicle as well as its working area. Therefore, the automation of any part of this process can constitute an important improvement in the maintenance of this kind of installations, with direct impact on the reduction of the number of errors, task execution time and monetary costs.

Apart from other solutions based on other sensors (e.g. acoustic), one form of automation based on vision cameras is the mere recording on video of the whole length of the cable, followed by the off-line analysis of the images acquired. A more sophisticated solution would also include a defect detection module, which would prevent the system from recording those frames in which the cable appears in good condition. In any case, in order to video-document the cable, the AUV control architecture must command the vehicle so as to let it fly over the cable, what leads to the tracking, frame by frame, of the pose (i.e. the position and the orientation) of the cable, in order to confine it within the *field of view* (FOV) of the camera during the mission. Thanks to the special visual features that artificial objects present, which allow distinguishing them in natural scenarios such as the seabed even in very noisy images, the automatic guidance of an AUV for such maintenance/inspection tasks by means of visual feedback turns out to be feasible. However, distracting background, such as rocks or algae growing on top and nearby cables, complicate the detection and tracking. Besides, ambiguities may occur when rocks or marine growth form shapes and textures that resemble a cable.

A novel tracking system for elongated structures, such as the aforementioned cables, was described in (Wirth et al., 2008). The approach was based on *Particle Fil-*

ters (PF) (Arulampalam et al., 2002; Isard and Blake, 1998) because of their natural ability to model multi-dimensional multi-modal probability density functions, what allows handling in a more appropriate way the aforementioned ambiguities. This property of PFs makes them of more general application than other popular stochastic approaches like the *Kalman Filter* and related variants (Chen, 2003; Ristic et al., 2004), although, as it is well known, at the expense of a larger computational cost.

This paper describes an evolution of the previous tracking system which allows considering different types of cables according to their visual appearance and presents an extensive set of experimental results which show the usefulness of the approach. More precisely, results for off-line processing of an extensive set of more than 10,000 images of real cables are provided. Since ground truth data have been manually generated for the image set, quantitative performance data for the cable tracker is available. Results of several experiments of autonomous cable tracking in a water tank by means of a UUV are as well available and are discussed in the experimental results section.

The paper is organized as follows: section 2 briefly enumerates other approaches for visually tracking undersea cables and pipes; section 3 describes in detail the particle filter-based approach; section 4 summarizes the most relevant results gathered so far about the performance of the tracker; and, finally, section 5 concludes the paper.

RELATED WORK

Several proposals can be found regarding visual cable and pipeline tracking and inspection. On the one hand, due to the line-like appearance of this type of installations, several groups have proposed trackers using essentially edge maps and the Hough transform: Matsumoto and Ito (Matsumoto and Ito, 1995) to follow power cables, Hallset (Hallset, 1996) to track a pipeline in a network of pipelines, and Balasuriya and Ura (Balasuriya and Ura, 1999) for telecommunication cables. On the other hand, Zingaretti et al. (Zingaretti et al., 1996) developed a system which detected underwater pipes and some other accessories attached to them using statistical information obtained from selected areas of the image. Rives and Borrelly stated the vehicle control problem as a visual servoing application and proposed a solution for it (Rives and Borrelly, 1997). Grau et al. (Grau et al., 1998) proposed an approach based on texture descriptors learnt from the appearance of the cable and the background in a previous stage. Ortiz et al. proposal involves, due to the complexity of the images to be processed, a first step of image segmentation followed by a second step where the cable sides were reconstructed from the contours of the resulting regions (Ortiz et al., 2002; Antich and Ortiz, 2003). Asif and Arshad (Asif and Arshad, 2006), in a similar way, also proposed, through a quite complex algorithm, a cable sides reconstruction step after the detection of image edges. More recently, Inzartsev and Pavin presented a tracker for narrow cables mixing an algorithm for detecting

the longest straight line on the current image and the use of electromagnetic sensors to improve the tracking performance (Inzartsev and Pavin, 2008).

THE PARTICLE FILTER

PFs approximate probability density functions by a set of N weighted *particles*, the sample set $S = \{(s^{(i)}, \pi^{(i)}) \mid i = 1,\ldots,N\}$. Each particle represents a particular (hypothetical) configuration s of the variables (i.e. one state) in the state space, together with an importance weight π, where the *state model* and the *state space* must be chosen for the given application. The evolution of the sample set is defined by two models: the *movement model*, which defines how the particles are moved in state space from one time step to the next, and the *observation model*, which is used to weight the particles according to a given observation (e.g. a camera image). The adequate combination of all these models within the particle filter paradigm allows estimating sequentially the likelihood of the cable pose: i.e. for every frame in the video sequence, the previously computed probability density function of the cable parameters is used to predict —via application of the movement model— the cable pose in the next frame; subsequently, the probability density function is updated by means of the observation model; the most appropriate cable pose estimate is finally determined from the resulting density. The following sections describe in detail the different models adopted for the cable tracker here described.

Cable Model

Figure 1(b) illustrates the model chosen for the undersea cable as it appears in camera images (see figure 1(a) for an example), while the state components are enumerated in table 1. As can be observed, the cable is modeled by two bi-dimensional straight lines separated by the apparent width the cable shows in the images, what implicitly assumes the cable does not exhibit an appreciable curvature in the images because of its rigidity or due to the distance to the sea bottom at which the vehicle navigates. While tracking a cable, the underwater vehicle is supposed to navigate at a constant distance to the seabed. Therefore, the vehicle only changes its yaw angle and performs longitudinal translations, being its movements confined within a 2D plane parallel to the ground.

In case of narrow cables, such as the ones used in telecommunications, the cable model can be further simplified to just one straight line, which would in general correspond to the cable main axis in the image. Such simplification is straightforward from the state model defined, just setting $w = 0$ and $\beta = 0$. In this way, the vehicle can be prevented from having to navigate extremely close to the seabed in order to "see" in the images a cable thick enough so as to allow the image processing algorithms to discriminate the two straight lines corresponding to the cable sides.

Several other benefits result from the adoption of this model for both thick and narrow cables:

— it allows avoiding or at least diminishing to an acceptable level the problem with suspended particles due to vehicle propellers when navigating close to the seabed;
— keeping constant the distance to the seabed is no longer critical provided the cable in the images can still be correctly modeled by a single line; and
— since the vehicle does not need to navigate close to the seabed, the part of the scene within the FOV of the camera enlarges, making more difficult to have the cable disappearing in the images.

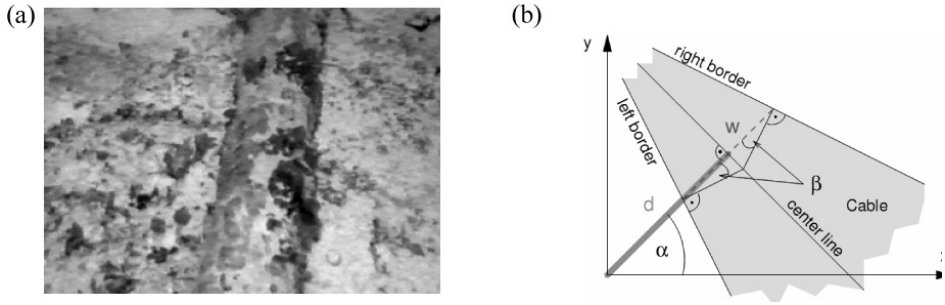

Figure 1: (a) Image of an undersea power cable. (b) Cable model (the coordinate system origin is at the center of the image).

Component	Description
d	Distance to cable centerline
α	Angle of cable centerline
w	Cable width
β	Cable skew

Table 1: Cable model components.

Movement Model

In accordance with the previous assumptions, the overall transition of a state $x = (d, \alpha, w, \beta)$ from time t to $t+1$ has been defined, by means of a constant velocity model for the cable distance and angle (Gustafsson et al., 2002), as:

$$x^*_{t+1} = x^*_t + (v_d, v_\alpha, \Delta w, \Delta\beta, \Delta v_d, \Delta v_\alpha)^T_t , \quad (1)$$

where the cable state has been augmented with an instant rotation velocity v_α and an instant translation velocity v_d, so that $x^* = (d, \alpha, w, \beta, v_d, v_\alpha)$. In equation (1), Δv_d, Δv_α, Δw and $\Delta\beta$ account for unmeasured or unknown components in the state dynamics (accelerations in cable distance/angle or velocities/accelerations in cable width/skew). In this work, they all are assumed small and, thus, are modeled as Gaussian random noise. On the other hand, in case of tracking narrow cables, the

state components relative to cable width and skew are removed or set permanently to 0, as indicated before.

At each time step, the sample state $s^{(i)}$ represented by each particle *(i)* is modified accordingly to the previous model:

$$s_{t+1}^{(i)} = s_t^{(i)} + (v_d^{(i)}, v_\alpha^{(i)}, 0, 0, 0, 0)_t^{\mathrm{T}} + \left(\mathrm{G}(\sigma_d^2), \mathrm{G}(\sigma_\alpha^2), \mathrm{G}(\sigma_w^2), \mathrm{G}(\sigma_\beta^2), \mathrm{G}(\sigma_{vd}^2), \mathrm{G}(\sigma_{v\alpha}^2)\right)^{\mathrm{T}}, \quad (2)$$

where $\mathrm{G}(\sigma^2)$ represents Gaussian zero-mean random noise. In particle filters terminology, the addition of the instant velocities is called *drift* and the addition of the random noise is the *diffusion*.

This model assumes that the different state components are mutually independent, which does not need to be the case. However, the different experiments performed have shown that this simple uncoupled constant velocity model is precise enough to follow cable movements in real sequences, such as those coming from inspection runs captured by ROVs.

Observation Model

In order to determine the weight $\pi^{(i)}$ for particle *(i)*, the (hypothetical) cable pose for such particle is first projected onto the current frame. Next, the response of a suitable filter for all the image points lying along the projection is determined (the filter is oriented orthogonally to the projection). The particle is finally scored with the average of filter responses. Two filters have been considered (see figure 2(a)): the *derivative of Gaussian* (DoG) filter, typically used for estimating image gradient information, and the unidimensional *mexican-hat* function (MeX filter from now on):

$$\mathrm{DoG}(x) = -\frac{x}{\sigma^3\sqrt{2\pi}} e^{-\frac{x^2}{2\sigma^2}}, \quad \mathrm{MeX}(x) = \left(1 - \frac{x^2}{\sigma^2}\right) e^{-\frac{x^2}{2\sigma^2}} \quad (3)$$

Figure 2(b) plots the respective filter responses for a 1D synthetic signal. As can be observed, the MeX filter emphasizes impulse-like signal changes with a larger response than the DoG filter, which tends to over-smooth such changes. On the other hand, the MeX filter produces a double response for step-like signal variations, while the DoG filter does not but emphasizes the step. Therefore, it must be expected better results from the MeX filter when tracking a cable which appears narrow in the images, while the DoG filter seems to be more appropriate for thick cables.

Finally, in order to speed up the calculation of particle weights, instead of using a filter oriented perpendicularly to each pose, horizontal and vertical mask filters are

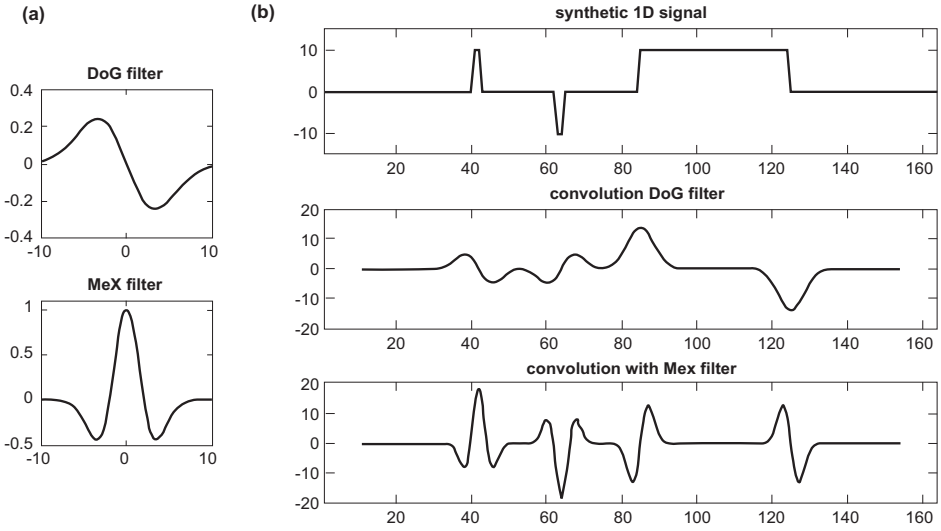

Figure 2: (a) Filters considered in the design of the observation model. (b) MeX and DoG ilter responses for a 1D synthetic signal.

defined and respective convolution images are computed for the current image. Oriented filter responses are then approximated for every particle *(i)* according to equation (4):

$$I_{\alpha^{(i)}} = \left(\cos\alpha^{(i)}\right) I_x + \left(\sin\alpha^{(i)}\right) I_y \ , \tag{4}$$

where I_x and I_y are, respectively, the "horizontal" and "vertical" response images.

Filter Initialization

In order for the tracker to follow the cable, the cable must first be detected so as to initialize the PF with a proper density. In this work, the PF is initialized in accordance with the results of analyzing selected rows and columns of the current frame. For such rows/columns, peaks in the Mex/DoG filter responses are located and the 1 or 2 largest magnitude peaks are kept depending on whether a narrow or a thick cable is tracked. Next, an initial particle set is generated by considering the lines joining every pair of selected peaks. If the image contains a cable, the best particle of the initial set can be expected to be scored very high (i.e. above a certain threshold) and coincide with the cable. In such a case, the cable is considered detected and the tracking starts; otherwise, the cable detection is considered unreliable, the image is discarded and the procedure is repeated with the next image. In such a case, the vehicle controller should not receive any motion order. Figure 3 illustrates this process for a narrow cable.

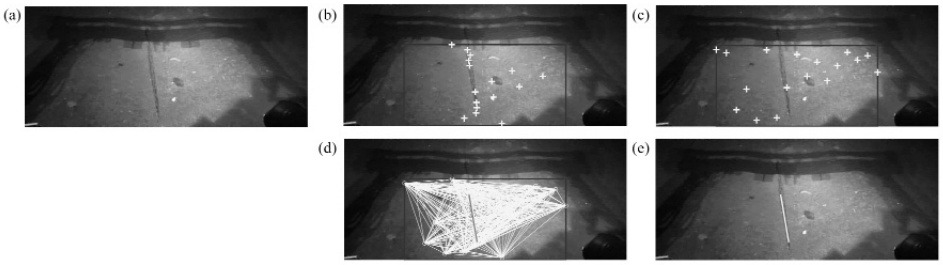

Figure 3: Illustration of the cable detection strategy: (a) original image; (b) crosses correspond to the maximum response of selected image rows; (c) crosses correspond to the maximum response of selected image columns; (d) particles generated (in yellow) and the best particle (in red); (e) best particle in yellow [The blue frame is a region of interest.].

EXPERIMENTAL RESULTS

An extensive set of experiments have been performed during the development of the cable tracker which has been described in this paper. A summary of results highlighting the most relevant facts about the tracker performance is presented in this section.

For a start, the tracker has been tested using a set of six video sequences of telecommunication cables and six video sequences of power cables. They all account for a total of around 150,000 images (approximately, one hour and a half of continuous video) and they all come from several sessions with an ROV navigating over real cables in a variety of situations: cables completely visible/partially hidden/totally hidden, uniform/cluttered background, scenes sufficiently/poorly illuminated, high/low contrast images, variations in the apparent thickness of the cable, etc. Figures 1(a) and 3(a) are examples of, respectively, the power (thick) and telecommunication (narrow) cables considered in these experiments. To obtain quantitative performance data, several excerpts representative of the previous sequences and com-

Excerpt	Number of frames	Average estimation error			
		Δd (pixels)	$\Delta\alpha$ (º)	Δw (pixels)	$\Delta\beta$ (º)
1	248	7.34	3.84	4.46	0.88
2	499	2.63	1.67	8.88	1.15
3	409	2.75	1.38	5.12	0.82
4	172	12.42	4.11	9.51	1.26
5	171	3.38	1.11	2.23	0.90
6	129	5.02	2.92	4.46	1.72
global average	1628	4.68	2.22	6.28	1.05

Table 2: Off-line processing results for thick cables.

Excerpt	Number of frames	Average estimation error	
		Δd (pixels)	$\Delta\alpha$ (º)
1	1400	6.44	3.41
2	500	1.79	0.88
3	4300	3.15	1.27
4	2600	4.34	0.96
5	900	3.42	1.26
6	600	9.37	1.92
global average	10300	4.21	1.50

Table 3: Off-line processing results for narrow cables.

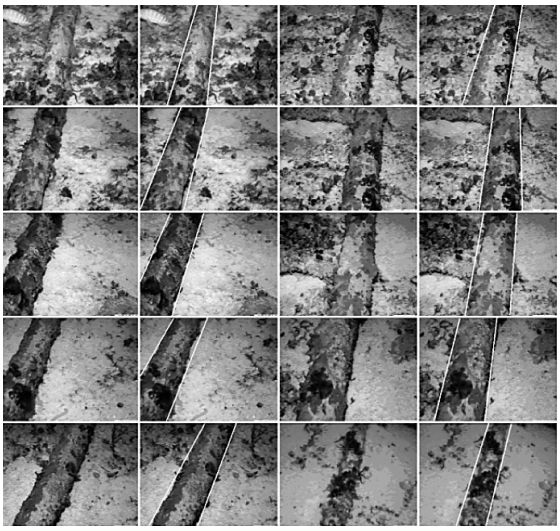

Figure 4: From top to bottom and left to right, tracking results for frames 1-225 of one of the power cable video sequences: (1st/3rd columns) original frames; (2nd/4th columns) processing results: yellow – cable estimate. (Every 25th frame is shown.)

prising more than 10,000 frames have been labelled with ground truth information. Performance has been measured by means of the average cable distance and angle errors with regard to the ground truth.

Apart from the off-line experiments, this section also provides results for a number of trials executed over a real vehicle navigating in a water tank.

In all the experiments, the filter handled sets of 500 particles and the Gaussian noise variances were determined experimentally. The filters used within the observation model made use of 21 pixel 1D masks. Finally, the state estimators used in the off-line and the on-line experiments were, respectively, the weighted average of the 5% best particles and the best particle.

Results of Off-line Experiments

Results for thick cables can be found in table 2, while table 3 provides results for narrow cables. As can be observed, on average, the error is of the order of 3-5 pixels for the cable distance and 1-2 degrees for the cable angle, what proves the usefulness of the approach. Additionally, a set of video sequences accounting for almost 150,000 frames and around 90 minutes of continuous video have been successfully processed. A sample of the results obtained for thick and narrow cables can be seen in, respectively, figures 4 and 5.

Results of On-line Experiments

Apart from the off-line experiments described in the previous section, the cable tracker has been tested along a number of trials with the ROV of figure 6. It is a small programmable ROV fitted with a compass, a depth sensor and a colour camera. The reduced size of this vehicle allowed us to perform the experiment in a 7.35m × 3.75m × 1.32m water tank. To carry out this experiment, the visual tracker was integrated with a subset of the control architecture described in (Antich and Ortiz, 2005).

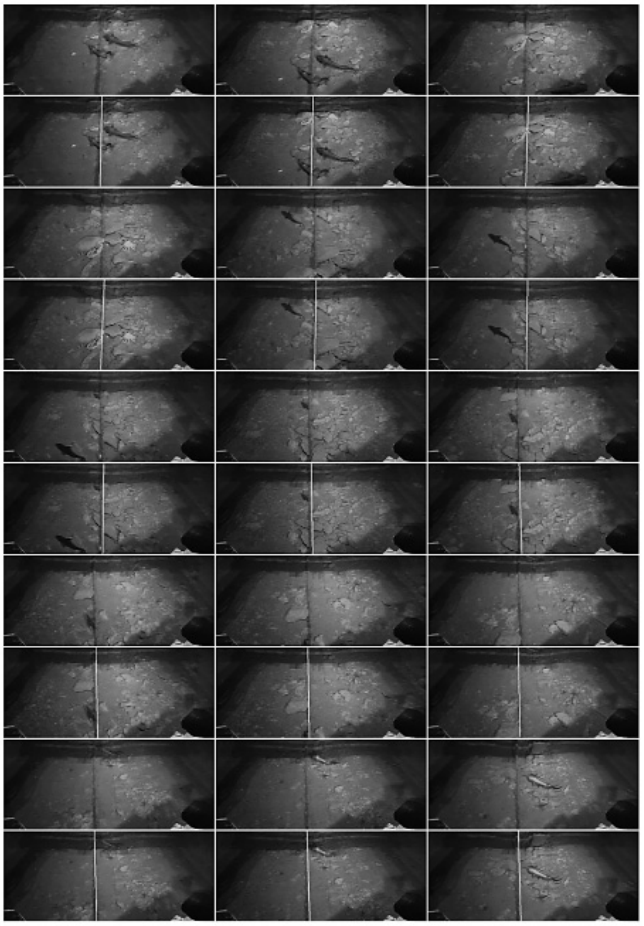

Figure 5: From left to right and top to bottom, tracking results for frames 20,800-21,450 of one of the telecommunication cable video sequences: (odd rows) original frames; (even rows) processing results: yellow-cable estimate (Every 50th frame is shown).

Figure 6: Nautilus microROV (from Albatros Marine Technologies).

Briefly speaking, those components of the architecture related with sensors not available in the experimental platform were deactivated.

Due to lack of space, figure 7 plots results for only two of the different trials that were performed. Each trial consisted in, without any human intervention, tracking the cable along four runs of the water tank, so that the vehicle had to turn autonomously at the end of every run. At the beginning of every run, the tracker had, thus, to look for the cable during the so-called *sweeping* stage, along which the vehicle performed a zigzag movement to sweep the tank in search for the cable. In order for the *sweeping* stage to last longer, the tracker was programmed so as to ignore the cable during the 2-3 first sweeping lines of the stage. Positioning information was available thanks to a visual positioning pattern at the bottom of the water tank. Table 4 provides quantitative performance results in the form of horizontal separation between the vehicle and the cable, to observe the capability of the tracker for making the vehicle "fly" over the cable. As can be observed, the vehicle did not detach from the cable more than 12 cm on average, and never more than about 40 cm.

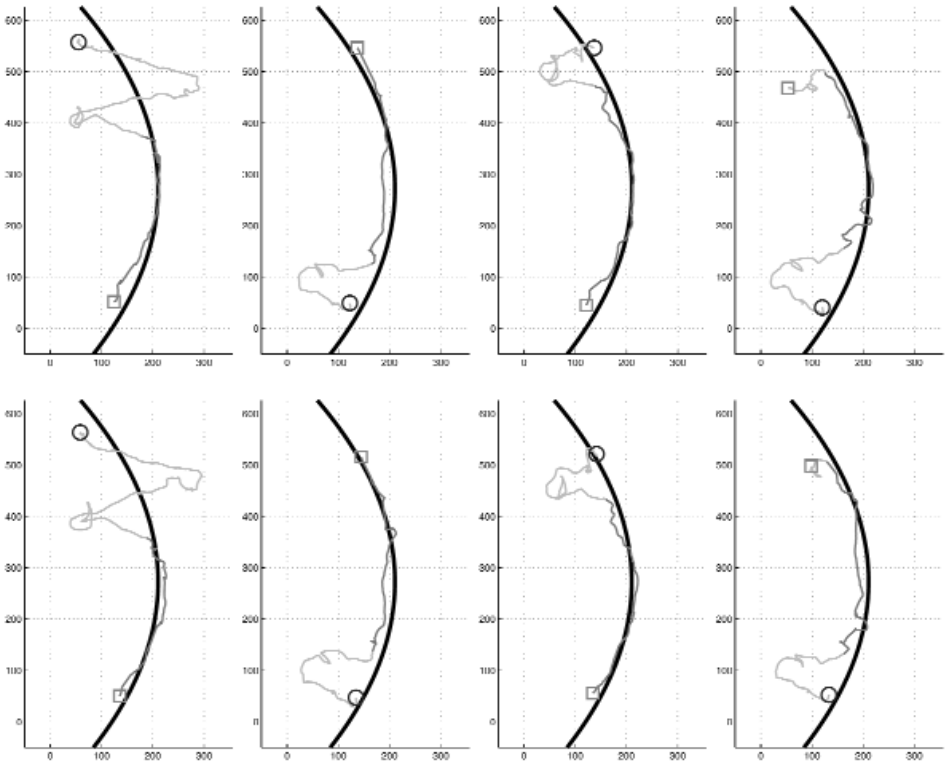

Figure 7: Paths followed by the vehicle during two trials (respectively, upper and lower rows) of a multiple-run experiment: the blue circle represents the position of departure while the magenta square indicates the end of the path; the sweeping and tracking stages are indicated in, respectively, green and red; from left to right, first, second, third and fourth runs of the trial; the thick black line is the cable at their real location.

	1st run	2nd run	3rd run	4th run	all runs
no. frames	127	149	159	139	574
AAD (cm)	10.16	15.92	10.69	12.56	12.38
MAD (cm)	35.94	32.94	34.77	41.31	41.31

	1st run	2nd run	3rd run	4th run	all runs
no. frames	133	146	137	157	573
AAD (cm)	9.27	12.39	9.74	14.70	11.66
MAD (cm)	19.26	30.26	24.27	38.60	38.60

Table 4: Tracking results for two trials (respectively, upper and lower tables): difference between vehicle and cable horizontal positions (tracking stage), AAD=Average Absolute Difference, MAD=Maximum Absolute Difference.

CONCLUSIONS

Extensive experimental results over a test set of more than 10,000 frames, for which ground truth data have been manually generated, have shown the usefulness of the cable tracking solution proposed.

Quantitative performance data in this regard has been gathered, yielding a global error for the cable tracker of, on average, between 4 and 5 pixels for the cable distance and between 1 and 2 degrees for the cable angle, what proves the usefulness of the approach. A set of video sequences accounting for almost 150,000 frames and around 90 minutes of continuous video have also been successfully processed. Besides, the cable tracker has been tested over a real vehicle in a water tank, yielding similar performance.

ACKNOWLEDGEMENTS

This study has been partially supported by project CICYT-DPI2008-06548-C03-02 and FEDER funds.

REFERENCES

Antich, J. and Ortiz, A. (2003): Underwater cable tracking by visual feedback, *Proceedings of the Iberian Conference on Pattern Recognition and Image Analysis*, 4-6 June, Puerto de Andratx (Mallorca), Spain, pp. 53-61.

Antich, J. and Ortiz, A. (2005): Development of the control architecture of a vision-guided underwater cable tracker. *International Journal of Intelligent Systems*, 20 (5), 477-498.

Arulampalam, S.; Maskell, S.; Gordon, N. and Clapp, T. (2002): A tutorial on particle filters for on-line non-linear/non-gaussian bayesian tracking. *IEEE Transactions On Signal Processing*, 50 (2), 174-188.

Asif, M. and Arshad, M.R. (2006): An active contour and kalman filter for underwater target tracking and navigation. In: Lazinica, A. ed. *Mobile Robots Towards New Applications*. Pro Literatur Verlag, 373-392.

Balasuriya, B. and Ura, T. (1999): Multi-sensor fusion for autonomous underwater cable tracking, *Proceedings of Oceans*, 13-16 September, Seattle, USA, pp. 209-215.

Chen, Z. (2003): Bayesian filtering: From kalman filters to particle filters, and beyond. *Technical report*, McMaster University.

Grau, A.; Climent, J. and Aranda, J. (1998): Real-time architecture for cable tracking using texture descriptors, *Proceedings of Oceans*, 28 September – 1 October, Nice, France, pp. 1496-1500.

Gustafsson, F.; Gunnarsson, F.; Bergman, N.; Forssell, U., Jansson, J.; Karlsson, R. and Nordlund, P.J. (2002): Particle filters for positioning, navigation, and tracking. *IEEE Transactions on Signal Processing*, 50 (2), 425-437.

Hallset, J.O. (1996): Testing the robustness of an underwater vision system. In: Laplante, P. and Stoyenko, A. eds. *Real-Time Imaging: theory, techniques, and applications*. IEEE Press, 225-260.

Inzartsev, A. and Pavin, A. (2008): AUV cable tracking system based on electromagnetic and video data, *Proceedings of Oceans*, 8-11 April, Kobe, Japan, pp. 1-6.

Iovenitti, L.; Venturi, M.; Albano, G. and Touisi, E.H. (1994): Submarine pipeline inspection: the 12 years experience of TRANSMED and future developments, *Proceedings of International Conference on Offshore Mechanics and Arctic Engineering*, 149-161.

Isard, M. and Blake, A. (1998): Condensation: conditional density propagation for visual tracking. *International Journal of Computer Vision*, 29 (1), 5-28.

Matsumoto, S. and Ito, Y. (1995): Real-time vision-based tracking of submarine cables for AUV/ROV, *Proceedings of Oceans*, 9-12 October, San Diego, USA, pp. 1997-2002.

Ortiz, A.; Simo, M. and Oliver, G. (2002): A vision system for an underwater cable tracker. *Machine Vision and Applications*, 13 (3), 129?140.

Ristic, B.; Arulampalam, S. and Gordon, N. (2004): *Beyond the Kalman Filter: Particle Filters for Tracking Applications*. Artech House.

Rives, P. and Borrelly, J.J. (1997): Underwater pipe inspection task using visual servoing techniques, *Proceedings of the IEEE International Conference on Intelligent Robotic Systems*, 7-11 September, Grenoble, France, pp. 63-68.

Whitcomb, L. (2000): Underwater robotics: out of the research laboratory and into the field. In *Proeedings of the IEEE International Conference on Robotics and Automation*, 24-28 April, San Francisco, USA, pp. 85-90.

Wirth, S.; Ortiz, A.; Paulus, D. and Oliver, G. (2008): Using particle filters for autonomous underwater cable tracking, *Proceedings of the IFAC Workshop on Navigation, Guidance and Control of Underwater Vehicles*, 8-10 April, Killaloe, Ireland.

Zingaretti, P.; Tascini, G.; Puliti, P. and Zanoli, S. (1996): Imaging approach to real-time tracking of submarine pipeline, *Proceedings of SPIE Electronic Imaging: Real-Time Imaging* (vol. 2661), 29 January, San Jose, USA, pp. 129-137.

SEGUIMIENTO VISUAL BAYESIANO PARA LA INSPECCIÓN DE CABLES DE POTENCIA Y DE TELECOMUNICACIONES SUMERGIDOS

RESUMEN

La operabilidad de una instalación submarina consistente en cables de transporte de energía eléctrica o de telecomunicaciones puede sólo ser garantizada a través de un programa de inspección capaz de proporcionar a tiempo información sobre condiciones de peligro potenciales o daños causados por la movilidad del suelo oceánico, la corrosión o actividades humanas tales como el tráfico marino y la pesca.

Hoy en día, estas tareas de vigilancia e inspección son realizadas por operadores que desde la superficie de un barco controlan un *vehículo operado remotamente* (ROV) sobre el que se han montado cámaras de vídeo. Evidentemente, ésta es una tarea tediosa en la que el operador debe permanecer largos periodos de tiempo concentrado frente a una consola, favoreciendo todo ello la aparición de errores cuyo origen es, principalmente, la pérdida de atención y la fatiga. Además, las peculiares características de las imágenes obtenidas del fondo marino —zonas difuminadas, bajo contraste, iluminación no uniforme, etc.— dificultan aún más la ya compleja operación. Por tanto, la automatización de cualquier parte de este proceso puede constituir una importante mejora en el mantenimiento de este tipo de instalaciones, no sólo en cuanto a la reducción del tiempo de inspección y de los errores, sino también de los costes asociados.

Con este objetivo, se propone un sistema visual de seguimiento de estructuras elongadas sumergidas capaz de proporcionar las consignas adecuadas para realizar el guiado de un *vehículo autónomo submarino*, de forma que a lo largo del guiado se pueda registrar en vídeo la estructura inspeccionada. La solución propuesta en este artículo se basa en los denominados *filtros de partículas* debido a su facilidad natural para modelizar funciones de densidad de probabilidad multi-dimensionales y multimodales, lo cual permite gestionar de forma más apropiada las ambigüedades que típicamente resultan de entornos no estructurados como el lecho marino. Esta propiedad de los filtros de partículas les permite abarcar un rango mayor de aplicaciones que otras soluciones como los Filtros de Kalman y sus variantes, aunque, como es bien conocido, a costa de un mayor coste computacional.

Los filtros de partículas aproximan funciones de densidad de probabilidad mediante conjuntos de *partículas* $S = \{(s^{(i)}, \pi^{(i)}) \mid i = 1,\ldots,N\}$. Cada *partícula* representa una particular (e hipotética) configuración s de variables (esto es, un estado) en el espacio de estados, al cual se le asocia un peso o importancia π; el modelo de estado, junto con el espacio de estados, se escoge para cada aplicación. La evolución del conjunto de partículas viene definido por dos modelos: el *modelo de movimiento*, que

define cómo se desplazan las partículas dentro del espacio de estados de un instante al siguiente, y un *modelo de observación*, el cual pondera las partículas de acuerdo con la observación actual (p.e. la imagen actual). La combinación adecuada de estos tres modelos a través del paradigma del filtro de partículas permite estimar secuencialmente la verosimilitud del estado del cable: para cada imagen de la secuencia, la función de densidad de probabilidad previamente estimada es utilizada para predecir —a través de la aplicación del modelo de movimiento— el estado del cable en la siguiente imagen; a continuación, la función de densidad de probabilidad es actualizada mediante la observación actual y el modelo de observación; el estado más probable del cable es finalmente determinado a partir de la densidad de probabilidad resultante.

En el artículo se describen los diferentes modelos utilizados en la solución actual, donde: el cable es modelizado por una o dos líneas rectas, dependiendo de su grosor aparente en las imágenes, el modelo de movimiento asume velocidad aproximadamente constante y el modelo de observación se define en base a la respuesta de un filtro de imagen especialmente adaptado para el tipo de cable a seguir.

CONCLUSIONES

La extensa colección de resultados experimentales presentados en este artículo, correspondientes a un conjunto de test de más de 10.000 imágenes etiquetadas manualmente con la detección correcta del cable que en ellas aparece, muestran la utilidad de la estrategia de seguimiento de cables sumergidos que se ha propuesto. En particular, a nivel cuantitativo, los experimentos realizados en cuanto a procesamiento de imágenes derivan en un error de, en promedio, entre 4 y 5 píxeles para la posición del cable, y 1-2 grados para la orientación del cable. Adicionalmente, un conjunto de secuencias de vídeo que comprenden casi 150.000 imágenes y alrededor de 90 minutos de vídeo continuo ha sido igualmente procesado con éxito. Finalmente, el seguidor de cables ha sido verificado en un tanque de agua con un vehículo submarino no tripulado, obteniendo un rendimiento igualmente satisfactorio.

INSTRUCTIONS FOR AUTHORS

http://www.jmr.unican.es

Description

Journal of Maritime Research (JMR) publishes original research papers in English analysing the maritime sector international, national, regional or local. JMR is published quarterly and the issues—whether ordinary or monographic—include both theoretical and empirical approaches to topics of current interest in line with the editorial aims and scope of the journal.

The objective of JMR is to contribute to the progress, development and diffusion of research on the maritime sector. The aim is to provide a multidisciplinary forum for studies of the sector from the perspective of all four of the following broad areas of scientific knowledge: experimental sciences, nautical sciences, engineering and social sciences.

The manuscripts presented must be unpublished works which have not been approved for publication in other journals. They must also fulfil all the requirements indicated in the 'Technical specifications' section. The quality of the papers is guaranteed by means of a process of blind review by two scientific referees and one linguistic reviewer. Although the journal is published in print format, the processes of submission and reception of manuscripts, as well as revision and correction of proofs are all done electronically.

The publication process

Submission and acceptance of manuscripts

Papers should be sent via the journal's web site at http://www.jmr.unican.es, following the guidelines indicated for the submission of manuscripts by authors. Submitting the manuscript involves sending electronically via the web site three different types of information: general information about the article and the authors, an abstract and the complete paper.

The general information about the article and the authors, as well as the acknowledgements, is to be introduced by means of an electronic form, in which the following data are requested:

- Title of the paper. Subtitle.
- Field of the manuscript presented (Experimental Sciences, Engineering, Nautical Sciences or Social Sciences) and sub-field.
- E-mail of the author to whom correspondence should be addressed.
- Personal data of each author including name, professional category or position, institution or organisation, postal address and e-mail.
- Acknowledgements, if included, should be no longer than 150 words without spaces between paragraphs.

The manuscripts submitted which are in line with the aims and scope of JMR will be submitted to a blind review process. The objective is to assess the scientific quality (two referees) and ensure that the text is linguistically acceptable (one reviewer). Only those works which are considered adequate from a scientific point of view will be reviewed linguistically. Manuscripts which do not pass the linguistic filter will be admitted with the condition that the author make linguistic and stylistic modifications as indicated.

Authors will be informed of the acceptance, rejection and/or modifications required no later than four months after the receipt of the manuscript. Once the paper has been accepted, authors can check on the status of their article via the web site. Any doubts or questions should be addressed to the Editor at jmr@unican.es

Copyright

After manuscripts have been definitively accepted, the authors must complete the copyright agreement assigning the copyright to JMR so that it can be published.

Proofs

Once the copyright transfer agreement has been completed, the Editors will assign the paper to an upcoming issue of JMR and proofs will be sent as a PDF file to the author who has corresponded with JMR throughout the reviewing process. The corrected proofs must be returned by e-mail to the Editor of JMR within 96 hours of receipt.

Reprints

Once the paper has been published, the authors will be sent a total of 12 free reprints, which will be sent the postal address of the corresponding author. Authors may also request, via the JMR web site http://www.jmr.unican.es, a maximum of 10 complete journals at 50% of the cover price.

Style and technical specifications

Manuscripts should be sent to JMR's web site in a format that is recognisable to Microsoft Word (.doc) in any of its versions for Windows. The maximum length of manuscripts is 23 double-spaced pages (approximately 7000 words) including the abstract, references and appendices. Manuscripts will be submitted using a specific application of the electronic form used to send personal data. The page layout should follow these guidelines:

- Size: DIN A4 (29 cm by 21 cm)
- Margins, 3 cm: top, bottom, left, and right.
- Font: Times New Roman, normal style, 12-point type.
- Double spacing should be used for all the paper except for the references which are to be single-spaced.
- Notes, when necessary, are to be placed at the end of the paper and numbered in their order of appearance in the text. Mathematical derivations should not be included in these endnotes.

The abstract is to be presented on one page and should include the following information:

- Title and subtitle of the paper
- Field and sub-field of the work presented.
- Abstract, which is to be no longer than 200 words, and should have no spaces between paragraphs.

- Key words (between 3 and 5) which will be used for computerised indexing of the work, in both Spanish and English.
- The complete work should be no longer than 23 pages (about 7000 words) and should be structured as is shown below.

The first page will contain the same information as the summary:

- Title of the paper, as specific and brief as possible, and subtitle if desired.
- Field and sub-field of the work presented.
- Abstract of 200 words.
- Key words.

The rest of the article:

- Introduction or Problem
- Methods
- Development (application and results)
- Conclusions
- Endnotes
- References. Only those included in the article in alphabetical order.
- Appendix containing a condensed version of the article in Spanish. This is to be 3 or at most 4 pages in length (approximately 1000-1200 words) with the following sections: abstract, methods and conclusions.

The body of the article is to be divided into sections (bold, upper-case), subsections (bold, italics) and optionally into sub-subsections (italics), none of which are to be numbered. Insert line spaces before and after the title of each section, subsection and sub-subsection. Symbols, units and other nomenclature should be in accordance with international standards.

References

The Harvard System is to be used, following the guidelines indicated below.

The way in which *bibliographic citations* are included in the text will depend on the context and the composition of the paragraph and will have one of the following forms:

- One author: Farthing (1987); (Farthing, 1987); (Farthing, 1987 pp. 182-5)
- Several authors: Goodwin and Kemp (1979); Ihere, Gorton y Sandevar (1984); Ihere et al.(1984); (Ihere et al., 1984)

The *bibliographic references* are to be arranged in alphabetical order (and chronologically in the case of several works by the same author), as is indicated in the following examples:

Books

Farthing, B. (1987) *International Shipping.* London: Lloyd´s of London Press Ltd.

Chapters of books

Bantz, C.R. (1995): Social dimensions of software development. In: Anderson, J.A. ed. *Annual review of software management and development*. Newbury Park, CA: Sage, 502-510.

Journal articles

Srivastava, S. K. and Ganapathy, C. (1997) Experimental investigations on loop-manoeuvre of underwater towed cable-array system. *Ocean Engineering* 25 (1), 85-102.

Conference papers and communications

Kroneberg, A. (1999) Preparing for the future by the use of scenarios: innovation shortsea shipping, *Proceedings of the 1st International Congress on Maritime Technological Innovations and Research,* 21-23 April, Barcelona, Spain, pp. 745-754.

Technical Reports

American Trucking Association (2000) *Motor Carrier Annual Report*. Alexandria, VA.

Doctoral theses

Aguter, A. (1995) *The linguistic significance of current British slang*. Thesis (PhD).Edinburgh University.

Patents

Philip Morris Inc., (1981). *Optical perforating apparatus and system*. European patent application 0021165 A1. 1981-01-07.

Web pages and electronic books

Holland, M. (2003). *Guide to citing Internet sources* [online]. Poole,
Bournemouth University. Available from:
http://www.bournemouth.ac.uk/library/using/guide_to_citing_internet_sourc.html
[Accessed 1 November 2003]

Electronic journals

Storchmann, K.H. (2001) The impact of fuel taxes on public transport — an empirical assessment for Germany. *Transport Policy* [online], 8 (1), pp. 19-28 . Available from:
http://www.sciencedirect.com/science/journal/0967070X
[Accessed 3 November 2003]

Equations, tables, Illustrations.

Equations are to be written with the Microsoft Word Equation Editor using right-justified alignment. They should be numbered consecutively using Arabic numerals within parentheses.

Tables should be inserted in the appropriate point in the text using Microsoft Word. They should be numbered consecutively with Arabic numerals and a concise title should be centred at the top of the table. The source is to be indicated at the bottom on the left. Any symbols used should be explained.

Illustrations are to be inserted in the appropriate point in the text using Microsoft Word. All illustrations (graphs, diagrams, sketches, photographs, etc.) will be denominated generically Figures and are to be numbered consecutively using Arabic numerals with the title centred at the top. The source is to be indicated at the bottom on the left. Photographs must be in black and white with a quality of at least 300 ppp.